Bulletin of Romanian Chemical Engineering Society

1 2017

ISSN 2360-4697
Edited by SICR and Matrix Rom

The journal is included in the international database
INDEX COPERNICUS INTERNATIONAL

ISSN 2360-4697

Bulletin of Romanian Chemical Engineering Society

Volume 4 2017 Number 1

Contents

APPLICATIONS OF CHEMICAL ENGINEERING PRINCIPLES IN MODELLING THE LIVING SYSTEMS: A TRADE-OFF BETWEEN SIMPLICITY AND MODEL QUALITY

Gheorghe MARIA[1]

Department of Chemical & Biochemical Engineering
University POLITEHNICA of Bucharest,
313 Independentei Spl., 060031 Bucharest

Abstract

The "whole-cell" simulation of cell metabolic processes under considering a variable-volume modelling framework, as developed by the author till present, has been reviewed to prove their advantages when building-up modular model structures that can reproduce complex protein syntheses inside cells. The more realistic "whole-cell-variable-volume" (WCVV) approach is reviewed regarding modular kinetic representations of the homeostatic gene expression regulatory modules (GERM) that control the protein synthesis and homeostasis of metabolic processes. The paper reviewed the general concepts of the WCVV modelling, while the cited literature includes past and current experience with GERM linking rules in order to point-out how optimized globally efficient kinetic models for the genetic regulatory circuits (GRC) can be obtained to reproduce experimental observations. Based on quantitative regulatory indices evaluated vs. simulated dynamic and stationary environmental perturbations, the reviewed literature exemplifies with GERM-s from E. coli, at a generic level, how this methodology can be extended: i) to characterize the module efficiency, species connectivity, and system stability; ii) to build-up modular regulatory chains of various complexity; iii) to prove feasibility of the cooperative vs. concurrent construction that ensures an efficient gene expression, system homeostasis, proteic functions, and a balanced cell growth during the cell cycle; iv) to prove the effect of the whole-cell content ballast in smoothing the effect of internal/external perturbations on the system homeostasis.

Key words: kinetic modelling of cell metabolic processes; homeostatic regulation of gene expression; regulatory modules of gene expression (GERM); linking GERM-s

1. Introduction

Living cells are organized, self-replicating, self-adjustable, evolvable and responsive structures to environmental stimuli.

Attempts to model metabolic cell reactions and processes are not new, an adequate model being the only one engineering alternative (reviews [22,24, 32-

[1] Corresponding author; Email: gmaria99m@hotmail.com

33]). *Synthetic Biology* and *System Biology* become emergent sciences focus on the engineering-driven model-based building of complex biological entities, aiming at applying engineering principles of systems design to biology with the idea to produce predictable and robust biological systems with novel functions in a broad area of applications, such as therapy of diseases (gene therapy), design of new biotechnological processes, new devices based on cell-cell communicators, biosensors, etc. "System Biology can be defined as "the science of discovering, modelling, understanding and ultimately engineering at the molecular level the dynamic relationships between the biological molecules that define living organisms." (Leroy Hood, President Institute for System Biology, Seattle, USA).

Due to the highly complex and partly unknown aspects of the metabolic processes, the detailed mathematical modelling at a molecular level remains still an unsettled issue, even if remarkable progresses and developments of extended simulation platforms have been reported. The general modelling rules, based on physico-chemical-biological & chemical engineering principles, and a statistical data treatment are more difficult to be applied to living systems. That is because metabolic cell processes present a low observability vs. the very large number of species (10^4), reactions (10^5), and transport parameters. Application of advanced lumping techniques can increase the model estimability by reducing the number of reactions and/or variables, and by keeping the most influential terms. Model quality tests, parameter and species sensitivity analysis, principal component and algorithms to find invariant subspaces are common rules to reduce extended model structures. The reduction cost is a loss of information on certain species and reactions, a loss in model generality, prediction capabilities, and physical meaning for some rate constants.

To overcome the structural low identifiability of living cell processes, the current trend is to use all types of information 'translated' from the 'language' of molecular biology to that of mechanistic chemistry, by preserving the cell structural hierarchy and species functions. Application of (bio) chemical engineering concepts and modelling methods, and of the nonlinear systems control theory allow improving the cell model quality, and may offer a detailed simulation of the cell metabolism adaptation to environmental changes, useful for designing modified genetic circuits and of modified micro-organisms.

Several case studies [32-33] exemplify application of such a gradual lumping analysis and modular approach to derive valuable models able to mimic the stationary and perturbed cell growth, cell response to stimuli, and system homeostasis under isotonic osmolarity.

The present paper is aiming at reviewing the general concepts of the WCVV modelling approach promoted by the author when developing modular kinetic representations of the homeostatic gene expression regulatory modules (GERM) that control the protein synthesis and homeostasis of metabolic processes. The

paper is also reviewing some published contributions including past and current experience with GERM linking rules in order to point-out how optimized globally efficient kinetic models for the genetic regulatory circuits (GRC) can be obtained to reproduce experimental observations.

2. Applied concepts when modelling the GRC dynamics

It is well-known that most of the concepts and numerical metods used in chemical engineering can be also used when modelling the dynamics of enzymatic [1-20] and metabolic cell processes [21-33]. This includes: mass conservation law (molecular and atomic species conservation, stoichiometric relationships, differential mass balances of specis[21-33]), thermodynamic laws (quantitative assignment of reaction directionality, set equilibrium of reactions, Gibbs free energy balance analyis, analysis of cyclic reactions, find species at quasi-steady-state, calculate the steady-state flux distribution that provide important information for metabolic engineering). Such kinetic analysis at a cell level includes modelling the kinetics of complex genetic regulatory circuits [21-33] controlling protein synthsis and cell metabolic fluxes distribution, and resource allocation in branched pathways through genetic switches according to environmental conditions. Such a cell model can eventually be used to design modified micro-organisms. Deterministic simulation platforms allow *in silico* design of modified cells with desirable gene circuits and 'motifs' of practical applications in the biosynthesis industry, environmental engineering, and medicine [30-31; 34-39], or for modelling and design of new drug delivery systems with a controlled drug release [40-46].

Some of these applications have been developed by the author in the framework of a NIH fellow at Texas A&M University (College Station, USA), Dept. of Chemistry and Molecular Biology, on cell modelling subjects related to gene expression regulation. Due to near astronomic complexity of cell processes (see Fig. 1 as an example of central carbon metabolism), and a huge number of involved species (10^4) and reactions (10^5) advanced lumping procedures [42] and modularization techniques [22,30] have been applied to obtain reduced models by lumpig species and/or reactions by keeping the main cell functions, and the structural, functional and temporal hierarchy.

When developing whole-cell models on a mechanistic (deterministic) basis by using continuous-variable models, all enzymatic processes are closely linked to ensure an optimum metabolism, that is an efficient use of resources (substrates) maintaining the species homeostasis and a balanced cell growth.

Moreover, for simplicity, the modelling problem was decomposed in modelling „functional modules" which, eventually will be linked to recreate the whole-cell structure [32-33], that is "modules that can be elaborated …..by

'translating' from the 'language' of molecular biology to that of mechanistic chemistry, by preserving the cell structural hierarchy and component functions"[22]. Other attempts to model cell complex continuous processes to reproduce the three main properties of the cell metabolis: i) dynamics; ii)feedback, and iii)optimality, by using „Electronic circuits" like models [22] (Fig. 2) failed.

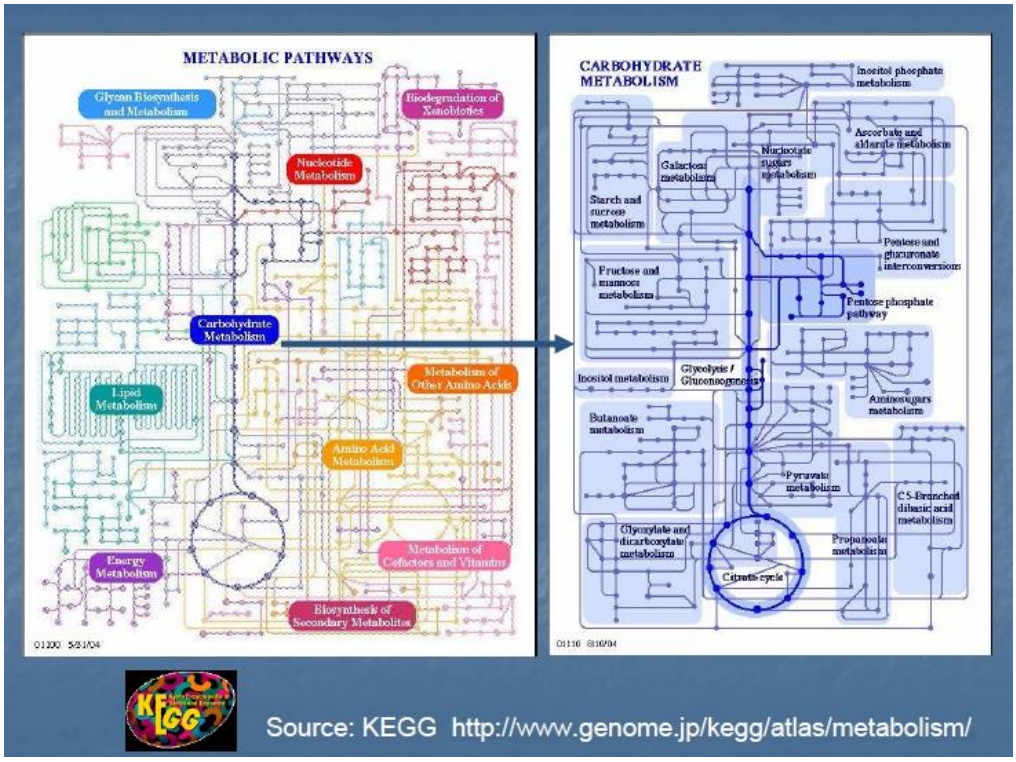

Fig. 1. The central carbon metabolism pathway in E. coli (from KEGG –omic free databank)

Because the deterministic model complexity sharply increases with the level of detail (Fig. 3), a satisfactory model complexity that realizes the best trade-off between model simplicity and its predictive quality should be adopted [23].

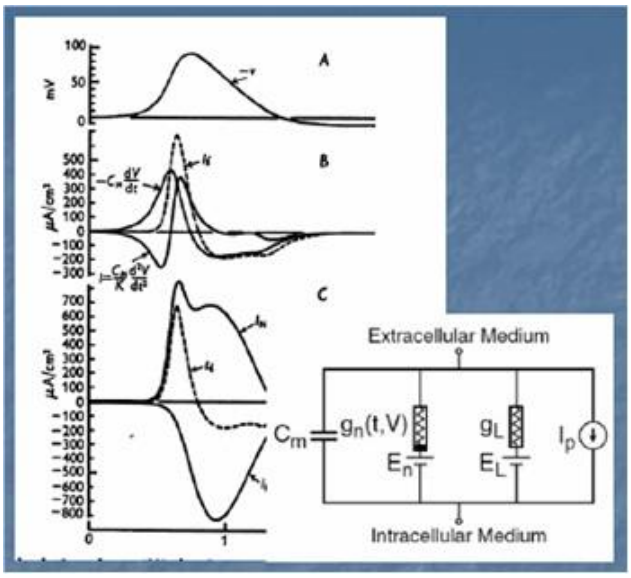

Fig. 2. Attempt to model oscillatory cell processes with electronic-like circuit models.

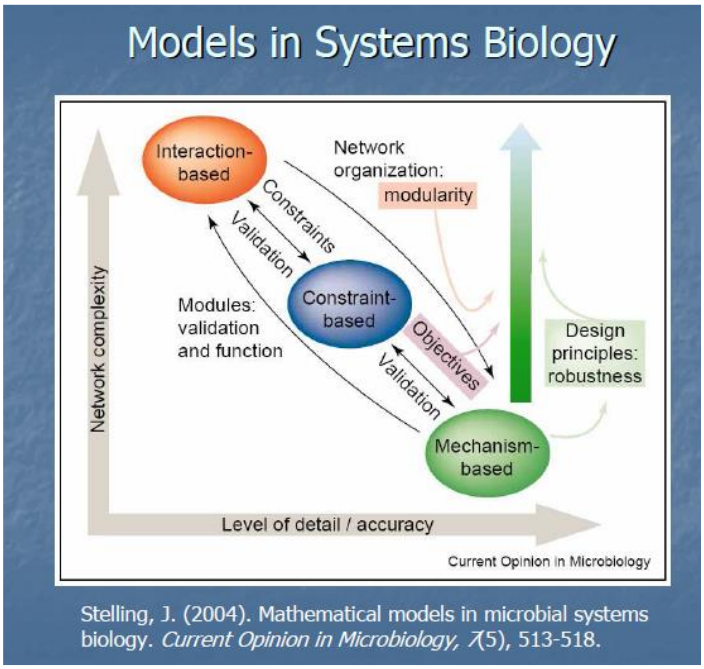

Fig. 3. The increase of the deterministic model complexity with the level of detail.

Starting from some case studies, G. Maria elaborated a procedure to build-up a whole-cell simulator of modular construction [22-31], useful for evaluation

of the genetic regulatory circuits (GRC) efficiency, and in designing genetic modified cells with desirable characteristics („motifs"). There are a large number of important contributions in modelling regulatory cell processes. Among the pioneers, the most important are: Heinrich, R., Schuster, S., 1996, The Regulation of Cellular Systems, Chapman & Hall, New York; Athel Cornish Bowden, The Pursuit of Perfection: Aspects of Biochemical Evolution, Oxford University Press, 2004. It is also to notice that the number of papers in the area of *System Biology* increases in the last 10-years with 3-orders of magnitude.

By working over several years in the area of modelling cell metabolic processes, G. Maria reported several contributions, as followings [21-33,39]:

- The more realistic "whole-cell-variable-volume" (WCVV) approach was proved to lead to a more effective representation of cell processes, being very useful when developing modular kinetic representations of the homeostatic gene expression regulatory modules (GERM) that control the protein synthesis and homeostasis of metabolic processes.
- Promotion of the new VVWC ('variable-volume whole-cell') modelling framework to buildup kinetic cell models that explicitely include the variable cell volume, its link with the cell reactions, and the role of the „cell ballast" (in a holistic approach) in smoothing the effect of perturbations coming from the environment. The VVWC modelling framework was succesfully used to derive effective kinetic models to describe the genetic regulatory circuits (GRC), and the individual gene expression modules (GERM) [21-30,32,33].
- Development of a methodology for a modular medelling of gene expression and for linking of GERMs to buidup complex GRC, thus offering the possibility i) to simulate the regulatory performances of a gene expression, of an aperon expression, or ii) of a GRC (switch, amplifier, filter, etc.), and also iii) to *in-silico* design of genetic modified or cloned micro-organisms with target plasmides to get desirable characteristics for industrial or medical applications (e.g. maximization of succinate production in *E. coli* [39], [13, 15, 18, 24,26, 27, 29]).
- The new VVWC modelling framework developed and promoted by G. Maria was used to simulate some cell metabolic processes by using the concept of a modular simulation platform, extensible, and linked to –omic databanks (Ecocyc, KEGG, Brenda, Prodoric, CellML, NIH, etc.[22]). By using conventional and non-conventional estimation techniques and incomplete experimental data from literature, applications have reproduced the protein synthesis homeostatic regulation, efficiency of some GRC, some essential cell processes such as glycolysis (Fig. 4), under stationary or perturbed growing conditions. Such a simulator can be used

to design genetic modified or cloned micro-organisms with industrial or medical applications. The case studies included simple micro-organisms (*Mycoplasma genitalium*, *Escherichia coli*, *Pseudomonas putida*) [21-33, 39]

- Proposal of structured kinetic models to simulate complex GRC-s of genetic-switch type, tested in the new VVWC modelling framework, that is whole-cell, variable cell volume, and isotonic conditions [21-33]. The cell kinetic models have been tested during collaborative works with international partners, or by using literature data collected from modified cells of *E. coli* (DFG grant 2006 TU Braunschweig; DAAD Grant, 2009 TU Hamburg; Chinese Academy grant, Tianjin Institute of Industrial Biotechnology, 2010).
- Proposal of a structured complex kinetic model (Fig. 4) to simulate the efficiency of the GRC responsible for induced expression of the *mer*-operon in gram-negative bacteria (*Pseudomonas putida*, *E. coli*) responsible for regulation of the reduction of mercury ions from wastewaters [13,15,18,27,29]. The model was tested in the new VVWC modelling framework vs. literature data and used to optimize operation of an industrial fluidized-bed bioreactor used for mercury removal from wastewaters [grant DAAD no. A/09/02572/2009, on the subject 'Dynamic modelling of some genetic regulatory circuits to simulate the bacterial resistance in a polluted environment by using the whole-cell modelling approach', at TU Hamburg, Institute of Bioprocess & Biosystems Engineering (2009)]. [27, 29, 13, 15, 30, 31].

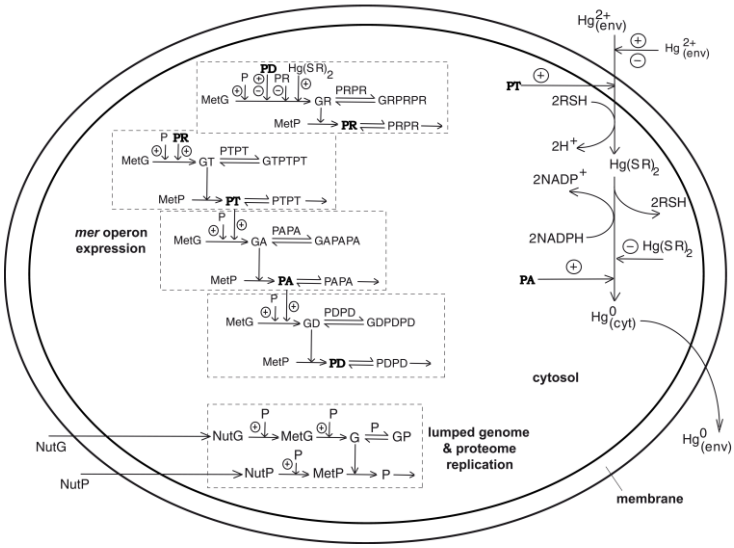

Fig. 4. Structured cell model of Maria, 2010, 2013 [15, 29] used to simulate the dynamics of mer-operon expression for mercury uptake in Escherichia coli.

- Proposal of a reduced kinetic model [31] to simulate the glycolysis under stationary or oscillating growing conditions glycolysis in *Escherichia coli* cells (Fig. 5). Such a model can be further used to coherently *in-silico* modelling of the central carbon metabolism of a bacteria aiming at designing modified bacteria of industrial use.

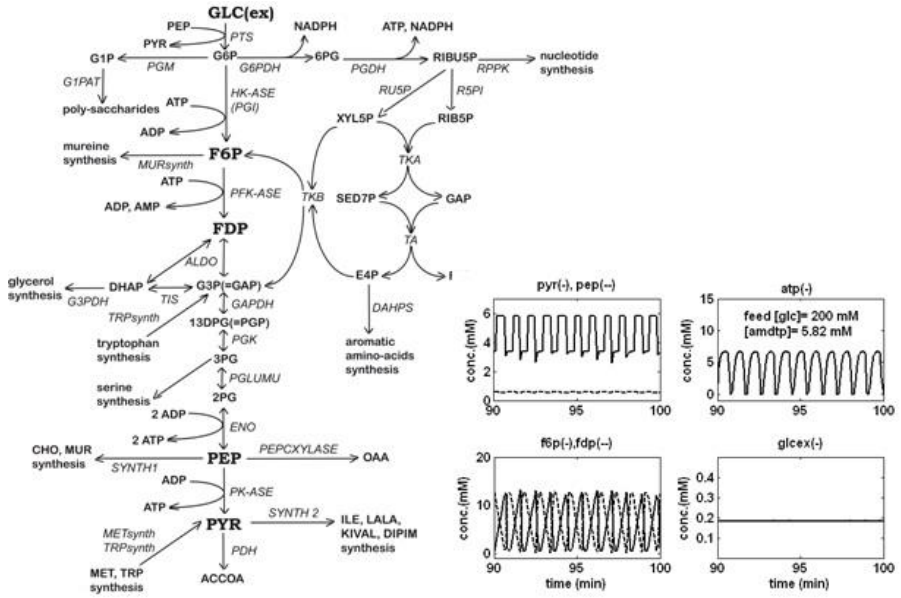

Fig. 5. Structured model of Maria, 2014 [31] to simulate the oscillating glycolysis in *Escherichia coli.*

3. Conclusions

In conclusion, general chemical engineering modelling principles are proved to be valuable tools for representing the both stationary and dynamic characteristics of the complex cell processes. Elaboration of reduced models of satisfactory quality is closely related to the ability of selecting the suitable lumping rules, key-parameters, and influential terms, and to apply multi-objective non-/conventional estimation criteria that realize the best trade-off between model simplicity and its predictive quality.

Acknowledgment
The author is grateful for the partial support from an NIH grant (GM46441/2002) and from a Romanian CNCSIS Project 1490/2004-2005.

REFERENCES

Modelling dynamics of some complex enzymatic or biological processes

[1] Maria, G., Ognean, T., An Adaptive Parameter Estimation used to Obtain Reduced Kinetic Models for the Biological Treatment Process, *Water Research* 23(2), (1989), 175-181.
[2] Maria, G., Rippin, D.W.T., Modified Integral Procedure (MIP) as a Reliable Short-Cut Method in Mechanistical Based ODE Kinetic Model Estimation: Non-Isothermal and Semi-Batch Process Cases, *Computers & Chemical Engineering* 19, (1995), S709-S714 [3]
[3] Maria, G., Rippin, D.W.T., Recursive Robust Kinetics Estimation by Using Mechanistic Short-Cut Technique and a Pattern-Recognition Procedure, *Computers & Chemical Engineering* 20, (1996), S587-S592.
[4] Maria, G., Rippin, D.W.T., Modified Integral Procedure (MIP) as a Reliable Short-Cut Method for Kinetic Model Estimation : Isothermal, Non-Isothermal and (Semi-) Batch Process Cases, *Computers & Chemical Engineering* 21, (1997), 1169-1190.
[5] *Ma*ria, G., Maria, C., Salcedo, R., Feyo de Azevedo, *S.*, Databank Transfer-of-Information, Shortcut and Exact Estimators Used in the Wastewater Biological Treatment Process Identification, *Computers & Chemical Engineering* 24, (2000), 1713-1718.
[6] Treitz, G., Maria, G., Giffhorn, F., Heinzle, E., Kinetic Model Discrimination via step-by-step Experimental and Computational Procedure in the Enzymatic Oxidation of D-Glucose, *Jl. Biotechnology* 85, (2001), 271-287.
[7] Maria, G., Model-Based Heuristic Optimised Operating Policies for D-Glucose Oxidation in a Batch Reactor with Pulsate Addition of Enzyme, *Computers & Chemical Engineering* 31, (2007), 1231-1241.
[8] Maria, G., Cocuz, A., Operating alternatives for the (semi)batch reactor used for D-glucose enzymatic oxidation with free-enzyme, *Revista de Chimie*, 62(3), (2011),318-327.
[9] Maria, G., Enzymatic reactor selection and derivation of the optimal operation policy by using a model-based modular simulation platform, *Computers & Chemical Engineering*, 36(1), (2012), 325–341.
[10] Maria, G., Ene, M.D., Jipa, I., Modelling enzymatic oxidation of D-glucose with pyranose 2-oxidase in the presence of catalase, *Journal of Molecular Catalysis B: Enzymatic*, 74(3-4), (2012), 209-218.
[11] *E*ne, M.D., Maria, G., Temperature decrease (30-25oC) influence on bi-enzymatic kinetics of D-glucose oxidation, *Journal of Molecular Catalysis B: Enzymatic* **81**(9), (2012), 19-24..
[12] Maria, G., Ene, M. D., Kinetics studies on enzymatic oxidation of d-glucose with pyranose 2-oxidase in the presence of catalase, *New Biotechnology*, 29, (2012), S86.
[13] Maria, G., Luta, I., Maria, C., Model-based sensitivity analysis of a fluidised-bed bioreactor for mercury uptake by immobilised *Pseudomonas putida* cells, *Chemical Papers*, 67(11), (2013), 1364–1375.
[14 Maria, G., Ene, M.D., Modelling enzymatic reduction of 2-keto-D-glucose by suspended aldose reductase, *Chemical & Biochemical Engineering Quarterly*, 27(4), (2013), 385–395.
[15] Maria, G., Luta, I., Structured cell simulator coupled with a fluidized bed bioreactor model to predict the adaptive mercury uptake by *E. coli* cells, *Computers & Chemical Engineering*, 58, (2013), 98-115.
[16] Maria, G., Crisan, M., Evaluation of optimal operation alternatives of reactors used for D-glucose oxidation in a bi-enzymatic system with a complex deactivation kinetics, *Asia-Pacific Journal of Chemical Engineering*, 10, (2015), 22-44.

[17] Crisan, M., Maria, G., Modular simulation to check performances of various reactors for the enzymatic D-glucose oxidation, *Revue Roumaine de Chimie*, 61(6-7), (2016), (in-press).
[18] Scoban, A.G., Maria, G., Model-based optimization of the feeding policy of a fluidized bed bioreactor for mercury uptake by immobilized *P. putida* cells, *Asia-Pacific Journal of Chemical Engineering*, in-press, 11(5), (2016), 711-734.
[19] Maria, G., Quick identification of a simple enzyme deactivation model for an extended-Michaelis-Menten reaction type. Exemplification for the D-glucose oxidation with a complex enzyme deactivation kinetics *Computers & Chemical Engineering*, 3, (2016), 323-330.
[20] Maria, G., Crisan, M., Modular simulation to determine the optimal operating policy of a batch reactor for the enzymatic fructose reduction to mannitol with the in-situ continuous enzymatic regeneration of the NADH cofactor, *Biochemical Engineering Journal*, submitted, 2016.

Modelling dynamics of some metabolic cell processes (metabolic fluxes, protein synthesis, glycolysis, genetic regulatory circuits, etc.)

[21] Maria, G., Evaluation of Protein Regulatory Kinetics Schemes in Perturbed Cell Growth Environments by Using Sensitivity Methods, *Chemical and Biochemical Engineering Quarterly* 17(2), (2003), 99-117.
[22] Maria, G., Modular-Based Modelling of Protein Synthesis Regulation, *Chemical and Biochemical Engineering Quarterly* 19, (2005), 213-233.
[23] Maria, G., Application of lumping analysis in modelling the living systems -A trade-off between simplicity and model quality, *Chemical and Biochemical Engineering Quarterly* 20, (2006), 353-373.
[24] Maria, G., Modelling bistable genetic regulatory circuits under variable volume framework, *Chemical and Biochemical Engineering Quarterly* 21, (2007), 417-434.
[25] Maria, G., Reduced modular representations applied to simulate some genetic regulatory circuits, *Revista de Chimie* 59, (2008), 318-324.
[26] Maria, G., Building-up lumped models for a bistable genetic regulatory circuit under whole-cell modelling framework, *Asia-Pacific Journal of Chemical Engineering* 4, (2009), 916-928.
[27] Maria. G., A whole-cell model to simulate the mercuric ion reduction by E. coli under stationary and perturbed conditions, *Chemical and Biochemical Engineering Quarterly* 23(3), (2009), 323-341.
[28] Maria. G., A whole-cell approach in modelling genetic circuits in living cells, New Biotechnology, 25, (2009), S338.
[29] Maria, G., A dynamic model to simulate the genetic regulatory circuit controlling the mercury ion uptake by E. coli cells, *Revista de Chimie* 61(2), (2010), 172-186.
[30] Maria, G., Extended repression mechanisms in modelling bistable genetic switches of adjustable characteristics within a variable cell volume modelling framework, *Chemical & Biochemical Engineering Quarterly*, 28(1), (2014), 83–99.
[31] Maria, G., Insilico derivation of a reduced kinetic model for stationary or oscillating glycolysis in *Escherichia coli* bacterium, *Chemical & Biochemical Engineering Quarterly*, 28(4), (2014), 509-529.
[32] Maria, G., Scoban, A.G., Setting some milestones when modelling gene expression regulatory circuits under variable-volume whole-cell modelling framework. 1. Generalities, *Revista de Chimie* (2016). in-press.
[33] Maria, G., Scoban, A.G., Setting some milestones when modelling gene expression regulatory circuits under variable-volume whole-cell modelling framework. 2. Case studies, *Revista de Chimie* (2016). in-press.

Design of genetic modified micro-organisms (Synthetic Biology)

[34] Heinemann, M., Panke, S., Synthetic Biology - putting engineering into biology, *Bioinformatics*, 22, (2006), 2790–2799.
[35] Banga, J.R., 2008, Optimization in computational systems biology, 6th Simon Stevin on Optimization in Engineering, Arenberg, Leuven, NL..
[36] Banga, J.R., Optimization in computational systems biology, *BMC Systems Biology*, 2, (2008), 47.
[37] Rodriguez-Fernandez, M., Mendes, P., Banga, J.R., A hybrid approach for efficient and robust parameter estimation in biochemical pathways, *BioSystems* 83, (2006), 248–265.
[38] Moles, C.G., Mendes, P., Banga, J.R., Parameter estimation in biochemical pathways: A comparison of global optimization methods, *Genome Res.*, 13, (2003), 2467-2474.
[39] Maria, G., Xu, Z., Sun, J., Investigating alternatives to in-silico find optimal fluxes and theoretical gene knockout strategies for E. coli cell, *Chemical & Biochemical Engineering Quarterly* 25(4), (2011), 403-424.

Design of drug release systems with a controlled drug release rate in biological fluids

[40] Maria, G., Luta, I., 2015, Kinetic models for the in-silico design of functionakized mesoporous supports for the controlled release of biological active principles, Ed. Printech, Bucharest, ISBN 978-606-23-0443-0 (in Romanian).
[41] Zhang, W., Tichy, S.E., Perez, L.M., Maria, G.C., Lindahl, P.A., Simanek, E.E., Evaluation of Multivalent Dendrimers Based on Melamine. Kinetics of Dithiothreitol - Mediated Thiol-Disulfide Exchange Depends on the Structure of the Dendrimer, *Journal of American Chemical Society* 125(17), (2003), 5086-5094.
[42] Maria, G., Relations between Apparent and Intrinsic Kinetics of Programmable Drug Release in Human Plasma, *Chemical Engineering Science* 60, (2005), 1709-1723.
[43] Maria, G., Luta, I., Precautions in using global kinetic and thermodynamic models for characterization of drug release from multivalent supports, *Chemical Papers*, 65(4), (2011), 542-552.
[44] Maria, G., Berger, D., Nastase, S., Luta, I., Modelling alternatives of the irinotecan release from functionalized mesoporous-silica supports, *Microporous and Mesoporous Materials* 149(1), (2012), 25-35.
[45] Maria, G., Stoica, A.I., Luta, I., Stirbet, D., Radu, G.L., Cephalosporin release from functionalized MCM-41 supports interpreted by various models, *Microporous and Mesoporous Materials*, **162**(11), (2012), 80-90.
[46] Luta, I., Maria, G., In-silico modulation of the irinotecan release from a functionalized MCM-41 support, *Chemical & Biochemical Engineering Quarterly*, 26(4), (2012), 309–320.

NITROGEN REMOVAL IN WASTEWATER TREATMENT PROCESSES

Cristina SINGUREANU[1], Alexandru WOINAROSCHY[1,2*]

[1]Department of Chemical and Biochemical Engineering, Faculty of Applied Chemistry and Materials Science, University Politehnica of Bucharest
[2]Academy of Technical Sciences of Romania

Abstract
Nitrogen-containing pollutants in different effluents have significant adverse effects on the aquatic environment by producing eutrophication of lakes and slow-flowing rivers, stimulating the development of algae and aquatic plants. Here are presented different procedures for the removal of nitrogen from municipal wastewater. An important such procedure is the Bardenpho process. As an application the advantage of Bardenpho process for ammonia removal compared with a classical wastewater treatment is exposed by the use of SuperPro Designer simulator.

Key words: Wastewater treatment, nitrogen nutrients, Bardenpho process

1. Introduction

Municipal wastewater treatment is the set of measures and procedures by which the chemical or biological impurities contained in the wastewater are reduced below certain limits, so that these waters do not harm the receptor in which they are evacuated and do not endanger the use of water.

Traditional objectives related to waste water treatment were initially related to the removal of suspended materials (settleable or floatable), through primary or mechanical treatment, then through the reduction of organic substances in the biological or secondary stage. The problem has become much more complex due to residual substances in wastewater that pose particularly serious environmental problems.

With the development of scientific knowledge of the pollutants found in wastewater, as well as the availability of an extensive information base from environmental monitoring studies, the requirements imposed on the quality of effluent discharged into the emissaries have become increasingly stricter. In most situations, severe conditions are imposed on the retention of organic substances,

*Corresponding author: E-mail address: a_woinaroschy@chim.upb.ro

suspensions, nutrients and specific toxic compounds, conditions that cannot be met only with conventional purification classical technologies [1-3].

2. The impact of discharging mechano-biologically treated wastewater into natural emissaries

At present, most of the treatment plants in Romania have only physico-chemical (primary) and biological (secondary) stages. The primary stage allows retention of suspended substances, settleable substances and fats, while the biological stage provides for the partial removal of the organic substance in either dissolved or colloidal form. A number of resistant or refractory substances are not retained, such as the compounds of nitrogen, phosphorus, heavy metals, persistent organic micropollutants, pesticides, certain pathogenic germs and other non-biodegradable substances. These substances are present in the treated effluent and reach the emissary. If they are a source of water supply to downstream communities, their cumulative effect and the continued exposure of humans to these substances may have negative (sometimes lethal) effects on human health. In addition, some of them are ideal food for algae and aquatic plants.

The impact of discharging wastewater into natural emissaries is manifested at various levels, from human health damage to complex ecological, technical and economic issues.

- nitrogen compounds endanger human health;
- ammonia is toxic, having cumulative sub-lethal effects, slowing the growth and development of children and adolescents;
- nitrites are very dangerous, both for humans (producing gastric cancer) and for aquatic fauna;
- nitrates are less dangerous for adults (may cause certain gastric disorders), but for newborns they cause methemoglobinemia or blue disease.

Nitrates as such are not toxic, so that in order to gain this quality they must undergo a reduction process and be converted into nitrites. Once infused into the blood, nitrites combine themselves with hemoglobin forming methemoglobin and creating an oxygen deficiency. Maladia is almost exclusively encountered at babies in the first year of life who are artificially fed, which is explained by the fact that in the first few months, the baby still has a much leaner maternal hemoglobin and the need for water is higher than that of adults. The amount of nitrates per unit of body weight is also higher [4].

Nitrogen-containing pollutants in different effluents have significant adverse effects on the aquatic environment by producing eutrophication of lakes and slow-flowing rivers (a phenomenon induced by the accelerated and massive development of microplankton and aquatic vegetation). Eutrophication is due to both nitrogen and phosphorus compounds that are nutrients for algae and

microplankton. The direct consequences of eutrophication correspond to the deterioration of water quality from the point of view of organoleptic properties, saturation's decrease in dissolved oxygen, transparency, and the fish stock with possible fish mortality and the occurrence of toxic effects on humans and animals.

The technical and economic effects of mechanical and biological treated effluents discharge into natural emissaries should not be omitted, meaning that:

- there is a need for technologically complicated and cost-effective drinking water treatment technologies;
- water is enriched with ethereal oils that cause unpleasant taste and are very difficult to remove in the treatment processes for drinking water;
- because of eutrophication, navigation and leisure activities are hindered.

3. Procedures for the removal of nitrogen from municipal wastewater

Due to the high cost of external sources of organic C, technologies were sought in which the C oxidation and nitrification/denitrification steps are combined in one process, using natural C available in wastewater. Advantages specific to this process include:

• reducing the required airflow to ensure nitrification and reduction of CBO_5;
• eliminating the need for additional organic C sources for denitrification;
• elimination of intermediate decanters and sludge recycling systems.

Most of these systems are capable of removing between 60 and 80% of total nitrogen but with proper process control, nitrogen could be reduced below provisions requirements.

The main physical and chemical processes used to remove nitrogen are:

• stripping;
• chlorination at breakpoint;
• selective ion exchangers.

4. The Bardenpho process for wastewater treatment

The Bardenpho process for wastewater treatment was developed by James Barnard from South Africa in the 1970s. The Bardenpho process uses both carbon from wastewater and carbon from endogenous decomposition to ensure denitrification. The separate reaction zones are used for carbon oxidation and anoxic denitrification. Initially, the wastewater enters into an anoxic denitrification zone where a nitrified mixture is recycled from the next compartment, which combines carbon oxidation with nitrification (Figure 1).

Carbon present in wastewater is used to denitrify the recirculating nitrate.

Denitrification occurs rapidly, because organic loading is increased. In the wastewater, the ammonia passes unchanged through the first anoxic basin and is nitrified in the first aeration basin [5].

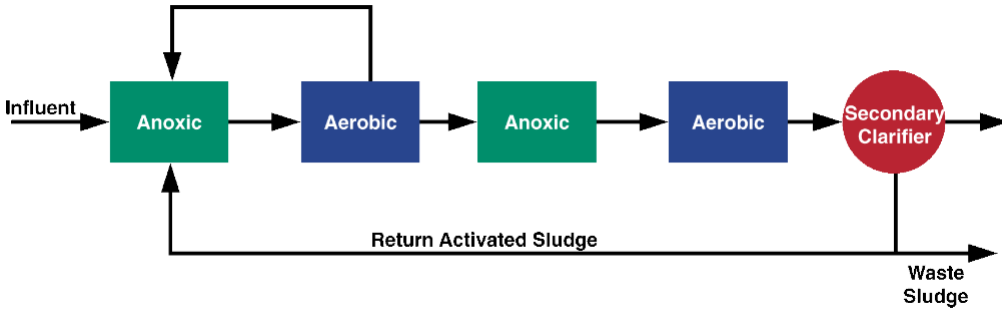

Fig.1 The Bardenpho Process

The nitrified mixture in the first aeration tank passes into the second anoxic zone, where the denitrification occurs on the basis of consumption of the endogenous C source. The second aerobic zone is relatively small and is mainly used for stripping the gaseous N which entered before rinsing. The ammonia released from the sludge in the second anoxic zone is also nitrified in the last aerobic zone.

• *Advantages of the Bardenpho process*

Since no chemical products are used, the operating costs are lower and there is no problem with the disposal of sludge. Wastewater treatment plants built on the Bardenpho process are simple and do not require re-qualification of the staff. The sludge obtained in the final stages does not require additional treatment and can be easily eliminated.

• *Disadvantages of the Bardenpho process*

One of the main drawbacks of the Bardenpho process is the number of tanks required, which considerably increases investment costs. Another disadvantage is the retention time that must be strictly monitored and evaluated.

4.1. Comparison between a base case and Bardenpho wastewater treatment process using SuperPro Designer simulator

An existing wastewater treatment plant (Figure 2) is designed to handle an average flow of 46,000 m^3/day.

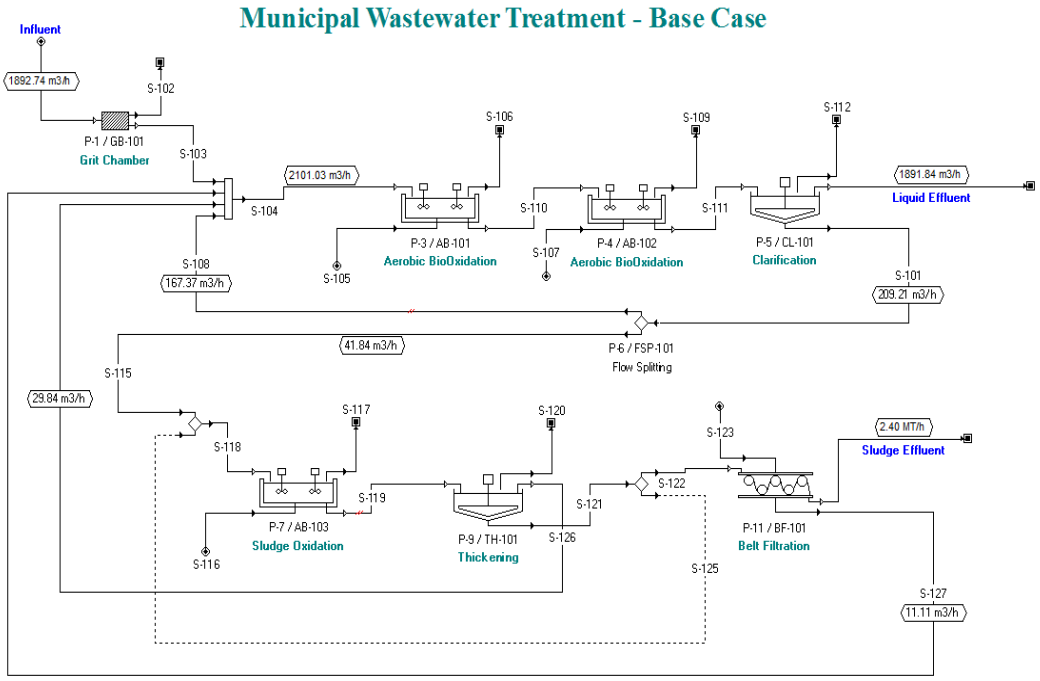

Fig.2 The base case of an existing wastewater treatment plant [6]

The dimensions of the equipment are [6]:

- Aeration Basin - 4 tanks each having a volume of 2,500 m^3 with a depth of 2 m; the four tanks form two pairs operating in sequence (AB-101 and AB-102).
- Secondary Clarifier (CL-101) - 4 tanks each having a surface area of 490 m^2 with a depth of 4 m.
- Aerobic Digester (AB-103) - 1 tank of 2,500 m^3 with a depth of 2 m.
- Sludge Thickener (TH-101) - 2 tanks each having a surface area of 250 m^2 with a depth of 4 m.
- Belt Filter Press (BF-101) - 1 unit with a belt width of 1.5 m. Note that a single icon on the flowsheet may represent multiple identical units operating in parallel.

For this reference case the input flowrate is aprox. 1892 m^3/h and the influent concentrations and the corresponding explanations are indicated in Table 1.

Table 1

The influent concentrations and the corresponding explanations

Component	Influent concentration (mg/L)	Explanation
DomWaste	105.667	substrate - organic, soluble, biodegradable material
X-vss-h	52.833	active volatile solids in suspension (heterotrophic biomass)
X-vss-i	51.248	inert volatile solids in suspension
X-vss-n	3.170	vss for nitrifiers (autotrophic biomass)
FSS	60.758	fixed suspended solids (non-biodegradable)
TDS	305.434	total dissolved solids (non-biodegradable)
NO_3	2.642	nitrite/nitrate
Ammonia	13.133	dissolved NH_3/NH_4 (not NH_3-N)
Carbon Dioxide	51.248	dissolved CO_2 (in the form of HCO_3 or H_2CO_3)

The detailed stoichiometry equations and kinetic constants of substrate (DomWaste) degradation, nitrification, biomass decay, and de-nitrification can be found in the literature [2, 3].

The SuperPro Designer flowsheet for the Bardenpho process for nitrogen removal (Figure 3) shows the two anoxic and two aerobic stages as separate process units. In reality, all four stages are accommodated by the four initial tanks. More specifically, one of the four tanks (25% of total volume) houses the first anoxic stage, two other tanks (50% of total volume) house the first aerobic stage, 80% of the fourth tank (or 20% of the total volume) houses the second anoxic zone, and the remaining 20% of the fourth tank (or 5% of the total volume) houses the second aerobic stage. The dimensions of the equipment are identical with the base case. The reaction stoichiometry and kinetics were assumed the same as in the base case. The input flowrate and the influent concentrations for the Bardenpho process are the same as in the base case (Table 1).

The effluent concentrations for the two cases computed using SuperPro Designer simulator are exposed in Table 2.

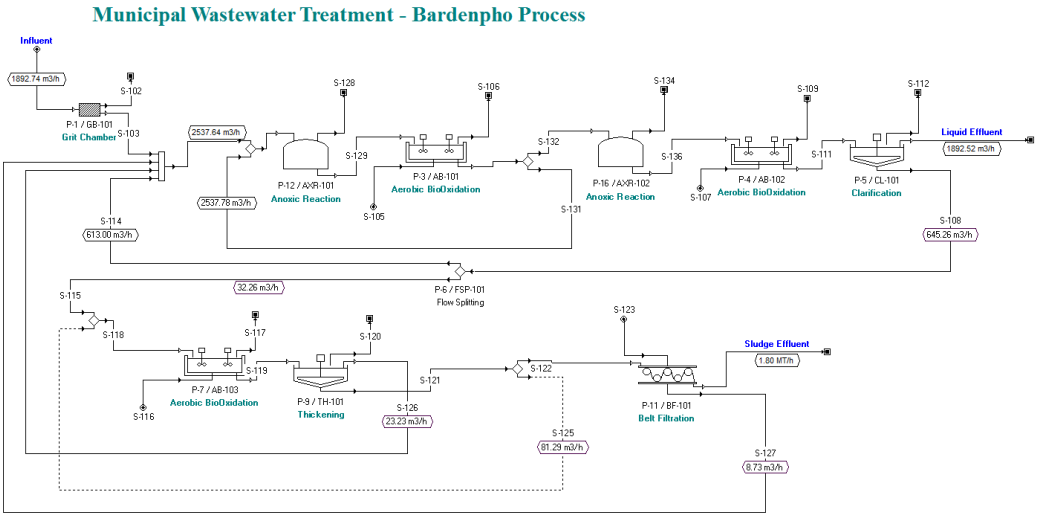

Fig. 3 The SuperPro Designer flowsheet of Bardenpho process [6]

Table 2

The effluent concentrations for the two cases

Component	Effluent concentration for base case (mg/L)	Effluent concentration for Bardenpho process (mg/L)
DomWaste	3.338	0.761
X-vss-h	12.449	38.116
X-vss-i	5.085	15.906
X-vss-n	0.332	0.962
FSS	4.172	14.597
TDS	306.288	306.258
NO_3	19.183	14.031
Ammonia	**8.904**	**0.670**
Carbon Dioxide	1.757	0.244

From Table 2 it can be observed that for the base case the effluent ammonia concentration is greater than the maximum admitted value of 2 mg/L [7], instead for the Bardenpho process the corresponding value is in the limit of legal concentrations. Here must be indicated that for the Bardenpho process the residence time for the anoxic reaction zones and for aerobic bio-oxidation zones were computed in order to minimize the ammonia effluent concentration [8].

5. Conclusions

Discharges of treated wastewater containing nitrogen compounds, such ammonia, can accelerate the eutrophication, and can stimulate the development of algae and aquatic plants. Despite the fact that the number of tanks required is higher than in a traditional wastewater treatment process, which considerably increases investment costs, the Bardenpho process is net superior for ammonia removal. This fact was demonstrated in this paper using the SuperPro Designer simulator.

REFERENCES

[1] Ianculescu O., Ionescu G., Racoviţeanu R., 2011. *Epurarea apelor uzate* , Matrix Rom, București.
[2] Tchobanoglous,G., Burton, F., 2003. *Wastewater Engineering: Treatment and Reuse*, 4th edition, Metcalf and Eddy, McGraw-Hill, New York, USA.
[3] Wesley W., Eckenfelder Jr., 2000. *Industrial Water Pollution Control*, 3rd edition, McGraw-Hill, New York, USA.
[4] Barnes D., Bliss P.J.,1983. *Biological Control of Nitrogen in Wastewater Treatment*, E. & F.N. Spon, London, UK.
[5] Jayant R Row, 2014. *The Bardenpho Wastewater Treatment Process*, http://www.brighthubengineering.com/geotechnical-engineering/78729-the-bardenpho-wastewater-reatment-process/2014;
[6] Intelligen Inc., 2011. SuperPro Designer 8.5: Examples, Scotch Plains, New Jersey, USA.
[7] H.G. 188/20.03.2002 pentru aprobarea unor norme privind condiţiile de descărcare în mediul acvatic a apelor uzate, modificată şi completată prin H.G. 352/11.05.2005.
[8] Singureanu, C., Woinaroschy, A., Simulation of Bardenpho Wastewater Treatment Process for Nitrogen Removal using SuperPro Designer Simulator, *U.P.B. Sci. Bull., Series B*, 79, (2017) – in press.

LABORATORY RESEARCH ON INTENSIFIED BIOLOGICAL TREATMENT BY ACTIVATED SLUDGE OF WASTEWATERS WITH HIGH CONTENT OF ORGANIC POLLUTANTS

Carmen TOCIU*, Irina Elena CIOBOTARU, Ecaterina MARCU, Bianca PETCULESCU

National Institute for Research and Development Institute in Environmental Protection, 294 Independentei Spl., 060031 Bucharest

Abstract
The necessity to optimize the biological treatment using activated sludge arises from the existence of deficient biological treatment processes within the wastewater treatment plants.
This paper proposes a methodology for the study of the process at a laboratory scale in order to establish the operating conditions so that the increase of the achievable treatment potential in a given capacity is accomplished.
Biological treatment using activated sludge at high load (intensified biological treatment) may be applied successfully for improving the treatment efficiency of wastewaters with high organic load and for obtaining of effluents with quality parameters that comply with the requirements regarding the protection of ecological systems.

Key words: intensified biological treatment, kinetic parameters, laboratory research methodology, wastewaters

1. Introduction

Conventionally, wastewaters with organic substances concentrations expressed as chemical oxygen demand (COD) higher than 1000 mg/L are designated wastewaters with high organic load (wastewaters with high content of pollutants or concentrated wastewaters).

Wastewaters with organic load may be treated biologically only when the organic pollutants are biodegradable and the contained inorganic species do not affect negatively the degradation process, thus the wastewater are biologically treatable [1].

[I1]In the recent years, the global environmental standards have become more stringent and the necessity to adapt the facilities used for influent treatment has arisen; however, the economic pressures regarding the energy efficiency and a minimum land use have to be taken into account. Under these circumstances, the intensification of wastewater treatment process may contribute to solving such issues.

One of the processes employed successfully for the treatment of concentrated wastewaters is the biological treatment using activated sludge at high load (intensified biological treatment). The biological treatment using activated

sludge involves the permanent contact between the wastewater and a mixed culture of microorganisms (activated sludge), followed by the separation of the phases in a gravitational decanter, where the activated sludge is either recirculated in the treatment facility or it is removed for further treatment and the treated water is discharged in the sewer or in the natural receptor. The aerobic biological treatment using activated sludge requires a permanent minimum concentration of dissolved oxygen of 1-2 mg/L [2].

The increase of the organic load of the microbial population leads to an increase of the concentration of activated sludge in the treatment system up to maximum values of 10000 mg/L. For this reason, the intensified aerobic biological treatment using activated sludge is defined as the treatment conducted in cases where high concentration of activated sludge (2500-10000 mg/L) is present in the reaction system and organic loads over 0.4 kg BOD/(kg·day) are applied [3].

The treatment processes using activated sludge are controlled usually by means of two key factors, namely the substrate concentration (provided by the the impurities from the wastewater) and the biomass (activated sludge) concentration from the tank. Organic substances from wastewater are removed through metabolism. The ability of the microorganisms to consume a variety of organic substances is their main characteristics and is provided by their extraordinary adaptation capacity. Also, a typical characteristic of the microorganisms is their preferential metabolism for specific substrates together with specific metabolic pathways [4,5].

The interdependence of these two factors (substrate-activated sludge) influences the kinetics of the biological treatment processes using activated sludge. The parameters employed so far to control and design the biological treatment using activated sludge derive from the kinetics of the bio-oxidation processes. The above-mentioned parameters are: the volumetric organic load of the aeration tank ($I_{OV,}$ kg BOD/(day·m^3)), the aeration time (t_a) and the age of the sludge (V_N) named also retention time (TRN) [6].

In fact, all the biochemical reactions are enzymatic reactions and thus the theory according to which the growth rate of the microorganisms *(μ)* varies with the substrate concentration (*S)* up to a limit concentration is accepted, as to the relationship established by Michaelis and Menten [7,8]:

$$\mu = \mu_m \frac{S}{K_S + S} \tag{1}$$

where:

μ_m - the maximum specific growth rate of the activated sludge, day^{-1}.

K_S - the substrate concentration for which the maximum specific growth rate of the activated sludge is halved, mg/L.

Also, a ratio between the weight of the formed microorganisms and the weight of the removed substrate exists and is given by the growth factor of the activated sludge *(Y)*. Usually, transformations of the substrate and biomass take place that in the treatment tank with recirculation (Figure 1) and may be described using the following mathematical relationships obtained from the material balance [7,8]:

$$\frac{1}{\mu} = \frac{1}{S} \cdot \frac{K_S}{\mu_m} + \frac{1}{\mu_m} \qquad \text{for the biomass} \tag{2}$$

$$\frac{\Delta X}{X \Delta t} = Y \cdot \frac{\Delta S}{X \Delta t} - K_D \qquad \text{for the substrate} \tag{3}$$

where:

V - the volume of the aeration tank, m^3
X - the concentration of the biomass in the aeration tank, g/L
Q - the flow rate of wastewater inlet, m^3/day
Q_R - the volume of the recirculated sludge m^3/day
Q_W - the volume of the discharged thickened sludge, m^3/day
X_E - the concentration of the activated sludge in the effluent, g/L
X_R - the concentration of the activated sludge in the recirculating flux, g/L
S_0 - the sludge concentration in the influent of the treatment tank, mg/L
S - the substrate concentration in the treatment tank mg/L
Y - the growth factor of the activated sludge, g/g.

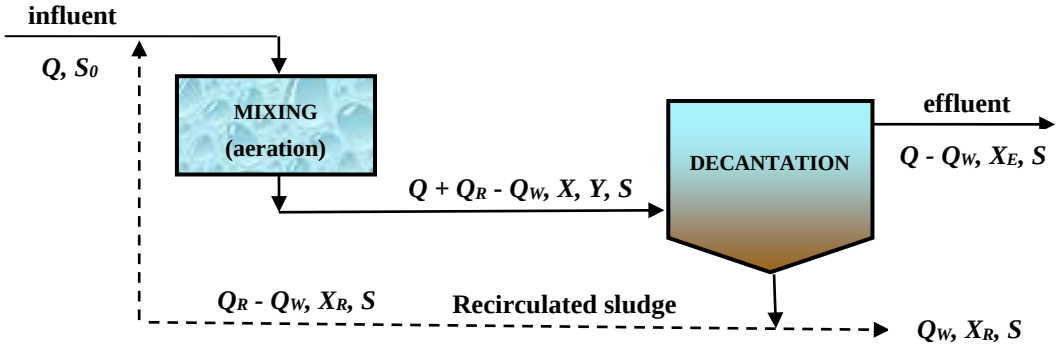

Fig. 1. The diagram of the contact biological treatment system using activated sludge

The values of the kinetic coefficients μ_m, K_S, K_D and Y from equations (2) and (3) are basic elements of the technological design of the intensified aerobic biological treatment using activated sludge, as they are turned into account in the

computation of the aeration tank and in the quality of the treated effluent according to the following equations [7,8]:

$$V = \frac{Y \cdot \gamma_S \, Q_S \, (S_0 - S)}{1 + K_D \, \gamma_S} \, / \, X \tag{4}$$

$$S = \frac{K_S \, (1 + \gamma_S \, K_D)}{\gamma_S \, (\gamma_m - K_D) - 1} \tag{5}$$

where γ_S is the specific growth rate of the activated sludge, equal to the quantity of microorganisms discharged daily from the treatment tank.

Each type of wastewater shows specific values of the kinetic coefficients; thus these coefficients must be computed from experimental data acquired from laboratory studies conducted for each particular case.

The intensified metabolism from the aerobic processes at high loads leads to an increased production of surplus sludge, and thus its assessment is required in order to adequately size the facilities where the sludge is treated prior to landfilling [9].

The objective of this study is to highlight a laboratory research methodology for the aerobic biological treatment of wastewaters with high content of organic pollutants in order to determine some computation elements of the optimal parameters of the technological design of the biological treatment installation using activated sludge at high load.

Through the qualitative and quantitative diversity of their composition, wastewaters show different behaviour in the biological treatment processes. Thus, the first condition for biological treatment to take place is that the organic impurities from the wastewater are biodegradable and the wastewater is biologically treatable. A BOD/COD ratio higher than 0.4 is important information and is related to a good biological treatability; however, it must be confirmed by means of the Zahn Wellens respirometry test [10].

The laboratory study on the aerobic biological wastewater treatment at high load should comprise three work phases, namely:

1. The characterisation of the wastewater as regards the degree of contamination and the biological treatability. This is achieved by determining the following wastewater characteristics: pH, suspended matter, chemical oxygen demand (COD), biochemical oxygen demand (BOD_5), total nitrogen, total phosphorus, toxic substances to aerobic microorganisms (heavy metals, pesticides etc.).

2. Experimental research conducted in laboratory installations with batch operation in order to establish the applicability of the process and the optimal operating conditions.

3. Experimental research conducted in continuous flow stirred-tank laboratory installations (small scale models of the industrial installations employed for aerobic treatment using activated sludge) in order to achieve the data required for the technological design of the process.

The estimation of the kinetic coefficients is accomplished by the mathematical processing of the experimental results where the two key factors vary, namely the substrate and the biomass.

2. Experimental

Wastewaters resulting from the manufacturing of polyester fibres were used for the study of the aerobic treatment at high load. The physicochemical characteristics of these wastewaters were attained using standardised analysis methods [11-13].

The laboratory installation with batch operation

The laboratory installation with batch operation comprised a series of reaction vessels (glass containers) each with a capacity of 1 L provided with a stirring or aeration system that would ensure the homogenisation of the reaction mixture and the aerobic conditions (minimum 2 mg/L of dissolved oxygen).

A known volume of wastewater and different quantities of activated sludge were added to the reaction vessels so that the ratio between the feed and the microorganisms (the organic load of the activated sludge) is below 1 g/g.

The experiments were conducted for 5 days at room temperature and the following were investigated:

- the treatment efficiencies expresses as COD and BOD;
- the sedimentation properties of the activated sludge expressed by means of the volume index (IVN);
- the growth rate of the activated sludge related to BOD.

Continuous flow stirred-tank laboratory installations

The continuous flow stirred-tank laboratory installation consisted mainly of the activated sludge tank and the secondary (gravitational) decanter. Additionally, tanks for feed water and treated effluent were employed as well as supplementary devices that ensured the continuous feed, aeration and homogenisation of the system and the recirculation and the discharge of surplus sludge (Figure 2).

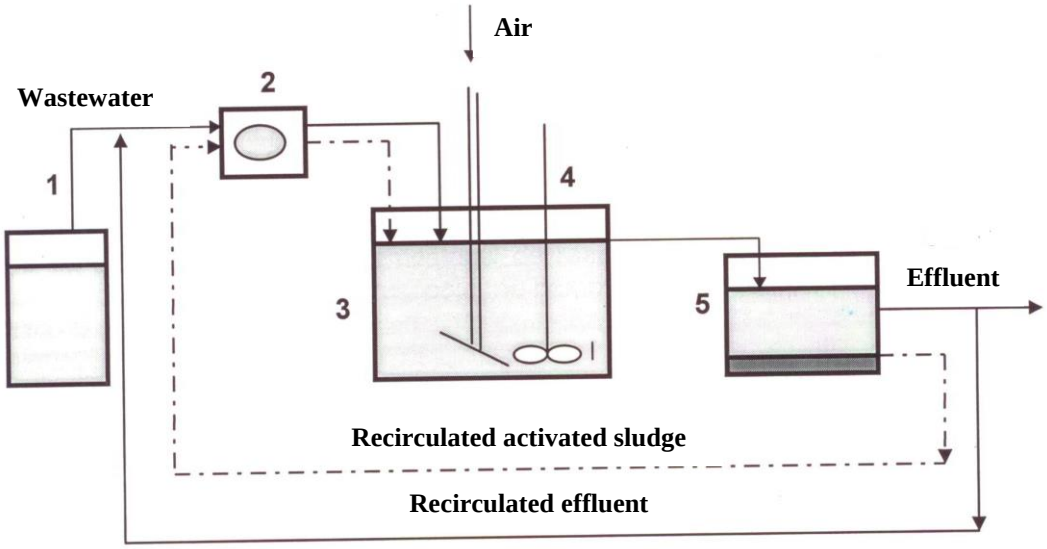

Legend: 1. Wastewater storage tank; 2. Peristaltic pump; 3. Storage tank with activated sludge; 4. Mechanical stirrer with blades; 5. Secondary decanter

Fig. 2. The continuous flow stirred-tank laboratory installation employed for intensified biological treatment using activated sludge

The laboratory installation was exploited for 40 days and the following parameters were considered:

- continuous feed with wastewater at a constant flow rate;
- a minimum concentration of 2 g/L activated sludge ensured by adjusting the flow rate of the recirculated sludge in the gravitational decanter and the discharge rate of the surplus sludge;
- continuous stirring and adequate oxygenation ensured by adjusting the air flow rate.

The main variable that may affect the treatment efficiency is the organic load of the activated sludge. During the experiments, the adjustment of the pollutant flow rate was performed in order to maintain a permanent equilibrium of the treatment system.

The operating parameters of the continuous flow stirred-tank laboratory installation were: feed flow rate 5 L/day wastewater, useful volume of the aeration tank 10 L and the recirculation degree for the sludge ranged within 30-90%.

The treatment process was monitored by periodic analysis of the composition of influents and effluents (COD, BOD, total nitrogen, total phosphorus and suspended matter) and of the reaction mixture (the sludge volume index, the concentration and the microscopic appearance of the sludge and the concentration of dissolved oxygen).

3. Results and discussions

The quality parameters describing the wastewater resulting from the manufacture of polyester fibres subjected to intensified biological treatment are depicted in Table 1.

Table 1

The characteristics of feed wastewater

Quality parameter	Unit	Limit values *(minimum - maximum)*	Average values
pH		7.5	7.5
Total suspended solids	mg/L	Absent	-
Chemical oxygen demand (COD)	mg O_2/L	1600 – 28900	20000
Biochemical oxygen demand (BOD_5)	mg O_2/L	750 – 13139	9000
Total nitrogen	mg/L	28 – 84	50
Total phosphorus	mg/L	7 - 10	9
Toxic substances	mg/L	absent	-
BOD_5 / COD-Cr ratio	-	0.45	0.45

Following the computation of the Symons criterion that establishes whether the wastewater is biologically treatable or not, the experimental design was performed based on the two work phases.

The experimental results obtained after the exploitation of the installation with batch operation are summarised in Table 2. Looking at the data regarding the treatment efficiencies, one may state that the aerobic biological treatment at high load may be employed for this type of wastewaters. The highlighted values are the optimal values that constitute the basis for the calculus of the average optimal values used in the installation with batch operation.

Table 2

Experimental results obtained for the installation with batch operation

No.	COD (mg O_2/L)		BOD_5 (mg O_2/L)		Concentration of activ. sludge	Organic load of activ. Sludge (g/g day)	
	Influent	Effluent	Influent	Effluent	(mg v.s./L)	COD	BOD_5
1.	3590	441	2424	50	4000	**0.9**	**0.6**
2.	7181	3206	4853	950	4000	**1.8**	**1.2**
3.	14907	9478	10075	5360	4000	5.7	2.5
4.	21758	14990	14706	9300	4000	5.4	3.7
5.	29083	19878	19675	13233	4000	7.2	4.9
6.	14700	5702	9936	2750	7200	**2.0**	**1.4**
7.	14700	7603	9936	-	5000	3.0	1.9
8.	14700	8830	9936	4680	3600	4.0	2.8
9.	14700	9068	9936	5000	1800	8.0	5.5

Optimal average values (OAV)	***1.6***	***1.1***

Treatment efficiencies:

No.	Treatment efficiency (%)		Removed substrate (g/g day)	
	COD	BOD_5	COD	BOD_5
1.	**97.7**	**97.7**	0.8	0.6
2.	**55.0**	**80.4**	1.0	0.9
3.	38.4	46.9	1.4	1.2
4.	31.1	36.7	1.6	1.3
5.	31.6	32.6	2.3	1.7
6.	**61.0**	**72.3**	1.2	1.0
7.	48.0	-	1.4	-
8.	40.0	52.8	1.6	1.5
9.	38.0	49.6	5.1	2.7
OAV	***71.2***	***83.5***		

The experimental results obtained after the exploitation of the continuous flow stirred-tank laboratory installation are summarised in Table 3. Starting from the available data, the kinetic coefficients of the treatment process were computed employing mathematical methods.

Table 3

Experimental data obtained for the continuous flow stirred-tank laboratory installation

No.	COD (mg O_2/L)		BOD_5 (mg O_2/L)		Concentration of activ. sludge (mg v.s./L)	Organic load of activ. sludge (g/g day)	
	Influent	Effluent	Influent	Effluent		COD	BOD_5
1.	1615	87	750	15	2270	0.4	0.2
2.	6400	266	3750	198	5480	0.6	0.3
3.	7171	1649	3456	1220	4556	0.8	0.4
4.	8446	3398	5120	2540	2130	2.0	1.2
5.	18500	5280	12000	3900	3990	2.3	1.5

Treatment efficiencies:

No.	Treatment efficiency (%)		Removed substrate (g/g day)		IVN (mL/g)
	COD	BOD_5	COD	BOD_5	
1.	94.6	98.0	0.3	0.2	71
2.	95.8	94.7	0.5	0.3	101
3.	77.0	64.6	0.6	0.3	123
4.	60.0	51.1	1.2	0.6	144
5.	71.4	66.7	1.6	1,0	156

The determination of the kinetic coefficients μ_m and K_S

The determination of the kinetic coefficients μ_m (the maximum specific growth rate of the activated sludge) and K_S (the substrate concentration for which the maximum specific growth rate of the activated sludge is halved) is accomplished using equation (2). For this purpose, experiments were conducted after which the interdependence between the removal rate and the concentration of the substrate in the treated effluent is acquired.

As one may notice, the relationship expresses a linear dependence between 1/μ and 1/S and the parameters characterising the straight line are $1/\mu_m$ and K_S/μ_m. These parameters were obtained by using the method of least squares. Table 4 shows the data required to apply this mathematical method presented as average values of multiple daily determinations (7 replicates).

Table 4

Elements required for the calculus of the kinetic parameters μ_m and K_S using the method of least squares

Measures	Unit	Experimental version				
		I	II	III	IV	Σ
S_0	g/L	1.600	6.400	7.000	8.000	
S	g/L	0.087	0.266	1.650	3.390	
X	g	2.300	5.500	4.550	2.200	
μ	day^{-1}	0.328	0.557	0.588	1.047	
$1/\mu$	day	3.050	1.790	1.770	0.950	8.09
$1/S$	L/g	11.500	3.840	0.610	0.290	16.44
$1/\mu \cdot 1/S$	day L/g	35.070	6.870	1.160	0.270	43.48
$(1/S)^2$	$(L/g)^2$	32.200	14.740	0.370	0.084	147.50

The method of least square provided the following results $K_S/\mu_m = 0.18$ and $1/\mu_m = 1.0$, that correspond to $\mu_m = 1\ day^{-1}$ and $K_S = 180$ mg/L.

The determination of the kinetic coefficients Y and K_D

The determination of kinetic coefficients Y (the growth factor of the activated sludge) and K_D (the coefficient of endogenous respiration) is accomplished using equation (3) which is the equation of a straight line described by the parameters Y and K_D. For this purpose, experiments were conducted after which the correlation between the quantities of activated sludge generated after the removal of organic pollutants is acquired. The results are shown in Table 5.

Table 5

Elements required for the calculus of the kinetic parameters Y and K_D using the method of least squares

Measures	Unit	Experimental version					
		I	II	III	IV	V	Σ
ΔS	g	7.560	30.670	26.750	23.050	73.700	
ΔX	g	2.420	12.260	12.300	11.950	46.400	
X	g	45.000	55.000	45.000	42.000	40.000	
$\Delta S/X$	-	0.170	0.560	0.590	0.550	1.840	3.71
$\Delta X/X$	-	0.056	0.220	0.270	0.280	1.160	1.98
$\Delta S/X \cdot \Delta X/X$	-	0.009	0.120	0.160	0.150	2.130	2.56
$(\Delta S/X)^2$	-	0.029	0.310	0.350	0.300	3.380	4.36

The method of least square provided the following results Y = 0.68 g sludge/g removed COD and K_D = 0.11 g/g day.

4. Conclusions

The use of intensified biological treatment using activated sludge is required for wastewater treatment plants that do not provide effluents that comply the regulations regarding the quality parameters (environmental authorisations and agreements etc.).

This methodology for the laboratory research regarding the intensified biological treatment of wastewater with high content of organic pollutants allows the determination of the main kinetic parameters of the process and is the basis of establishing the technological parameters for the exploitation of the treatment facility considering the nature of the wastewater.

The experimental program employed for the determination of the kinetic parameters of the biological treatment using activated sludge at high load takes into account the following objectives:

- establishing the applicability of the treatment for the wastewaters (indirect assessment of the biological treatability of the wastewaters using the specific Zahn-Wellens test based on the monitoring of the degradation process of the organic pollutants);
- establishing the optimal conditions for attaining maximum treatment efficiencies in economically favourable conditions (tests in installations with batch operation and continuous flow stirred-tank laboratory installations);
- achievement of data required for the technological design of treatment installation used at industrial scale.

REFERENCES

[1] Degrémont, 2007, *Water Treatment Handbook*, 5th edition, **1**, Lavoisier, Paris.
[2] Robescu Diana, Stroe F., Presura A., Robescu D., 2011, *Wastewater treatment techniques*, Technical Publishing House, Bucharest.
[3] Tchobanoglous G., Burton F. L., Stensel H. D., 2003, *Wastewater Engineering. Treatment and Reuse*, 4th edition., Mc. Graw Hill, New York.
[4] Martin A., 1999, *Biodegradation and Bioremediation*, Academic Press, London.
[5] Maria C., Tociu C., Maria G., Improvement of Aquatic Pollutant Partition Coefficient Correlations Using 1D Molecular Descriptors – Chlorobenzene Case Study, *Chemical Papers*, **67**, (2013), 173-185.
[6] Judd S., Stephenson T., 2002, *Process Science and Engineering of Water and Wasterwater Treatment*, IWA Publishing, London.
[7] Benefield L. D., Randall W., 1980, *Biological Process Design for Wastewater Treatment*, Prentice Hall, Englewood Cliffs, New Jersey.
[8] Vaicum L., 1981, Wastewater treatment with active sludge. Biochemical bases., Academy Publishing House, Bucharest.
[9] Robescu D., Lanyi S., Robescu Diana, Constantinescu I., 2000, *Technologies, Facilities and Equipment for Water Treatment*, Technical Publishing House, Bucharest.
[10] Bailey J. E., Ollis D. F., 1986, *Biochemical Engineering Fundamentals*, 2nd edition, McGraw-Hill Education, London.
[11] SR ISO 6060:1996, Water quality standard. Determination of chemical oxygen demand., Romanian Association for Standardization (ASRO), Bucharest.
[12] SR EN 1899:2003, Water quality standard. Determination of biochemical oxygen demand., Romanian Association for Standardization (ASRO), Bucharest.
[13] Marinescu F., Tociu C., Ilie M., Anghel A.M., The influence of toxic pollutants on the absolute value and on the kinetics of the degradation of organic substances quantified as BOD, *Biointerface research in applied chemistry*, **7**(1), (2017), 1955-1958.

APPLICATIONS OF SOME INORGANIC COMPOUNDS RECOVERED FROM METALLURGICAL WASTES IN THE TREATMENT OF OIL REFINERY WASTEWATERS

Carmen TOCIU[1], Cristina MARIA, Ecaterina MARCU,
Irina-Elena CIOBOTARU,

Research and Development Institute for Environmental Protection, 294 Independentei Spl., 060031 Bucharest

Abstract
The subject of this paper is related to the reduction of impact of some polluting substances on water resources by means of removing them from wastewaters received and to the support of the development of recovery technology for some wastes with few applications.
Aluminium sulphate recovered from secondary aluminium slags is employed within this case study for the chemical treatment of wastewater resulting from oil refinery activities. As proven by the experimental results, an insignificant difference exists between the behaviour of the recovered aluminium sulphate compared to a classical coagulation agent (commercially available aluminium sulphate) considered as benchmark, based on the treatment efficiencies for the main water quality indicators, on the volume and characteristics of the resulting sludge and on the dynamics of the gravitational separation of insoluble impurities.
Although the production of aluminium-based coagulants is based on using the hydrated alumina obtained from bauxite, lately a worldwide tendency of using inferior raw materials is noted, as the aluminium requirements have increased and its recycling has gained a paramount economic, environmental and social importance.

Key words: aluminium sulphate, metallurgical slag, wastewater treatment

1. Introduction

The European strategy and politics regarding water management start from the premise that water is a legacy for future generations and the protection of water resources, quality improvement and sustainable development are actions of general interest.

The main pressure applied on surface water status is exerted by human population through the discharge of untreated or insufficiently treated wastewater. The technical issue that needs to be taken into consideration regarding the protection of water quality is the restriction of discharged residues to values that

[1] Corresponding author: Email address: tociucarmen@yahoo.com, Phone: +4021.304.26.75, Fax: +021.318.20.01.

do not exceed the capacity of self-purification so that the natural resource maintains the quality required for aquatic fauna and land use development [1].

On the other hand, the aluminium industry is under a continuous development and significant amounts of slags are generated annually that tend to hinder the activity of economic operators. The landfill of metallurgical wastes is a globally issue as the leakage of metallic ions may cause severe pollution of underground water and soil contamination due to their toxicity and bioaccumulation potential [2, 3].

Having clearly stated the objectives regarding the protection of environmental factors, a technology for the aluminium recovery as aluminium sulphate was developed and patented in Romania, based on a chemical and hydrometallurgical method for processing the secondary aluminium slag [4, 5].

Generally, aluminium sulphate is obtained from natural raw material and has important uses in wastewater treatment [6,7]. Previous studies have proven that aluminium sulphate recovered from secondary aluminium slags is a valuable coagulation agent and may be used successfully for the removal of pollutants from wastewater [8,9].

Wastewater resulting from oil refinery activities is one of the most important source of pollution for water bodies due to its highly harmful characteristics. Water resulting from the technological processes is contaminated with a wide variety of pollutants: oil, various oil products (kerosene, diesel, benzine, oil etc), suspended substances, phenols, naphtenate, sulfonate, mercaptans, acids, detergents, chlorides and other organic and inorganic substances. The concentrations of such pollutants are variable and exceed the allowable limits required for their discharge in the water body. The contaminants are present as floating particles, emulsions, dissolved substances or adsorbed on suspended matter.

Practice on oil refineries exploitation shows that wastewater treatment is achieved mainly through [10, 11]:

- local pretreatment using lye and other harmful substances and the reuse of treated wastewater or the discharge of wastewater resulting from specific processes to a central sewerage and the treatment of mixed wastewaters;
- mechanical, physicochemical and biological treatment of wastewaters contaminated with oil products.

This paper proposes the use of aluminium sulphate recovered from matallurgical slags in the treatment of wastewater resulting from an oil refinery facility provided with final treatment plant whose effluent is insufficiently treated as regards the organic substances expressed as COD, suspended substances and extractible substances. The effluent resulting from the mechanical treatment is subsequently treated with aluminium sulphate in order to improve the global performances of the treatment plant and to obtain an effluent that meets the

quality requirements provided by the law before the discharge in a natural receptor.

2. Experimental

The experiments were conducted using 5 products (P1-P5) based on aluminium sulphate recovered from metallurgical slags by means of a Romanian technology, in which the raw materials are derived from waste landfills of some low and medium capacity smelters [4, 5].

The experiments involving the treatment of wastewater using recovered aluminium sulphate were conducted in comparison with a referential coagulation agent (considered as benchmark and noted with M), respectively the commercially available aluminium sulphate Kemira ALG provided by Kemwater Cristal (EN 878:2004).

The pH was adjusted with NaOH in order to achieve an adequate treatment as regards to the optimum precipitation of the Al^{3+} ion as aluminium hydroxide [12].

In order to facilitate the sedimentation of the generated sludge, a flocculation agent was used, namely a specific anionic polyelectrolyte Floerger FR 1023.

The prepared solutions had the usual concentrations used at industrial scale.

The experiments were conducted on a laboratory setup consisting of 6 mixing units using Jar-test [13]. The operating conditions took in consideration the rapid dispersion of the coagulant within the sample (n = 160 rpm) for 2 minutes, followed by the adjustment of pH to the optimum value (pH = 7) and the slow mixing of the flocculation agent (n = 40 rpm) for a time period longer than 20 minutes, so that the flocs were allowed to aggregate. The retention time of the sludge sedimentation phase was 120 minutes.

Water quality indicators and sludge characteristics were determined according to standardised analysis methods [14-18].

3. Results and discussions

The experiments involved the simulation of coagulation and flocculation processes at a laboratory scale and comprised two phases, as follows:

- Establishing of the optimum dose of coagulant;
- Investigation of the efficiency of the application of such products as coagulation agents in the treatment of wastewater resulting from oil refinery processes.

Table 1 shows the quality of wastewater used in the coagulation-flocculation treatment experiments.

Table 1

Quality parameters for wastewater subjected to chemical treatment

Quality parameter	Determined value
Colour	grey
pH (pH units)	7.5
COD (mg/L)	927
Suspended solids (SS, mg/L)	510
Extractable substances (ES, mg/L)	82

The establishing of the optimum dose of coagulation agent

Experiments of wastewater treatment were conducted and increasing doses of commercially available coagulant were tested ranging from 300 to 1500 mg/L of wastewater. Using the statistical data correlation technique, the correlation between the variables of the treatment process was obtained and is shown in Figure 1. The proposed mathematical model describes the behaviour of the physicochemical system with a high level of confidence (95%). The regression function that fits most adequately the data set is power type and is described by the equation $y = a - bc^x$, where y is the concentration of suspended solids resulted after the treatment of wastewater (expressed as mg/L) and x is the applied dose of commercially available aluminium sulphate, expresses as mg Al^{3+}/L wastewater.

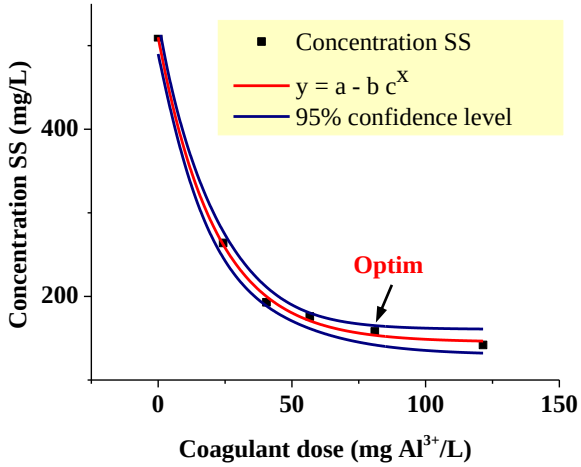

Parameter	Value	Standard deviation
a	145.3764	0.8231
b	-364.6659	7.6647
c	0.9542	0.0024

Fig. 1. The correlation between the concentration of suspended solids and applied coagulant dose for chemical treatment of wastewater

The analysis of the experimental results allowed the identification of an optimum dose of coagulant of 1000 mg/L wastewater. The efficiency of the treatment process was 57.2% for COD, 69.0% for suspended matter and 80.4%

extractable substances. The volume of sediment decanted after 2 hours was 110 mL/L (1.4% dry matter and 68.1% volatile substances).

Chemical treatment of wastewater

The experimental results and the investigation conducted on the treatment of wastewater resulting from oil refinery activities using aluminium sulphate recovered from metallurgical slags and commercially available aluminium sulphate may be summarized as follows:

- coagulant dose applied: 1000 mg product/L wastewater
  P1-P5 = 59.3-73.8 mg Al^{3+}/L wastewater;
  M = 81.0 mg Al^{3+}/L wastewater);
- flocculant dose applied: 5 mg/L wastewater;
- removal efficiency:
  COD: minimum 53.6% (P8), maximum 62.8% (P11), 59.7% (M);
  SS: minimum 72.5% (P12), maximum 81.2% (P9), 73.5% (M);
  ES: minimum 79.2% (P8), maximum 89.0% (P9), 85.3% (M);
- chemical sludge*:*
  P1-P5 = 110-145 mL/L wastewater (0.9-1.5% dry matter and 68.2-70.5% volatile substances);
  M = 115mL/L wastewater (1.3% dry matter and 69.3% volatile substances);
- observation on the treatment process: medium and large flocs, supernatant without staining, chemically stable sludge.

The products P1-P5 and the benchmark had high efficiency for the removal of specific pollutants and in some cases (as is the case of suspended matter), the results are better compared to the benchmark. The results were analysed and interpreted using simple statistical indicators for data variation (Figure 2). The maximum deviation of the treatment efficiencies corresponding to the tested products compared to the commercially available coagulant were 6.1%, 7.7% and 6.1% for COD, suspended solids and respectively, extractible substances. These results prove that the aluminium sulphate recovered from metallurgical slags is of good quality in respect to commercially available aluminium sulphate with low differences between the medium efficiencies compared to commercially available aluminium sulphate, namely 0.2%, 3.0% and 1.2% for COD, suspended solids and extractible substances.

Figure 3 shows the evolution of the sedimentation of the chemical sludge generated and as one may see from the curve shape, the mass sedimentation took place very rapidly. The sludge volumes represented maximum 15% of the wastewater volumes subjected to treatment and the product P1 led to the smallest volume of decanted sediment after 2 hours. The experimental results show good

sedimentation rates for all tested products and characteristics of the resulting sludge similar to the characteristics of the benchmark.

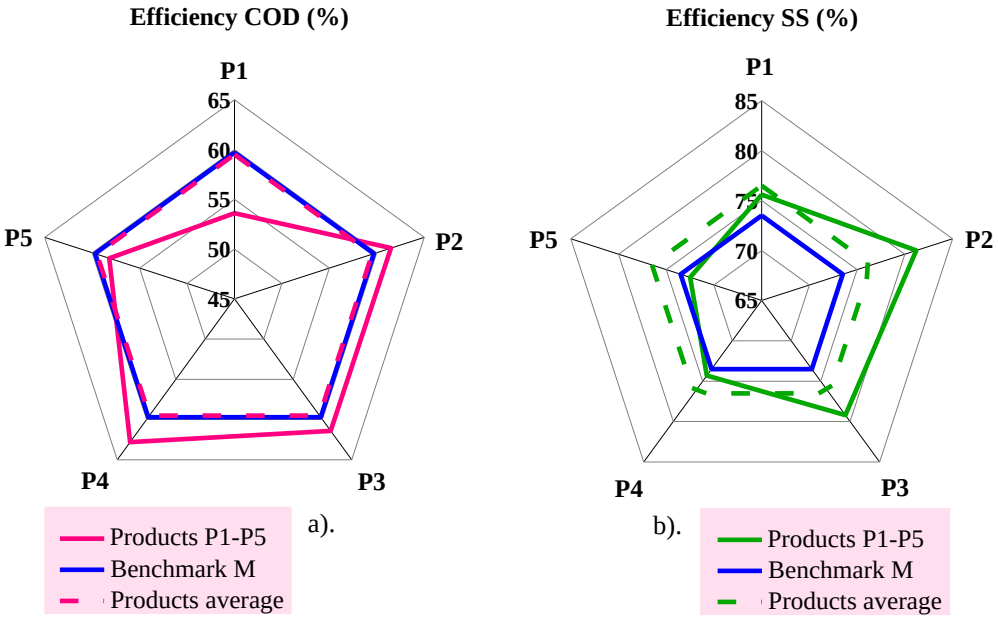

Fig. 2. The effect of using the coagulation agent in oil refinery wastewater:
a) reduction of organic substances (COD); b) reduction of suspended solids (SS)

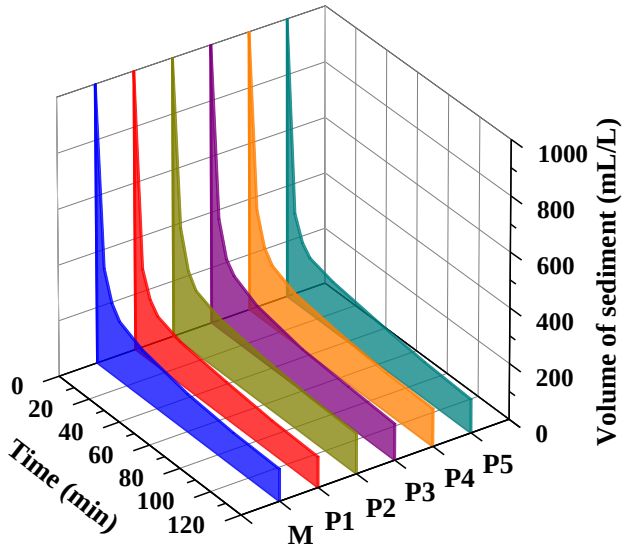

Fig. 3. The dynamics of the gravitational sedimentation of chemical sludge resulting from the treatment of oil refinery wastewater

The evaluation of the overall efficiency of the tested products used for the treatment of wastewater resulting from the oil refinery activities and the process of sedimentation of the generated chemical sludge was achieved by drawing the characteristics curves and provide hard evidence that products P1-P5 have coagulation properties equivalent to commercially available aluminium sulphate considered as benchmark.

4. Conclusions

In the context of worldwide issues concerning the production of aluminium related to the significant volumes of slags of variable chemical and mineralogical composition generated, a simple and efficient technology was developed in Romania for metal recovery as sulphate aluminium by means of a chemical-hydrometallurgical processing of secondary aluminium slags. As we know, aluminium sulphate has various applications in the treatment of wastewater and primary and secondary sludge.

In order to achieve maximum efficiency for pollutants removal, the treatment process has to be conducted in certain conditions, specific to each wastewater type. Thus, the pH where the precipitation occurs and the optimum dose of coagulation/flocculation agent were determined by means of Jar test, as this is the most employed technique for establishing the operating conditions for chemical treatment of wastewater.

The experiments conducted on wastewater resulting from oil refinery activities highlighted good coagulant properties of the products based on aluminium sulphate recovered from metallurgical slags, as these products have successfully contributed to the aggregation of suspended and colloidal matter and to the adsorption and/or absorption of dissolved substances and dyes.

The study of the performances reached by the chemical treatment of wastewater resulting from oil refinery activities using aluminium sulphate recovered from secondary aluminium slags offers a support for promoting this product as a viable alternative for the conventional chemical coagulation agents used nowadays in wastewater treatment.

REFERENCES

[1] Directive 60/2000/EC, 2000, Water Framework Directive establishing a framework for Community action in the field of water policy, European Parliament and Council, *Official Journal of the European Union*, **L 327**, Brussels.

[2] Haupin W., 2001, Aluminium production and refining, *Encyclopedia of Materials: Science and Technology*, 1st edition, Elsevier Science, Amsterdam.

[3] Maria C., Tociu C., Maria G., Improvement of aquatic pollutant partition coefficient correlationsusing 1D molecular descriptors – chlorobenzene case study, *Chemical Papers*, **67**(2), (2013), 173–185.
[4] Teodorescu R., Roman M., Tociu C., Gheorghe M., Crișan A., The technology for aluminum recovery from various Al slag for environment depolution, *Metalurgia International*, **14(**2), (2009), 131-134.
[5] Teodorescu R., Bădiliță V., Roman M., Purcaru V, Capotă P., Tociu C., Gheorghe M., Crișan A., Optimization of process for total recovery of aluminum from smelting slag: Removal of aluminum sulfate, *Environmental Engineering and Management Journal*, **13**(1), (2013), 7–14.
[6] Mackenzie L. D., 2010, *Water and Wastewater Engineering*, 1st edition, Mc. Graw Hill, New York.
[7] Frank W. B., Haupin W. E., Vogt H., Bruno M., Thonstad J., Dawless R. K., Kvande H., Taiwo, O. A., 2009, Aluminum, *Ullmann's Encyclopedia of Industrial Chemistry*, Wiley-VCH, New Jersey.
[8] Tociu C., Diacu E., Maria C., Minimization of chemical risk by using recovered aluminium from metallurgical slag as coagulant in wastewater treatment, *Environmental Engineering and Management Journal*, **13**(2), (2014), 429–434.
[9] Tociu C., Diacu E., Quality assessment of the aluminium sulphate coagulant recovered from metallurgical slag based on a correlation of the removed phosphorous from municipal wastewaters, *U.P.B. Sci. Bull., Series B - Chemie*, **77**(2), (2014), 29-40.
[10] Negulescu M., 1987, *Industrial Wastewater*, **1**, Technical Publishing House, Bucharest.
[11] Judd S., Stephenson T., 2002, *Process Science and Engineering of Water and Wasterwater Treatment*, IWA Publishing, London.
[12] Nistreanu V., Nistreanu Viorica, 1999, *The Arrangement of Water Resources and Environmental Impact*, BREN Publishing House, Bucharest.
[13] Satterfield Z., 2005, Jar testing, Tech Brief, The National Environmental Services Center at West Virginia University, West Virginia.
[14] SR ISO 10523:2012, Water quality standard. Determination of pH., Romanian Association for Standardization (ASRO), Bucharest.
[15] SR ISO 6060:1996, Water quality standard. Determination of chemical oxygen demand., Romanian Association for Standardization (ASRO), Bucharest.
[16] SR EN 872:2005, Water quality standard. Determination of total suspended solids by method of filtering on glass fiber filters., Romanian Association for Standardization (ASRO), Bucharest.
[17] SR 7587:1996, Water quality standard. Determination of substances extractable with solvents. Gravimetric method., Romanian Association for Standardization (ASRO), Bucharest.
[18] Marinescu F., Tociu C., Ilie M., Anghel A.M., The influence of toxic pollutants on the absolute value and on the kinetics of the degradation of organic substances quantified as BOD, *Biointerface research in applied chemistry*, **7**(1) (2017), 1955-1958.

POTENTIAL RISK ASSESSMENT OF HEAVY METALS IN SEDIMENTS FROM SOME BUCHAREST LAKES

Petra IONESCU[1*], Elena DIACU[2], Ecaterina MARCU[1], Violeta - M. RADU[1], Carmen TOCIU[1], Andreea MONCEA[1]

[1]National Institute for Research & Development in Environmental Protection, Spl. Independentei, 294, 6th District, Code 060031, Bucharest, Romania
[2]University "Politehnica" of Bucharest, Polizu 1, 1st District, Code 011061, Bucharest, Romania

Abstract

Evaluation of the potential environmental risk of the presence of heavy metals in surface sediments collected from lakes situated in heavily urbanized areas has been performed. Five heavy metals (Cu, Cr, Cd, Pb and Ni) were determined in sediments of urban lakes called Plumbuita and Circului Lakes, from five sampling sections S1 – S5, to assess the risk of the the presence of mentioned metals. The potential harmful effects of heavy metals were evaluated by Potential Ecological Risk Index method (PERI) based on the applicability of specialized evaluation methods, which could quantify the potential ecological risk levels of heavy metals.

The degree of contamination was evaluated using the contamination factor C_f and the contamination degree C_d indices. The risk assessment was performed using the potential ecological risk factor E^i_r and the potential ecological risk index RI. In determining the interdependencies between studied metals and the nature and sources of pollution, Cluster Analysis was applied.

The ecological risk levels of heavy metals in the sediments from this area were low. The Potential Ecological Risk Indices for heavy metals had low potential ecological risk to the ecological environment in the sediments from Plumbuita and Circului Lakes.

Key words: Heavy metals, Potential Ecological Risk Index (PERI), Sediments, Circului Lake, Plumbuita Lake.

1. Introduction

Being well known that water plays an important role in maintaining ecological balance and that it is the major constituent of living organisms [1-3], identifying contaminants such as heavy metals and studying the effects of their presence in water sources continues to be important public health issues [4]. Heavy

[*]Corresponding author; E-mail adress: mileapetra@yahoo.com

metals are found naturally in the environment as part of the composition of all media and as part of the bio-geochemical cycles in nature and/or surface runoff through soil erosion as well as from human activities [5].

The bio-geochemical role and effects of the metals depends on the form in which they are found in the environment, as well as on their concentration. Depending on the concentration level present in the environment, some metals (Fe, Cu, Zn, Co, Mn, Ca and Mg) are essential for the conduct of biological processes of the body, while others (Hg, Cd and Pb) are particularly toxic even at very low concentrations, causing numerous health problems [6-8].

The analysis of the relationship between the heavy metals and environmental factors is extremely important as it provides information on the impact of heavy metals on the ecosystem [9]. Heavy metals are persistent in the environment and under the influence of various processes, biological and chemical properties can be converted from a chemical compound to another, they can volatilize into the atmosphere, can be processed from the aqueous phase to the solid phase, and finally they can become immobilized into the sediment [10, 11].

Thus, the sediments as a component of aquatic ecosystems act as a reservoir for the accumulation of heavy metals, demonstrating the natural (geogenical) and human impact [12]. Studies in this area concluded that certain heavy metals (Cd, Cu, Pb and Zn) were significantly accumulated in lake sediments collected in congested urban areas, thus presenting a high environmental risk [13]. As a result, the risk assessment of heavy metals in sediment areas is a priority for the assessment of sediment quality variation due to the influence of human activities [14].

The objectives of this research were to investigate the potential ecological risk related to the heavy metal content (cadmium (Cd), chromium (Cr), copper (Cu), nickel (Ni) and lead (Pb)) of urban sediments in Plumbuita and Circului Lakes and to apply Cluster Analysis method for establishing the interdependence relationships between the analysed heavy metals.

2. Experimental

In the Bucharest area of Romania most of the aquatic ecosystem is represented by the Colentina River. The Plumbuita Lake (44 ha) is of anthropic origin and is part of the chain of 15 lakes along Colentina River [15]. Due to potential effects involved by the discharge of the various types of waste from human activities in the area, the health of the lake raises a big concern. Also, along with this, Lake Circus is affected as well by the human activities in the area, particularly by the development of the underground infrastructure [16].

In order to assess the heavy metal environmental risk of urban lake sediments, surface sediment samples from five sections marked from S1 to S5 were

collected in March 2015, of which 3 sections (S1, S2 and S3) established for Plumbuita Lake and another 2 sections (S4 and S5) set for Circului Lake.

Approximately 0.5 g of dried sample of sediment (fraction < 63 μm) were digested with 9 mL of hydrochloric acid (37 %) and 3 mL of nitric acid (65 %). A microwave digestion system (Ethos 1 Milestone) equipped with a temperature and pressure control was used to digest the sediment samples. After bringing all the samples in solution, for determining the heavy metals content (Cd, Cr, Cu, Ni and Pb), a High-Resolution Continuum Source atomic absorption spectrometer - ContrAA 700 was used.

To assess the synergic effect of multiple metals pollution in the sediments, the Potential Ecological Risk Index method PERI proposed by Hakanson in 1980 has been applied [17]. This method is a useful tool in order to control water pollution, as a result of the heavy metals tendency to accumulate in sediments, being issued retroactively in water under certain conditions, endanger therefore the health of the ecosystem.

The contamination factor (C^i_f) and the contamination degree (C_d) were estimated based on the average concentration values of metals following the method of Hakanson. The applied equations are as follows [17]:

$$C_f^i = \frac{C_s^i}{C_r^i} \quad (1)$$

$$C_d = \sum_{i=1}^{5} C_f^i \quad (2)$$

were C^i_f is the pollution coefficient of a single element of *"i"*; C^i_s represents the measured values of heavy metals in surface sediments; C^i_r represents the parameters for calculation. In this study, the C^i_r values were considered to be the limit values of chemical quality standards for sediment (fraction <63 μm) listed in national legislation (Cd=0.8; Cr=100; Cu=40; Ni=35 and Pb=85 mg/kg) [18].

Table 1 presents the terminology that may be used in this risk index approach to get a uniform way of describing the contamination factor and the degree of contamination [12, 17].

The potential ecological risk factor (E^i_r) of a single element and the potential ecological risk index (*RI*) of the multielement can be computed using the following equations [17, 19, 20]:

$$E_r^i = C_f^i \, x \, T_f^i \quad (3)$$

$$RI = \sum_{i=1}^{5} E_r^i \quad (4)$$

were T^i_f is the response coefficient for the toxicity of the single heavy metal.

Table 1

Classes of contamination factor and degree of contamination

Contamination factor (C^i_f)	Description	Degree of contamination (C_d)	Description
$C^i_f < 1$	low	$C_d < 8$	Low degree of contamination
$1 \leq C^i_f < 3$	moderate	$8 \leq C_d < 16$	Moderate degree of contamination
$3 \leq C^i_f < 6$	considerable	$16 \leq C_d < 32$	Considerable degree of contamination
$C^i_f \leq 6$	very high	$C_d \leq 32$	Very high degree of contamination

were T^i_f is the response coefficient for the toxicity of the single heavy metal. The toxic response factors were Cd=30, Cr=2, Cu=Ni=Pb=5, and in table 2 the potential risk standards for heavy metals are shown [17].

Table 2

Relationship among E^i_r, *RI* and pollution levels

Potential ecological risk factor (E^i_r)	Ecological risk level of single-factor pollution	Potential ecological risk index (RI)	General level of potential ecological risk for the lake
$E^i_r < 40$	low	RI < 150	low
$40 \leq E^i_r < 80$	moderate	$150 \leq RI < 300$	moderate
$80 \leq E^i_r < 160$	considerable	$300 \leq RI < 600$	considerable
$160 \leq E^i_r < 320$	high	RI ≤320	very high
$E^i_r \leq 320$	very high		

3. Results and Discussions

The contamination factor and the contamination degree are two indicators used for the assessment of the sediment in aquatic ecosystems. The contamination factor reveals the metal load of the sediment with a single heavy metal, while for the overall evaluation, the sum of contamination factors for the studied heavy metals is calculated [17]. Table 3 shows the obtained values of the heavy metal contamination factors analysed (Cd, Cr, Cu, Pb and Ni) in the sediments collected from Plumbuita and Circului Lakes.

Table 3

Contaminations factors (C_f^i) values in Plumbuita and Circului Lakes

Sampling sections		C_f^i				
		Cd	Cr	Cu	Ni	Pb
Plumbuita Lake	S1	0.17	0.43	1.63	0.61	3.86
	S2	1.12	0.46	2.28	0.44	1.77
	S3	0.50	0.59	1.12	0.60	0.62
Circului Lake	S4	0.85	0.39	2.49	0.35	1.40
	S5	0.67	0.32	2.44	0.42	1.60
Reference lake (unpolutted)		1.0	1.0	1.0	1.0	1.0

In accordance with the classification made by Hakanson for this index (Table 1), the contamination level was determined for each metal.

For the sediments collected from the Plumbuita Lake sections S1, S2 and S3, there has been a moderate contamination with Cd (C_f = 1.12) in S2 and with Cu for all three locations, the maximum value recorded for Cu being in S2 (C_f = 2.28). For Pb, the value recorded in S1 (C_f = 3.86) revealed a considerable contamination.

For sediments collected from Circului Lake, a moderate contamination with Cu and Pb for both sampling sections was observed.

The degrees of sediment contamination (C_d) for the studied heavy metals in the sampling sections of the lakes were 6.71 (S1), 6.07 (S2), 3.42 (S3), 5.48 (S4) and 5.46 (S5) respectively, indicating a low degree of contamination with these heavy metals (Fig. 1).

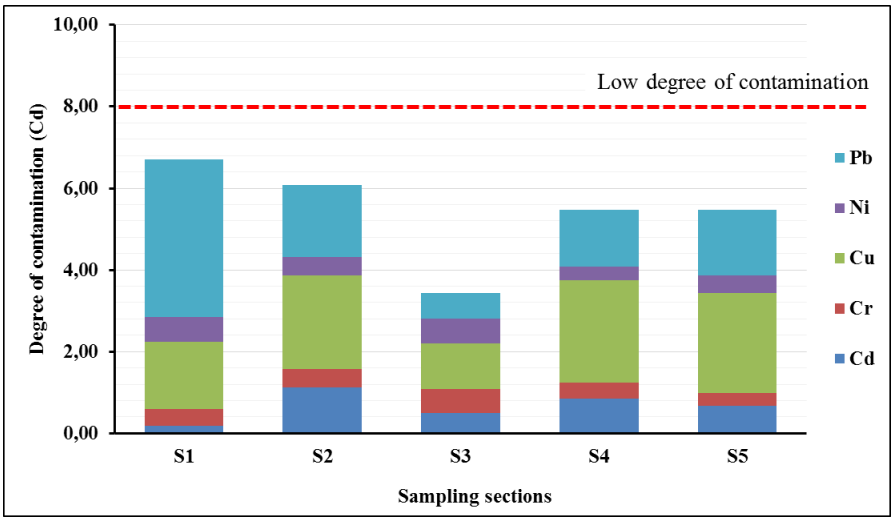

Fig. 1. Degrees of sediment contamination of selected metals in sediments from Plumbuita and Circului Lakes

Table 4 presents the values for ecological risk factor (E_r^i) and potential risk index (*RI*) in sediments collected from two studied lakes.

The order of potential ecological risk factor (E_r^i) of heavy metals in sediments was: S1-Pb > Cu > Cd > Ni > Cr; S2-Cd > Cu > Pb > Ni > Cr; S3-Cd > Cu > Cr > Pb > Ni; S4-Cd > Cu > Pb > Ni > Cr and S5-Cu > Cd > Pb > Ni > Cr.

The potential ecological risk factors for Cd, Cr, Cu, Ni and Pb were all lower than 40, demonstrating a low ecological risk. All the sampling sections had a low risk level correlating with the potential risk index values much lower than 150 (Table 4).

Table 4

Ecological risk factor (E_r^i) and potential risk index (*RI*) for the surface sediments

Sampling sections		E_r^i					RI
		Cd	Cr	Cu	Ni	Pb	
Plumbuita Lake	S1	5.24	0.85	8.16	3.06	19.31	36.63
	S2	33.74	0.92	11.42	2.21	8.83	57.11
	S3	15.00	1.17	5.59	3.02	3.08	27.86
Circului Lake	S4	13.49	0.62	12.15	1.57	6.40	34.23
	S5	8.24	1.17	18.62	2.97	5.44	36.43
Min		5.24	0.62	5.59	1.57	3.08	27.86
Max		33.74	1.17	18.62	3.06	19.31	57.11
Average		15.14	0.95	11.19	2.56	8.61	38.45
± SD		11.12	0.23	4.92	0.66	6.33	11.02

Cluster Analysis (CA) was performed using the statistical software package JMP 10 for Windows [21]. Cluster Analysis was applied to identify the variables grouping. Figure 2 shows the dendrogram obtained for the sediments collected from the three sections (S1, S2 and S3) of the Plumbuita Lake (Fig. 2.a) and the other two sections (S4 and S5) of the Circului Lake (Fig. 2.b).

The cluster analysis results indicate two similar clusters for the metals analyzed in the sediment samples collected from two lakes: (1) Cd-Ni-Cr; (2) Cu-Pb in terms of similarities. This indicates that Cu and Pb appear to have originated mainly from natural sources. In addition, Cd, Ni and Cr probably originate from anthropogenic sources.

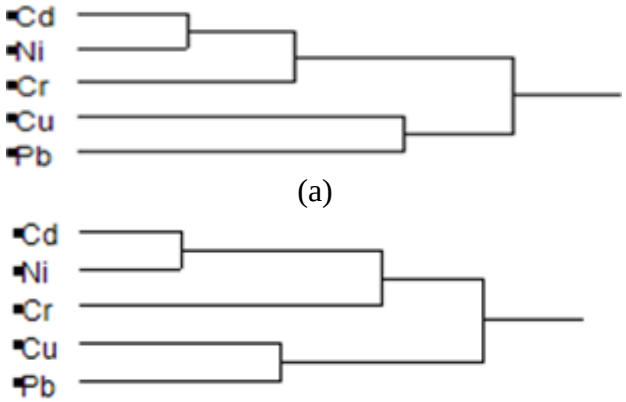

Fig. 2. Dendrogram of heavy metals
(a) - Plumbuita Lake, (b) - Circului Lake

4. Conclusions

This study provides useful information regarding the potential environmental risk of heavy metals contamination in sediments from Plumbuita and Circului lakes. The degree of contamination was evaluated using the contamination factor C_f and contamination degree C_d indices. The risk assessment was conducted using the potential ecological risk factor E_r^i and the potential ecological risk index *RI*.

From the analysis of contaminants factors (C_f), the characteristic values of a slightly pollution have been revealed: with Cd (C_f = 1.12) in S2, with Cu in all five sampling sections, the maximum value being registered in S4 (C_f = 2.49), and with Pb in S2, S3 and S4. For S1, the value recorded for Pb (C_f = 3.86) indicated a considerable pollution.

Considering the sum of all contamination factors, the Cd index indicated that the sediments had a low degree of contamination with the investigated heavy metals (Cd, Cr, Cu, Pb and Ni).

Cluster Analysis applied to data obtained for the content of heavy metals in sediments demonstrated significant correlations between: Fe, Mn, Co, Cr and Ni, suggesting similar sources of pollution and/or similar geochemical processes controlling the occurrence of these metals in the sediments.

The numerical values obtained for the potential ecological risk factor for investigated heavy metals in sediment samples indicated a low ecological risk level and all the sampling section indicated a low general level of potential ecological risk for the lakes.

Considering the fact that various contaminants are introduced into the environment daily, sediment quality assessment should be long term monitored for a continuous environmental protection and water management in the urbanization area.

Acknowledgements. This work was financially supported by the National Authority for Scientific Research and Innovation, in the frame of Nucleu Program-Project (PN 09 06 01 13 and PN 09 06 02 40). The authors would like to thank the management and employees of the National Institute for Research & Development in Environmental Protection for their valuable assistance and suggestions.

REFERENCES

[1] Deák Gy., Daescu V., Holban E., Marinescu P., Tanase G. S., Csergo R., Daescu A. I., Gaman S., Health–environment relation: a key issue of Romanian environmental protection, *Environmental Engineering and Management Journal*, 16(1-2), (2015), 304-315.

[2] Tociu C., Marcu E., Ciobotaru I. E., Maria C., Risk assessment of population exposure to nitrates/nitrites in groundwater: a case study approach, *Journal of Environmental Research and Protection*, 13, (2016), 39-45.

[3] V.-M. Radu, P. Ionescu, Gy. Deák, A. Ivanov, E. Diacu, Multivariate statistical analysis for quality assesment of aquatic ecosystem on lower Danube, *Journal of Environmental Protection and Ecology* 15(2), (2014), 412-424.

[4] Resetar-Deac A.-M., Diacu E., Assessment of aquatic environment contamination with heavy metals from abandoned mines of Northwestern Romania, *Rev. Chim. (Bucharest)*, 66(9), (2015), 1535-1539.

[5] V.-M. Radu, A. Ivanov, Gy. Deák, E. Diacu, Assessment of Heavy Metals Content in Water and Sediments from the Lower Danube River Using EcoIndex, *Rev. Chim. (Bucharest)*, 67(2), (2016), 649-653.

[6] Pandey G., Madhuri S., Heavy Metals Causing Toxicity in Animals and Fishes, *Research Journal of Animal, Veterinary and Fishery Sciences*, 2(2), (2014), 17-23.

[7] Grund S., Higley E., Schönenberger R., Suter M. J. F., Giesy J. P., Braunbeck T., Hecker M., Hollert H., The endocrine disrupting potential of sediments from the Upper Danube River (Germany) as revealed by in vitro bioassays and chemical analysis, *Environmental Science and Pollution Research*, 18, (2011), 446-460.

[8] Khan K., Khan H., Lu Y., Ihsanullah I., Nawab J., Khan S., Shah N. S., Shamshad I., Maryam A., Evaluation of toxicological risk of foodstuffs contaminated with heavy metals in Swat, Pakistan, *Ecotoxicology and Environmental Safety*, 108, (2014), 224-232.

[9] Aly Salem D. M. S., Khaled A., El Nemr A., El-Sikaily A., Comprehensive risk assessment of heavy metals in surface sediments along the Egyptian Red Sea coast, *Egyptian Journal of Aquatic Research*, 40, (2014), 349-362.

[10] Popescu I., Biasioli M., Ajmone-Marsan F., Stănescu R., Lability of potentially toxic elements in soils affected by smelting activities, *Chemosphere*, 90, (2013), 820-826.

[11] Radu V.-M., Raischi S., Szep R., Tănase G.S, Ionescu P., Evaluation of priority hazardous substances present in the sediments of the Lower Danube section using multivariate statistical analysis, *Water resources, forest, marine and ocean ecosystems, SGEM*, 1, (2015), 277-283.

[12] El-Sayed S. A., Moussa E. M. M., El-Sabagh M. E. I., Evaluation of heavy metal content in Qaroun Lake, El-Fayoum, Egypt. Part I: Bottom sediments, *Journal of Radiation Research and Applied Sciences*, 8, (2015), 276-285.
[13] Yu G. B., Liu Y., Yu S., Wu S. C., Leung A. O. W., Luo X. S., Xu B., Li H. B., Wong M. H., Inconsistency and comprehensiveness of risk assessments for heavy metals in urban surface sediments, *Chemosphere*, 85, (2011), 1080-1087.
[14] Yang J., Chen L., Liu L.-Z, Shi W.-L., Meng X.-Z, Comprehensive risk assessment of heavy metals in lake sediment from public parks in Shanghai, *Ecotoxicology and Environmental Safety*, 102, (2014)129-135.
[15] Ionescu P., Deák Gy., Diacu E., Radu V.-M, *Assessment of heavy metal levels in water, sediment and fish from Plumbuita Lake, Romania*, *Rev. Chim. (Bucharest)*, 67(11), (2016), 2148-2150.
[16] Gogu C. R., Serpescu I., Perju S., Gaitanaru D., Bica I., Urban groundwater modeling scenarios to simulate a Bucharest city lake disturbance, *Hydrogeology, engineering geology and geotechnics, SGEM*, 1(2), (2015), 834-840.
[17] Hakanson L. An ecological risk index for aquatic pollution control. A sedimentological approach, *Water Res.*, 14, (1980), 975-1001.
[18] Ministerial Order No. 161, Approving the Norms on surface water quality classification to determine the ecological status of water bodies, 2016. (Including Quality Standards for Sediments).
[19] Guo W., Liu X., Liu Z., Li G., Pollution and potential ecological risk evaluation of heavy metals in the sediments around Dongjiang Harbor, Tianjin, *Procedia Environmental Sciences*, 2, (2010), 729-736.
[20] Soliman N. F., Nasr S. M., Okbah M. A, Potential ecological risk of heavy metals in sediments from the Mediterranean coast, Egypt, *Journal of Environmental Health Science & Engineering*,13, (2015), 70.
[21] https://www.jmp.com/en_us/home.html

STATISTICAL ANALYSIS OF HEAVY METALS IN LOWER DANUBE SEDIMENTS

Violeta -M. RADU[1*], Alexandru A. IVANOV[1], Petra IONESCU[1], Elena DIACU[2], Iustina POPESCU[1], Carmen TOCIU[1]

[1]National Institute for Research & Development in Environmental Protection, 294, Spl. Independentei, 6th District, Code 060031, Bucharest, Romania
[2]University "Politehnica" of Bucharest, Polizu 1, 1st District, Code 011061, Bucharest, Romania

Abstract

Sediments quality assessment may give important information regarding the pollution status of a hydrographic basin, heavy metals present in sediments posing significant risks on aquatic environment, hence to human health.

This paper describes the assessment of heavy metals concentration in the sediments of Lower Danube River between km 375 and km 175, performed through multivariate statistical methods. To do this, sediment samples were collected during September 2013 – August 2015 timeframe from 20 locations along the study area, and the following indicators were monitored: cadmium, chromium, copper, nickel, zinc, lead and water flow.

Based on statistic method Principal Component Analysis (PCA) two principal components with a percentage of 60% from total were identified, while the Cluster Analysis (CA) use highlighted indicators aggregation in groups, being outlined the heterogeneity of sediment samples.

Useful information on the distribution trend of heavy metals in sediments has been obtained, with emphasis on the utility of multivariate statistical techniques in the processing and interpretation of complex data sets.

Key words: sediments, statistical analysis, Danube River

1. Introduction

One of the major environmental problems is caused by heavy metals presence - sometimes above the legislation thresholds - in all environmental compartments: air, water, sediments and soil [1-4].

[*]Corresponding author; E-mail: radumonica33@yahoo.com

Waterbodies quality assessment represents a complex action due to many factors, among which the most important are the continuous variation of chemical substances concentration and the climatic changes [5, 6]. The evolution of pollutants stocked in sediments highlights water long-term tendencies, sediments constituting one of the basic elements of a water body [7]. During time, scientific world concluded that sediments are a reservoir for a large variety of pollutants, both organic (such as persistent organic pollutants) and inorganic (such as heavy metals) [8, 9].

The load of heavy metals in sediment can have industrial, agricultural or urban pollution sources [10, 11]. These harmful elements are stored in aquatic media as non-biodegradable persistent pollutants offering a clear overview of river's historical pollution [12-14].

One of the main pollution sources of the Black Sea represents Danube River which enters on Romanian territory with a large load of pollutants gathered from the 14 crossed countries [15-18].

The main aim of this study was to perform a statistical evaluation of the sediments from the Lower Danube River regarding heavy metals concentration correlated with water flow, highlighting the interdependencies between the monitored indicators.

2. Experimental

The study area is represented by Lower Danube River between km 375 and km 175, where were undertaken hydro-technical works for improving navigation conditions (figure 1) to respect the Danube Commission recommendations to maintain minimum water flow during droughts, in order to ensure normal navigation conditions during the whole year [19].

In this purpose, 500 sediment samples were collected from 20 locations chosen for monitoring.

Sediment samples were collected from both river banks, monthly from L1-L7, L18-L20 locations and quarterly from L8-L17 locations, during September 2013 – August 2015, and the content of cadmium (Cd), chromium (Cr), copper (Cu), nickel (Ni), lead (Pb), zinc (Zn) was analysed in correlation with water flow (Q). For sediment sampling a *sediment core sampler* was used, and the samples were stored in PTFE recipients and preserved in dark and at 4°C until being transported to the laboratory. Prior to analysis, they were air-dried at room temperature, grinded and mixed to ensure a representative sample. From the fraction < 63 μm, around 0.5 g of sediment have been mineralized with *Aqua Regia*, using the microwave digestion method DG-EN-30 from Milestone ETHOS.

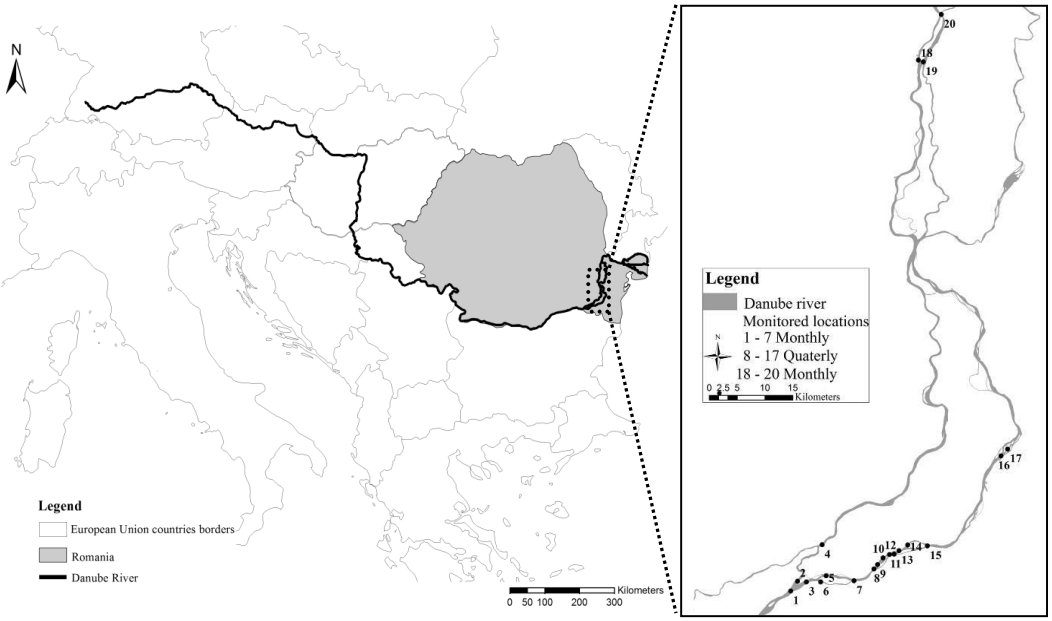

Fig. 1. Map of the study area indicating monitoring locations of sediments on the Lower Danube River, km 375 – km 175 [20]

Heavy metal concentrations (Cd, Cr, Cu, Ni, Pb and Zn) have been determined using Atomic Absorption Spectrometry equipped with flame and graphite furnace (GFAAS) (Solaar M5, Thermo) after *Aqua Regia* digestion [21].

Quality assurance of the results was performed by verifying the analytical performances with river sediment standard reference material LGC 6187.

All reagents used in this study were of analytical grade and all glassware used was thoroughly washed with nitric acid 1.5 mol/L and rinsed in double distilled water and deionized water before use.

The water flow (Q) was measured onsite in all established locations, under the monitoring program.

3. Results and discussions

In order to perform the statistical evaluation of sediments quality, Principal Component Analysis (PCA) and Cluster Analysis (CA) were applied

with the statistical software package JMP 10 for Windows on the sediments data (about 3000 results) obtained in 2013- 2015 period.

Principal Component Analysis (PCA) is one of the multivariate statistical techniques used for identifying important factors or components which explain the majority of system variance [22]. During Principal Component Analysis (PCA), the Pearson correlation matrix was obtained, the results being presented in table 1.

Table 1

Correlation matrix for monitored parameters

	Cd	***Cr***	***Cu***	***Pb***	***Zn***	***Ni***	***Q***
Cd	1.0000						
Cr	0.1931	1.0000					
Cu	***0.4788***	*0.3216*	1.0000				
Pb	*0.3354*	0.1253	**0.5062**	1.0000			
Zn	***0.4933***	0.2753	**0.7791**	***0.4612***	1.0000		
Ni	*0.3541*	0.2793	**0.5752**	0.2934	**0.6117**	1.0000	
Q	-0.1367	-0.0310	-0.0465	-0.1385	-0.0437	0.0321	1.0000

The obtained correlation between the monitored heavy metals may provide useful information regarding their sources, migration probability and accumulation potential.

High correlations between two heavy metals may suggest that they have the same pollution source or that they were subject of the same biochemical process.

In table 1 there can be seen significant correlations, having a Pearson correlation coefficient higher that 0.5, between zinc and copper (Pearson correlation coefficient 0.78), nickel and zinc (Pearson correlation coefficient 0.61) and between lead and copper (Pearson correlation coefficient 0.51). Also, the correlation between copper and cadmium should not be neglected, having a Pearson correlation coefficient of 0.48.

Chromium distribution in monitored sediments was probably affected by the oxidation-reduction potential, being known that chromium is sensitive at oxidation and reduction phenomena.

From the correlation matrix (table 1) we can notice an insignificant direct proportional influence of the water flow on nickel concentration, with a Pearson

coefficient of 0.03, while the other metals have insignificant indirect correlations with negative values of Pearson coefficients. This is mostly due to water level increases and decreases with the river flow rate leading to sampling slightly different riverbank locations. On low flow rates, historically more contaminated sediment was available for sampling, on higher flow rates almost only newly submerged river bank areas were available to sampling.

A representative load values for the first two principal components are presented in table 2. The first principal component is formed by the monitored heavy metals evolutions and confirms the similarity of these components, while the second principal component is associated to water flow. These distributions emphasize the independent evolution of the heavy metals group with water flow, on the studied section.

Table 2

The matrix of sediment heavy metals load and water flow

Parameters	*PC1*	*PC2*
Cd	0.66607	
Cr	0.43928	
Cu	0.88258	
Pb	0.63453	
Zn	0.87826	
Ni	0.73833	
Q		0.90585

In figure 2 are presented the values associated to the principal components and the variability percentage of each component, showing that the first two principal components cumulate about 60 % of the total variation in the data set.

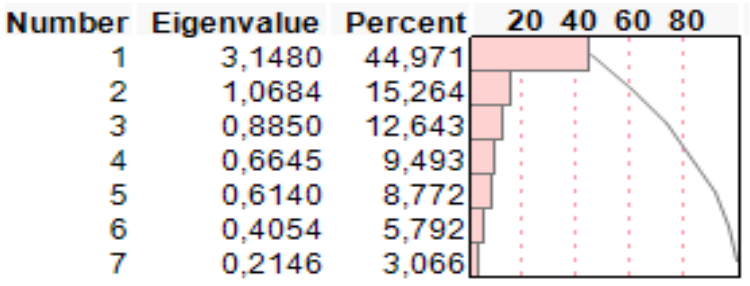

Fig. 2. Eigenvalues and percentage of data variability accounted by each PC

The representation of the data in terms of the first two components is presented in figure 3, showing that sediment samples have a strong, uniformly dispersed character, without any apparent aggregated groups.

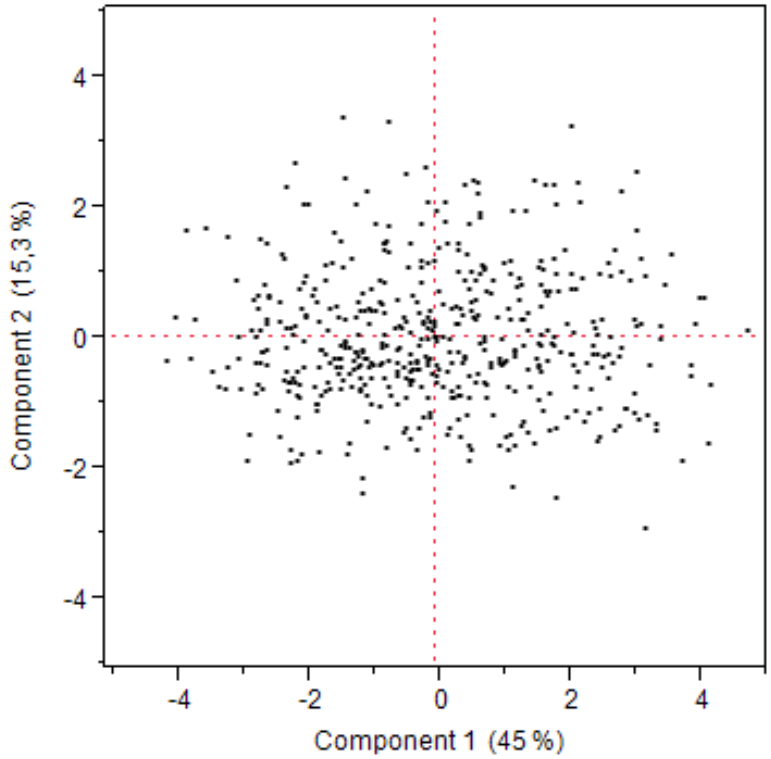

Fig. 3. Score plot of the first two principal components

The spatial distribution of the monitored parameters is presented in figure 4, stressing on the relations between them. As it can be seen, Cu Zn and Cr Ni pairs are included in the ++ quadrant, probably being affected by the same factors, while Cd and Pb can be associated in another group in the +−. Water flow had the most separated behaviour, being situated in −+ quadrant.

Another multivariate statistical technique applied in this study is Cluster Analysis which provides useful information regarding the similarity between monitored parameters groups and offers a detailed evaluation of the relation between them [23].

The result of Cluster Analysis is presented in figure 5 – a dendrogram which emphasise the grouping of parameters.

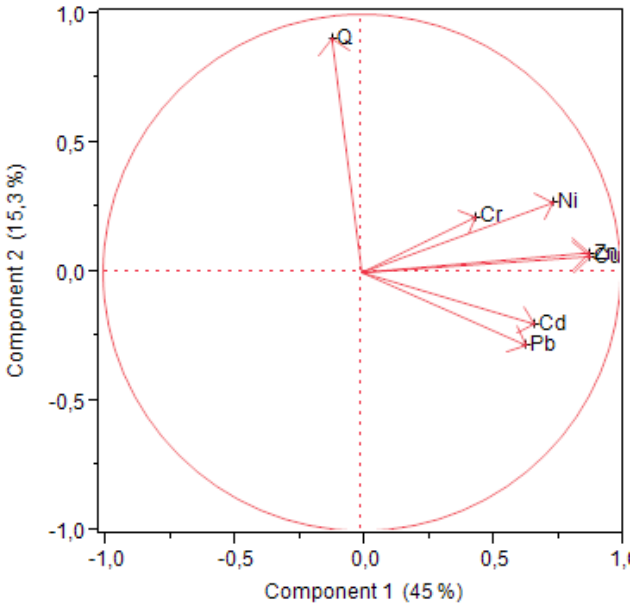

Fig. 4. The Loading Plot between PC1 and PC2

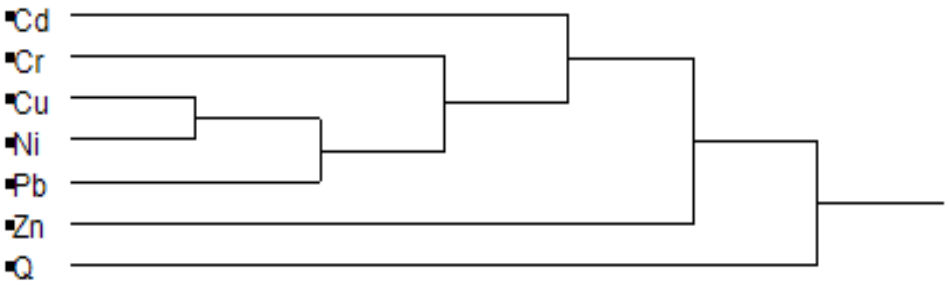

Fig. 5. Dendrogram of the monitored parameters

From figure 5 we can conclude that the monitored heavy metals from the surface of the sediment from the studied area have probably the same anthropogenic sources.

Ionescu et al. [21] have represented a heavy metals distribution in 2013-2014 period from 10 monitoring locations and obtained a dendrogram with the same variation, which helps us to conclude that the hydro-technical works that occurred in the studied area have not significantly influenced the heavy metals content in sediments.

6. Conclusions

The multivariate statistical analysis accomplished on heavy metal content of the sediments in Lower Danube, showed that the hydro-technical works undertaken for improvement of navigation conditions between km 375 and km 175 did not significantly affected the sediments composition, in terms of heavy metals concentration variability.

By using the PCA statistical method, an independent evolution of heavy metals concentration in sediments relative to water flow has been highlighted. Moreover, this conclusion was reinforced by the contributions in the principal components, confirming the similarity between the studied heavy metals. At the same time, the CA method showed that the concentration of Ni and Cu in the analysed sediments were strongly influenced by the anthropogenic activities.

The application of these multivariate statistical techniques in integrated monitoring programmes on environment can plays an important role, constituting an accurate overview of large data sets.

Acknowledgments

The authors acknowledge the management and employees of National Institute for Research & Development in Environmental Protection for their valuable assistance and suggestions and to the POS-T Project ”Monitoring of Environmental Impact of the Works for Improvement of the Navigation Conditions on the Danube between Calarasi and Braila, km 375 - km 175”, (http://www.afdj.ro/en/content/romomed).

REFERENCES

[1] Pallavi D., Kumar M., Sarma K. P., Speciation of heavy metals in surface sediment of the Brahmaputra river, Assam, India, *Journal of Environmental Research and Development*, 9, (2015), 944-952.

[2] Milanovđ R.., Krstić P. M., Marković V. R.., Jovanović A. D., Baltić M. B., Ivanović S. J., Jovetić M., Baltić Ž. M., Analysis of heavy metals concentration in tissues of three different fish species included in human diet from Danube river, in the Belgrade region, Serbia, *Acta Veterinaria-Beograd*, 66, (2016), 89-102.

[3] Ionescu P., Radu V.-M., Deák Gy., Diacu E., Distribution, partition and fluxes of trace heavy metals in the Lower Danube River, *Rev. Chim. (Bucharest)*, 65, (2014), 1092-1095.

[4] Popescu I., Nimirciag R., Vina G., Ajmone-Marsan F., Spatial distribution of potentially toxic elements in soils polluted by mining activities, *Rev. Chim. (Bucharest)*, 5, (2013), 477-481.

[5] Voza D., Vukovic M., Takic L., Nikolic D., Mladenovic-Ranisavljevic I., Application of multivariate statistical techniques in the water quality assessment of Danube river, Serbia, *Archives of Environmental Protection*, 41, (2015), 96–103.

[6] Tan K. W., Evaluation of Water Quality snd Benthic Macrointervebrates Fauna Relationship Using Principal Component Analysis (PCA): A Case Study of Cameron Highlands Malaysia, *Environmental Management and Sustainable Development*, 5, (2016), 187-208.
[7] Wang Y.-B., Liu C.-W., Wang S.-W., Characterization of heavy-metal-contaminated sediment by using un-supervised multivariate techniques and health risk assessment, *Ecotoxicology and Environmental Safety*, 113, (2015), 469–476.
[8] Montuori P., Aurino S., Garzonio F., Sarnacchiaro P., Nardone A., Triassi M., Distribution, sources and ecological risk assessment of polycyclic aromatic hydrocarbons in water and sediments from Tiber River and estuary, Italy, *Science of the Total Environment*, 566–567, (2016), 1254–1267.
[9] Khan M. Z. H., Hasan M. R., Khan M., Aktar S., Fatema K., Distribution of Heavy Metals in Surface Sediments of the Bay of Bengal Coast, *Journal of Toxicology*, 1-7, (2017), https://doi.org/10.1155/2017/9235764.
[10] Zhao C., Dong S., Liu S., Sylvie I., Li J., Liu Q., Wang C., Spatial distribution and environmental risk of major elements in surface sediments associated Manwan Dam in Lancang River, China, *Eurasian Journal of Soil Science*, 4, (2015), 22-29.
[11] Hacısalihoğlu S., Karaer F., Relationships of Heavy Metals in Water and Surface Sediment with Different Chemical Fractions in Lake Uluabat, Turkey, *Pol. J. Environ. Stud.*, 25, (2016), 1937-1946.
[12] Jun R., Zhen S., Ling T., Xia W., Multivariate Analysis and Heavy Metals Pollution Evaluation in Yellow River Surface Sediments, *Pol. J. Environ. Stud.*, 24, (2015), 1041-1048.
[13] Resetar-Deac A.-M., Diacu E., Assessment of aquatic environment contamination with heavy metals from abandoned mines of Northwestern Romania, *Rev. Chim. (Bucharest)*, 66, (2015), 1535-1539.
[14] Soliman N. F., Nasr S. M., Okbah M. A., Potential ecological risk of heavy metals in sediments from the Mediterranean coast, Egypt, *J Environ Health Sci Eng.*, 13, (2015), doi: 10.1186/s40201-015-0223-x.
[15] Vigiak O., Malagó A., Bouraoui F., Grizzetti B., Weissteiner C. J., Pastori M., Impact of current riparian land on sediment retention in the Danube River Basin, *Sustainability of Water Quality and Ecology*, 8, (2016), 30–49.
[16] Ionescu P., Radu V.-M., Deák Gy., Ivanov A. A., Diacu E., Lower Danube water quality assessment using heavy metals indexes, *Rev. Chim. (Bucharest)*, 66, (2015), 1088-1092.
[17] Nacar S., Satilmis U., Temporal Variation of Organic and Inorganic Carbon Transport from the Southeastern Black Sea (Trabzon Province) Rivers, *EJENS*, 2, (2017), 149-153.
[18] Pagliero L., Bouraouia F., Willemsb P., Diels J., Large-Scale Hydrological Simulations Using the Soil Water Assessment Tool, Protocol Development, and Application in the Danube Basin, *Journal of Environmental Quality – Article*, 43, (2014), 145-154.
[19] POS-T Project Monitoring of Environmental Impact of the Works for Improvement of the Navigation Conditions on the Danube between Calarasi and Braila, km 375 - km 175 (http://www.afdj.ro/en/content/romomed).
[20] Radu V.-M., Ivanov A. A., Ionescu P., Deák Gy., Tudor M., Development of a multiparametric quality index for water quality monitoring, *Environmental Engineering and Management* Journal, 15, (2016), 1069-1074.
[21] Ionescu P., Radu V.-M., Diacu E., Sediments as indicators of heavy metal contamination in the Lower Danube River, *Rev. Chim. (Bucharest)*, 66, (2015), 1725-1727.
[22] Shekha Y. A., Evaluation of Water Quality for Greater Zab River by Principal Component Analysis/ Factor Analysis, *Iraqi Journal of Science*, 57, (2016), 2650-2663.
[23] Usman U. N., Toriman M. E., Juahir H., Abdullahi M. G., Rabiu A. A., Isiyaka H., Assessment of Groundwater Quality Using Multivariate Statistical Techniques in Terengganu, *Science and Technology*, 4, (2014), 42-49.

SIMULATION AND OPTIMIZATION OF A METHANOL SYNTHESIS PLANT CONSIDERING THE EFFECT OF CATALYST DEACTIVATION

Georgiana-Cristina BÎLDEA, Grigore BOZGA[1]

University Politehnica of Bucharest, Department of Chemical and Biochemical Engineering

Abstract

This article considers the optimal design of a cooled multi-tubular methanol reactor, taking into account catalyst deactivation. The optimal values of reactor length and purge fraction are found, for a plant producing 150 kt methanol/year in a quasi-isothermal reactor operated at 242°C. Next, a reactor model including catalyst deactivation is developed. The model can be solved by an iterative procedure, where the steady state reactor model and catalyst deactivation equation are successively solved. Due to the almost isothermal regime along the reactor, the assumption of constant catalyst activity along the reactor bed is reasonable. Finally, the average hourly profit is calculated for different values of operation time between two catalyst replacements and the optimal operation time is calculated. The cost of the catalyst replacement affects the optimal value of the operation time. The cost of syngas has a strong effect on the profit, but is less important when considering the optimal operation time.

Key words: methanol synthesis, cooled multi-tubular reactor, catalyst deactivation, optimal design and operation

1. Introduction

Synthesis of methanol from syngas is a catalytic, exothermal, reversible process, which requires cooling of the reaction mixture in order to obtain high conversion with small amounts of catalysts. The adiabatic external and indirect cooling reactor (Fig. 1a) consists of several catalyst beds. Cooling is achieved by several heat exchangers placed between the catalytic beds. The reaction proceeds in the vicinity of the maximum reaction curve, while all the gas passes through the catalyst. The major drawback of this system is the need for a large number of high pressure reactors, heat exchangers and interconnecting piping which inhibit cost savings [1]. The adiabatic quench cooling reactor (Fig. 1b) requires a relatively large catalyst volume, since the syngas passes only through a part the catalyst bed and the reaction path is still away from the maximum reaction rate curve. This reactor has many variables to control and is somehow complex to optimize [1]. The cooled multi-tubular reactor uses reaction heat to pre-heat the feed and to

[1] Corresponding author: Email address: g_bozga@chim.upb.ro

generate steam. This reactor requires a smaller catalyst volume since the reaction curve closely follows the maximum reaction rate curve. Other advantages are low by-product formation due to almost isothermal reaction conditions, high recovery of the reaction heat, and easy temperature control by regulating steam pressure. The methanol reaction heat is removed by partial evaporation of the boiler feed water, thus generating 1 metric ton of high-pressure steam per 1.4 metric tons of methanol. Boiler feed water is pumped to the shell side, where it is heated and fed to the steam separator. The resulting steam pressure can be controlled from 36 – 43 bar [1].

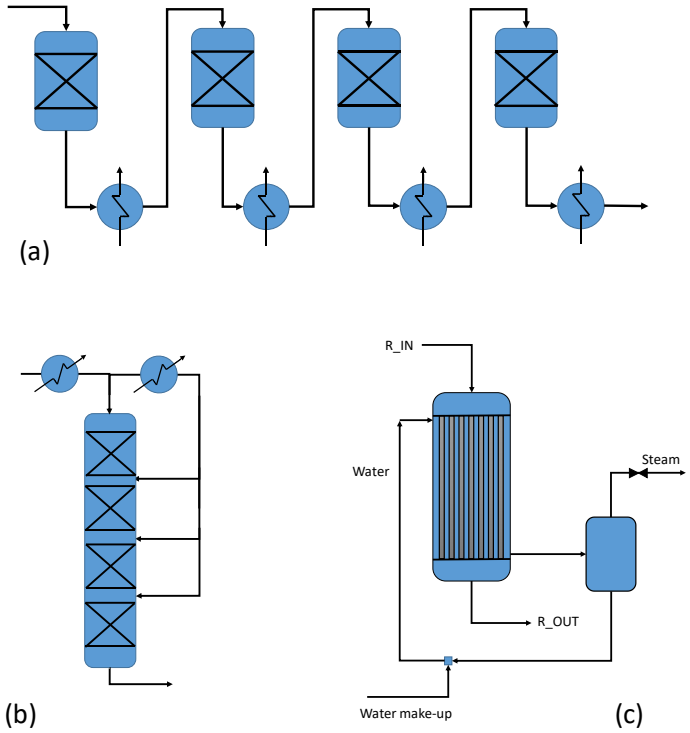

Fig. 1. The reactors used in the methanol industry ((a) – adiabatic external and indirect cooling reactor, (b) – adiabatic quench cooling reactor, (c) – cooled multi-tubular reactor).

2. Process design data

Synthesis gas (syngas) is a very versatile energy product. It is well suited as the feedstock for a range of different products, including electricity and transport fuel. Syngas is the favoured feedstock for the major clean coal technologies. As a mix of mostly hydrogen (H_2), carbon monoxide (CO), nitrogen (N_2), carbon dioxide (CO_2) and methane (CH_4), syngas provides opportunities for its use as either a heating gas (due to the heating value of CO, H_2 and CH_4), or by

using H_2 and CO as the basic building blocks for chemical and fuel production applications [2].
There are three chemical reactions that take place in the methanol reactor. The first one is the synthesis of methanol through the reaction between carbon monoxide and hydrogen (1). The second one is the transformation of carbon dioxide and hydrogen in carbon monoxide and water – the reverse water gas shift reaction (2). The third reaction that takes place is the synthesis of methanol from carbon dioxide and hydrogen (3). The selectivity of the process is high, very small amounts of dimethyl ether, acetone and higher alcohols (such as n-butanol) being obtained.

$$CO + 2H_2 \leftrightarrow CH_3OH \qquad \Delta H_1 = -90.6 \text{ kJ/mol} \qquad (1)$$

$$CO_2 + H_2 \leftrightarrow CO + H_2O \qquad \Delta H_2 = 41.2 \text{ kJ/mol} \qquad (2)$$

$$CO_2 + 3H_2 \leftrightarrow CH_3OH + H_2O \qquad \Delta H_3 = -49.4 \text{ kJ/mol} \qquad (3)$$

Fig. 2 shows the equilibrium yield, defined by equation (4), versus temperature, for different values of the reaction pressure, considering that the reactor is fed with syngas containing 15% CO, 74% H_2, 8% CO_2 and 3% CH_4 [3]. The results were obtained by using the equilibrium reactor model *REQUIL* implemented in Aspen Plus.

$$\eta_{tot} = \frac{\left(n_{CH_3OH,out} - n_{CH_3OH,in}\right)}{\left(n_{CO} + n_{CO_2}\right)_{in}}, \quad \frac{\text{kmol } CH_3OH}{\text{kmol oxides}} \qquad (4)$$

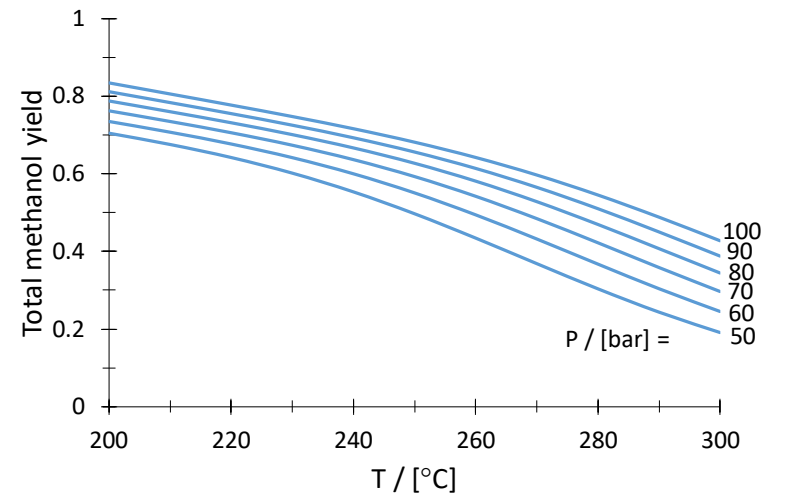

Fig. 2. The variation of the equilibrium yield with temperature and pressure.

Typical catalysts are based on copper and zinc oxides supported on alumina ($CuO\text{-}ZnO\text{-}Al_2O_3$), with a particle density of 2000 kg/m^3 and a bed voidage of 0.5. The reaction rates are described by LHHW-type equations, which use fugacities instead of partial pressures, since the mixture is non-ideal. The intrinsic rates of reactions (1) - (3) are given by equations (5) - (7) [4].

$$R_1 = \frac{k_1 \cdot K_{CO} \cdot \left[f_{CO} \cdot f_{H_2}^{\frac{3}{2}} - \frac{f_{CH_3OH}}{f_{H_2}^{\frac{1}{2}} \cdot K_{p1}} \right]}{\left(1 + K_{CO} \cdot f_{CO} + K_{CO_2} \cdot f_{CO_2}\right) \left[f_{H_2}^{\frac{1}{2}} + \left(\frac{K_{H_2O}}{K_{H_2}^{\frac{1}{2}}} \right) \cdot f_{H_2O} \right]} \tag{5}$$

$$R_2 = \frac{k_2 \cdot K_{CO_2} \cdot \left[f_{CO_2} \cdot f_{H_2} - f_{H_2O} \cdot \frac{f_{CO}}{K_{p2}} \right]}{\left(1 + K_{CO} \cdot f_{CO} + K_{CO_2} \cdot f_{CO_2}\right) \left[f_{H_2}^{\frac{1}{2}} + \left(\frac{K_{H_2O}}{K_{H_2}^{\frac{1}{2}}} \right) \cdot f_{H_2O} \right]} \tag{6}$$

$$R_3 = \frac{k_3 \cdot K_{CO_2} \cdot \left[f_{CO_2} \cdot f_{H_2}^{\frac{3}{2}} - \frac{f_{CH_3OH} \cdot f_{H_2O}}{f_{H_2}^{\frac{3}{2}} \cdot K_{p3}} \right]}{\left(1 + K_{CO} \cdot f_{CO} + K_{CO_2} \cdot f_{CO_2}\right) \left[f_{H_2}^{\frac{1}{2}} + \left(\frac{K_{H_2O}}{K_{H_2}^{\frac{1}{2}}} \right) \cdot f_{H_2O} \right]} \tag{7}$$

The kinetic parameters are calculated using equations (8)-(15), where R = 8.314 J/(mol·K) is the gas constant and T the temperature in K.

$$k_1 = 4.89 \cdot 10^3 \cdot \exp\left(\frac{-113000}{R \cdot T} \right), \ \frac{\text{mol}}{\text{bar}^{1.5} \cdot \text{kg}_{\text{cat}} \cdot \text{s}} \tag{8}$$

$$k_2 = 9.64 \cdot 10^{11} \cdot \exp\left(\frac{-152900}{R \cdot T} \right), \ \frac{\text{mol}}{\text{bar} \cdot \text{kg}_{\text{cat}} \cdot \text{s}} \tag{9}$$

$$k_3 = 1.09 \cdot 10^5 \cdot \exp\left(\frac{-87500}{R \cdot T}\right), \ \frac{\text{mol}}{\text{bar}^{1.5} \cdot \text{kg}_{\text{cat}} \cdot \text{s}} \tag{10}$$

$$K_{CO} = 2.16 \cdot 10^{-5} \cdot \exp\left(\frac{46800}{R \cdot T}\right), \ \text{bar}^{-1} \tag{11}$$

$$K_{CO_2} = 7.05 \cdot 10^{-7} \cdot \exp\left(\frac{61700}{R \cdot T}\right), \ \text{bar}^{-1} \tag{12}$$

$$\frac{K_{H_2O}}{K_{H_2}^{\frac{1}{2}}} = 6.37 \cdot 10^{-9} \cdot \exp\left(\frac{84000}{R \cdot T}\right), \ \text{bar}^{-1} \tag{13}$$

$$\lg K_{p1} = \left(\frac{5139}{T} - 12.621\right), \ \text{bar}^{-2} \tag{14}$$

$$\lg K_{p2} = \left(-\frac{2073}{T} + 2.029\right), \ - \tag{15}$$

To calculate the actual rate of reaction, the internal effectiveness factor (η_i) is needed to account for the influence of the mass and heat transport inside the catalyst particle. The internal effectiveness factor can be estimated as follows [5].

$$\eta_{i,n} = \frac{1 - e^{-2 \cdot u_n}}{u_n \cdot \left(1 + e^{-2 \cdot u_n}\right)}, \ n=1,2; \qquad \eta_{i,3} = \eta_{i,1} \tag{16}$$

$$u_n = a_n \cdot e^{-b_n / T} \tag{17}$$

$$a_1 = 1.302 \cdot 10^8; \quad a_2 = 6.722 \cdot 10^4 \tag{18}$$

$$b_1 = 1.008 \cdot 10^4; \quad b_2 = 5.6272 \cdot 10^3 \tag{19}$$

The reaction kinetics has been implemented in a Fortran subroutine, which has as input the reaction conditions (temperature, pressure, and molar fractions). The subroutine calls Aspen Plus' engine for the physical properties and fugacities, calculates the kinetic parameters, the reaction rates and component formation rates. The component formation rates are sent back to Aspen Plus and used to solve the reactor model.

3. Process design

Aspen Plus was used for the design and simulation of the methanol plant. The process takes place at two different pressure levels, higher pressure for methanol synthesis and lower pressure for methanol purification. For the first part, a standard selection is an equation-of-state model, while a liquid activity model is suited for the second part. The property methods used were SRK (for the reaction section), and NRTL-RK with CO, CO_2, CH_4, and H_2 declared as Henry components (for the separation section). The main equipment in the methanol plant is presented in **Fig. 3**.

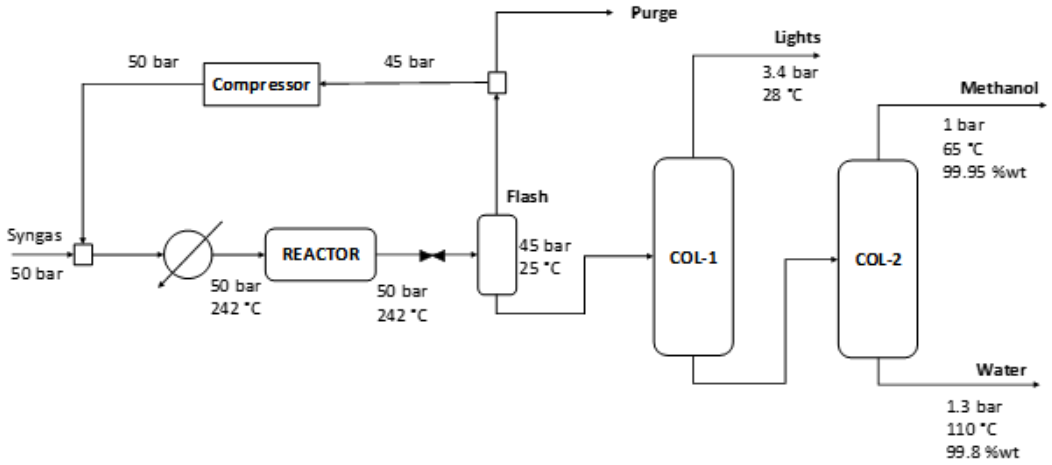

Fig. 3. Process flow diagram of the methanol process

The sizing of the reaction section consists of finding the number of tubes (n_t) and catalytic bed length (L) required to achieve the required methanol production of 150 kt/year (about 600 kmol/h). Additional decision variables are the purge fraction and the flow rate of fresh syngas. The objective function to be minimized is the total annual cost, taking into consideration the CAPEX, OPEX, and syngas cost.

The installed cost of the reactor includes the cost of the equipment and the cost of the catalyst:

$$C_{\mathrm{Re}actor} = C_R + C_{Catalyst} \tag{20}$$

$$C_{\mathrm{R}} = \frac{M\,\&\,S}{280} \cdot 474.7 \cdot A_R^{\,0.65} \cdot \left(2.29 + F_m\left(F_d + F_p\right)\right) \tag{21}$$

where *M&S* is the Marshall & Swift equipment cost index (*M&S*=1536.5 in 2012), A_R is the area of the reactor tubes (m^2), F_m = 1 (carbon steel), F_d = 0.8, and F_p is calculated by equation (22).

$$F_p = 1 + 0.0074 \cdot \left(P - 3.48\right) + 0.00023 \cdot (P - 3.48)^2 \tag{22}$$

The cost of catalyst is calculated as:

$$C_{Catalyst} = n_{tubes} \cdot \frac{\pi \cdot d_t^{\,2}}{4} \cdot L \cdot \rho_{cat} \cdot \left(1 - \varepsilon\right) \cdot C_{cat,sp} \tag{23}$$

where $C_{cat,sp}$ = 4 \$/kg; ρ_{cat} = 2000 kg/m^3; ε = 0.5

The cost of the compressor used for syngas recycle is the second major component of the investment cost (CAPEX).

$$C_{compressor} = \frac{M\,\&\,S}{280} \cdot 664.1 \cdot Power^{0.82} \cdot F_c \tag{24}$$

Besides the investment cost (CAPEX), the total annual cost (TAC) includes the cost of energy necessary for running the compressor (16.8 \$/GJ) and the cost of syngas (30 \$/thousand cubic meters [6]).

$$TAC = \frac{CAPEX}{payback\ period} + OPEX + C_{Syngas} \tag{25}$$

The objective function to be minimized is the total annual cost (25). The decision variables are the length of the reactor (*L*), the purge fraction (φ), the feed of syngas (F_0), and the total number of tubes (*NT*). The minimization is subject to the constrains showed in equation (26), namely a production rate F^* = 600 kmol/h of methanol, a constant superficial velocity of the mixture inside the reactor of 0.5 m/s, and the mass, energy, and momentum balance of the units involved in the reaction loop. Thus, the optimization problem is formulated as follows:

$$\min_{L,\varphi,F_0,NT} \quad TAC$$

$$\text{s.t.} \begin{cases} F = F^* \\ u = 0.5, \ \dfrac{m}{s} \\ mass,\ energy,\ and\ momentum\ balance \end{cases} \tag{26}$$

The composition of the fresh syngas is: 0.2179 CO, 0.0774 CO_2, 0.6753 H_2, and 0.0294 CH_4 (mole fractions) [7]. Reactor inlet temperature and the coolant temperature are both set to 242°C (515 K). The heat transfer coefficient from the reaction mixture to the coolant is calculated, by a FORTRAN block, according to the following relationships:

$$K_T = \frac{Nu \cdot \lambda}{d_t} \tag{27}$$

$$Nu = 2.26 \cdot \mathrm{Re}_p^{\,0.8} \cdot \mathrm{Pr}^{0.33} \cdot \exp\left(\frac{-6 \cdot d_p}{d_t}\right) \tag{28}$$

$$\mathrm{Pr} = \frac{c_p \cdot \eta}{\lambda} \tag{29}$$

$$\mathrm{Re}_p = \frac{u \cdot \rho \cdot d_p}{\eta} \tag{30}$$

The optimization problem is solved by performing the following steps:
Sensitivity analysis: Four length values (L_k) have been chosen to cover the usual values used in the industry. Smaller reactors are cheaper, but the conversion is lower, leading therefore to increased recycling costs. For better use of the high-cost syngas, the purge fraction (φ) should be as small as possible. On the other hand, low purge fraction means higher recycle rates, which require a more expensive compressor. After setting the initial values for the length and the purge fraction, the production and the corresponding cost are calculated and recorded, after which the same steps are repeated for the next value in the length set. Once the cost has been calculated for all lengths, the iterations are repeated for the other values of the purge fraction.
Production: During the sensitivity analysis, the mathematical model of the reaction section is solved for each value of the reactor length and purge fraction. If the methanol production rate is not equal to the required production rate (within a

certain tolerance), then the flow of the inlet stream (syngas) is adjusted and the calculations are redone.

Solution of the mathematical model: The component flow, temperature, and pressure of the reactor-inlet stream are initialized. Then, Aspen Plus solves the mathematical model for the reactor, flash, splitter, compressor, mixer, heat exchanger, and the inlet stream of the reactor. If the newly calculated value of the reactor-inlet stream is different from the previous value (within the tolerated error), the reactor-inlet stream is adjusted and the calculations are redone.

The results are presented in **Fig. 4**, where the lowest TAC was obtained using an eight-meter reactor and a purge fraction of 0.016. The reactor's characteristics, designed and optimized as explained, are presented in *Table 1*.

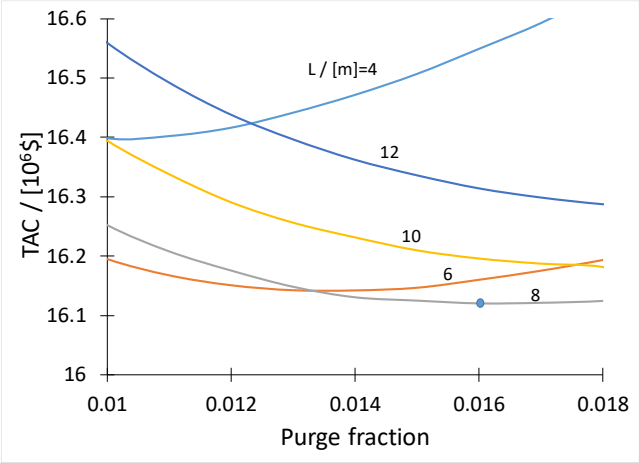

Fig. 4. Total annual cost versus the purge fraction, for different values of the reactor length.

Table 1.

Reactor sizing

Amount of catalyst / [kg]	61243
Length / [m]	8
Number of tubes	6092
Tube diameter / [m]	0.04

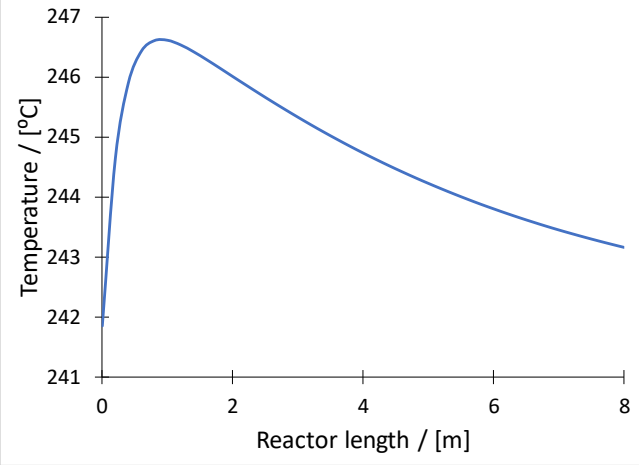

Fig. 5. Temperature profile along the reactor (purge fraction = 0.016).

Table 2 presents the temperature, pressure, flow rates and composition of the streams from the reaction section.

Table 2

Stream table of the reaction section

	SYNGAS	RIN	ROUT	LIQ	VAP	PURGE	RECYCLE
Temperature / [°C]	850	241.9	306.1	25.0	25.0	25.0	37.2
Pressure / [bar]	50	50	50	45	45	45	50
Mole Flows / [kmol/h]	2274.7	15679.4	14431.8	809.0	13622.7	217.9	13404.7
Mass Flows / [kg/h]	25801	124484	124484	24198	100288	1605	98683
Mole Fractions							
CO	0.21790	0.05967	0.03104	0.00102	0.03283	0.03283	0.03283
H_2	0.67530	0.69514	0.65936	$1.04 \cdot 10^{-5}$	0.69851	0.69851	0.69851
CO_2	0.07740	0.03153	0.02483	0.04303	0.02375	0.02375	0.02375
CH_4	0.02940	0.21090	0.22914	0.01750	0.24170	0.24170	0.24170
CH_3OH	0	0.00190	0.04438	0.75432	0.00222	0.00222	0.00222
H_2O	0	0.00016	0.01006	0.17625	0.00019	0.00019	0.00019
DME	0	0.00068	0.00119	0.00786	0.00080	0.00080	0.00080

Methanol purification is achieved in a sequence of two distillation columns. The first column (*COL-1*) separates methanol and water from the light components (DME, H_2, CO, CO_2 and CH_4). The column works as a stripper (feed on the first tray, no condenser), the reboiler duty being adjusted such that the recovery of methanol in the bottoms stream is 99.5% (the mole fraction of methanol in the *LIGHTS* is about 5%). This ensures that the bottoms stream is free of DME and lighter components. The methanol column (*COL-2*) separates methanol from water. The product purity exceeds 99.8 % molar.

Table 3.

Sizing of the distillation columns

	Lights column	Methanol column
Number of theoretical trays	7	36
Number of trays	9	50
Feed tray	1	39
Reflux ratio	-	0.59
Diameter / [m]	0.93	1.88
Height / [m]	7.8	32.4

4. Catalyst deactivation

It is important to consider the deactivation of the catalyst ($Cu/ZnO/Al_2O_3$), as the reaction rate will decrease due to a lower number of active sites. The deactivation is caused by thermal sintering, chemical poisoning due to sulphur compounds, chlorine, and heavy metals, and the oxidation of the active sites [8]. The thermal sintering occurs due to high temperatures, at which the catalyst tends to recrystallize to larger agglomerates, increasing the size and decreasing the active surface area [9].
The model used in this chapter has been implemented in a Matlab program that solves the mathematical model (heat, mass, and impulse balances) for an 8-meter reactor. The deactivation model is presented in (31), with the parameter values presented in *Table 4*.

$$\frac{da}{dt} = -K_{act}\, e^{\frac{E_{act}}{R}\left(\frac{1}{T_0}-\frac{1}{T}\right)} a\left(t,z\right)^5 \qquad a\left(t=0\right)=a_0 \tag{31}$$

where T_0 is the reference temperature, E_{act} the activation energy, and K_{act} the deactivation constant of the catalyst.

Table 4

Parameter values for the deactivation model

Parameter	Value
K_{act} / [h^{-1}]	$4.39 \cdot 10^{-3}$
E_{act} / [J/mol]	91270
T_0 / [K]	523
a_0 / [-]	0.4

The reaction rates are calculated at each point along of the reactor, at different times, using equation (32). Because the temperature varies in the reactor, and the catalyst's activity is affected by temperature, the activity will be different along the reactor's length (*z*).

$$R_i = R_i^0 \cdot \frac{a(t,z)}{a_0}, \quad i = 1,2,3 \tag{32}$$

Dynamic model of an isothermal plug flow reactor with catalyst deactivation
Let us consider the simple case of the single reaction A -> products which takes place in an isothermal plug flow reactor (PFR). The catalyst inside the reactor is slowly deactivating over time. The pressure drop inside the reactor is neglected.
The dynamic model is presented in (33), where ε is the bed voidage, C_A the concentration of *A* (kmol/m^3), *u* the superficial velocity (m/s), *a* the activity of the catalyst, R_A the consumption rate of *A*, *t* the time, and *z* the axial coordinate. Let us suppose that the change of the catalyst activity depends on the concentration of *A* and the activity itself (34).

$$\varepsilon \frac{\partial C_A(z,t)}{\partial t} = -\frac{\partial\left(u \cdot C_A(z,t)\right)}{\partial z} - \frac{a(z,t)}{a_0} R_A(C_A) \tag{33}$$

$$\frac{da(z,t)}{dt} = f(C_A, a) \tag{34}$$

Equations (33) and (34) have the following initial and boundary conditions:

$$\begin{aligned} &C_A(z,0) = C_A^0(z) \\ &\frac{a(z,0)}{a_0} = 1 \\ &C_A(0,t) = C_{A,0}(t) \\ &t \in (0, t_f) \end{aligned} \tag{35}$$

The dimensionless form of equation (33) is obtained by introducing the dimensionless time τ, where t_f is the time of the operation, $t_r = L / u$ the characteristic reaction time, and $x = z / L$ the length of the reactor.

$$\tau = \frac{t}{t_f}, \ \tau \in (0,1) \tag{36}$$

Thus, the dimensionless model of the isothermal PFR with deactivating catalyst can be written as

$$\varepsilon \frac{t_r}{t_f} \frac{\partial C_A}{\partial \tau} = -\frac{\partial C_A}{\partial x} - t_r \cdot \frac{a}{a_0} \cdot R_A \tag{37}$$

Since the ratio t_r / t_f is very small, the left-hand side can be neglected:

$$\begin{aligned} &\frac{dC_A}{dx} = -t_r \cdot \frac{a}{a_0} \cdot R_A \\ &C_A(0) = C_{A,0} \end{aligned} \tag{38}$$

The dimensionless form proves that the mass balance equation can be simplified and solved independently from the catalyst deactivation model. Thus, the algorithm of solving the deactivation model starts with initial activity $a(x,0) / a_0 = 1$. Solution of equation (38) gives the profile of reactant concentration along the reactor, at time $t = 0$. This allows performing one step of integration (in time) of equation (34) at several points ($k = 1 \ldots N$) along the reactor, for $t \in (0, t_1)$, leading to new values of catalysts activity along the reactor length. The procedure is repeated until the final operation time is reached.

In conclusion, the behaviour of the reactor when the catalyst is deactivating can be obtained by using the steady state model of the PRF (a dynamic model is not needed).

Steady state model of the methanol multi-tubular catalytic reactor

The steady state model of the methanol multi-tubular catalytic reactor contains the mole, energy and pressure drop equations:

$$\frac{d\xi_{mi}}{dz} = \frac{1}{\dot{D}_m} \cdot \nu_{Ri} \cdot \rho_{SC}, \; i = 1...3 \tag{39}$$

$$\frac{dT}{dz} = \frac{S \cdot \bar{M}}{D_m \cdot \bar{C}_p} \cdot \left(\sum_{i=1}^{3} (-\Delta H_{Ri}) \cdot R_i \right) \cdot \rho_{SC} - \frac{\pi \cdot d_t \cdot K_T \cdot (T - T_a)}{D_m \cdot \bar{C}_p} \tag{40}$$

$$\frac{dP}{dz} = -\left(150 \cdot \eta \cdot \frac{1-\varepsilon}{d_p} + 1.75 \cdot u \cdot \rho \right) \cdot \frac{u \cdot (1-\varepsilon)}{\varepsilon^3 \cdot d_p \cdot g \cdot 10^4}, \; \frac{\text{atm}}{\text{m}} \tag{41}$$

At $t = 0$: $\xi_{m,i} = 0$; $T = 515$ K; $P = 50$ atm

At each point of the reactor, the mole flow rate of each component can be calculated as follows, and then used for the quantities necessary for reaction rate and physical properties calculations:

$$\xi_i = D_m \cdot \xi_{mi} \tag{42}$$

$$D_{Mj} = D_{Mj,0} + \sum_{i=1}^{r=3} \nu_{ij} \cdot \xi_i \tag{43}$$

Deactivation model

Integrating equation (31) over a time interval (t_{old}, t_{new}) leads to

$$a_{k,new} = \left[a_{k,old}{}^{-4} + 4 \cdot K_{act}\, e^{\frac{E_{act}}{R}\left(\frac{1}{T_0} - \frac{1}{T_k}\right)} \cdot \left(t_{new} - t_{old}\right) \right]^{-0.25} \tag{44}$$

which allows calculation of the change of catalyst activity, at several points k along the reactor.

Fig. 6 shows the results of solving the reactor model including catalyst deactivation for a period of 50 hours (left) and 4 years (right). Deactivation occurs slowly over time. The deactivation rate is higher at the points in the reactor where the temperature is higher. However, deactivation takes place at almost constant rate along the reactor, property that will be used in the next section. This can be explained by the flat temperature profile (see Fig. 5, where the maximum temperature is only 5 °C higher than the feed temperature).

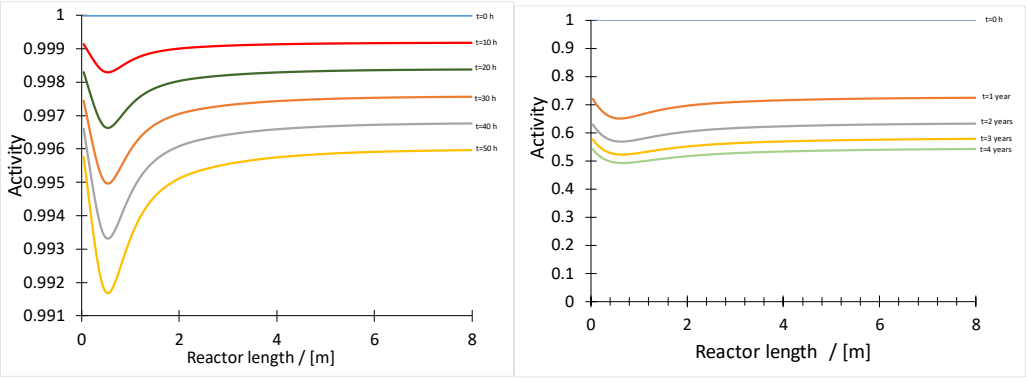

Fig. 6. The catalyst's activity, a/a_0, in the reactor, for 50 hours of operation, respectively 4 years of operation.

Optimization

In this section, a procedure for finding the optimum operation time before changing the catalyst will be presented. Frequent change of the catalyst (low operation time) is inefficient, due to the costs related to catalyst and plant down-time. On the other hand, operating over very long time-periods is also inefficient because of the deactivating catalyst. Therefore, an optimum value of operating time exists.

In order to determine the optimum value, an average of the activity a_{av} has been calculated for the whole reactor, at each t, as shown in equation (45). **Fig. 7** presents the change of the average catalyst activity in time, starting from a fresh catalyst (a_{av} = 1), and dropping to approximately 50% of the initial activity, after 4 years of operating the plant.

$$a_{av}(t) = \frac{1}{L}\int_0^L \frac{a(z,t)}{a_0}\,dz \tag{45}$$

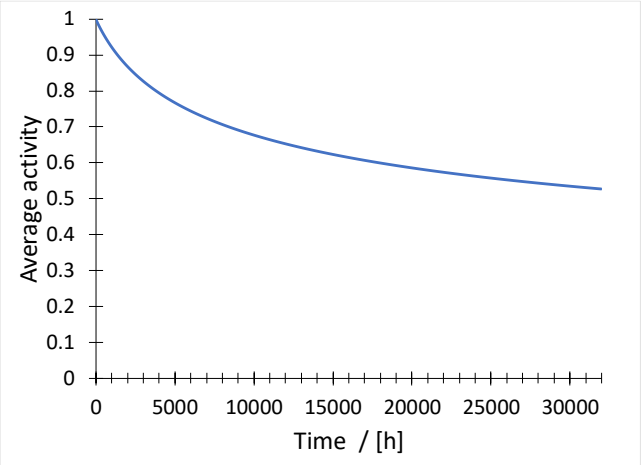

Fig. 7. Change of the average catalyst activity.

To find the optimum operation time before changing the catalyst, a cost/profit analysis was performed on the installation, using Aspen Plus. The cost elements were: syngas (constant); duty of feed pre-heater and distillation reboiler, and compressor energy (variable); catalyst (one time). The price of the syngas is 30 $/TCM (thousand cubic meters, in normal conditions (Pei et al., 2014)). The reboilers use low-pressure (LP) steam (6 bar, 160°C, 7.78 $/GJ), the compressor electricity (16.8 $/GJ), and the heat exchanger high-pressure (HP) steam (42 bar, 254°C, 9.88 $/GJ). For the solid catalyst, a cost of 10 $/kg was considered, resulting a cost of approximately 600,000 $ for every catalyst replacement. The methanol selling price was taken as 500 $/t (alibaba.com, 2017).

The results are presented in **Fig. 8**, where due to the catalyst deactivation the hourly profit drops in time. After 4 years of operating without renewing the catalyst, the hourly profit drops by 15%.

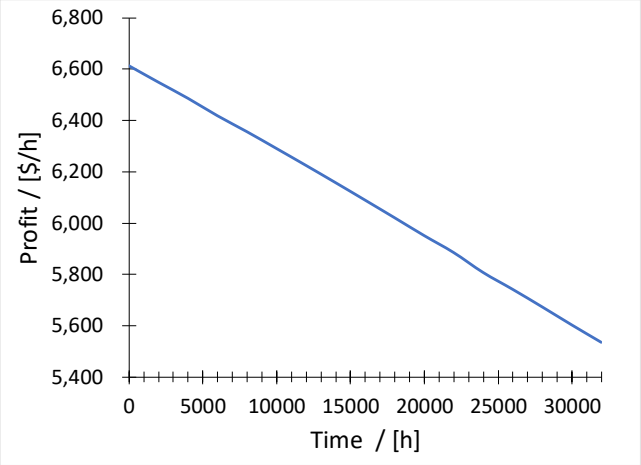

Fig. 8. The change of profit due to catalyst deactivation.

The next step was to determine the optimum time to change the catalyst. This is done by calculating the hourly average profit if the catalyst has been changed, considering the downtime of the installation (no methanol is produced, but also no utilities or syngas are being used), and the cost of the fresh catalyst.

Fig. 9 presents the results of the aforementioned analysis. The maximum hourly profit is obtained if the catalyst is changed after 16000 hours (2 years) of operation. Before the determined maximum, it would be too soon to change the catalyst, since the deactivation has not affected the profit sufficiently to require catalyst replacement. If the catalyst is changed later, the average profit drops.

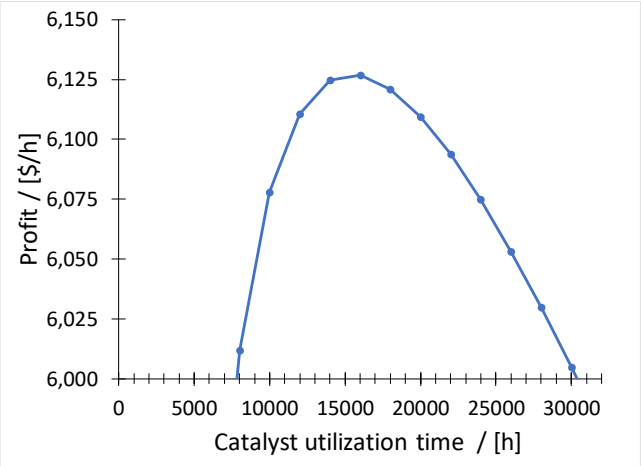

Fig. 9. The average profit variation with the catalyst's utilization time.

Cheap catalyst scenario

A scenario that can be considered is if the catalyst is cheap, resulting a lower cost for the changing of the catalyst. A catalyst cost of 4 $/kg was considered and the results are presented in **Fig. 10**. Now, the optimum time to change the catalyst is only 12000 hours (1.5 years). As expected, the price of the catalyst affects the optimum time to change it, as the more expensive the catalyst is, the better it is to use it for a longer period of time.

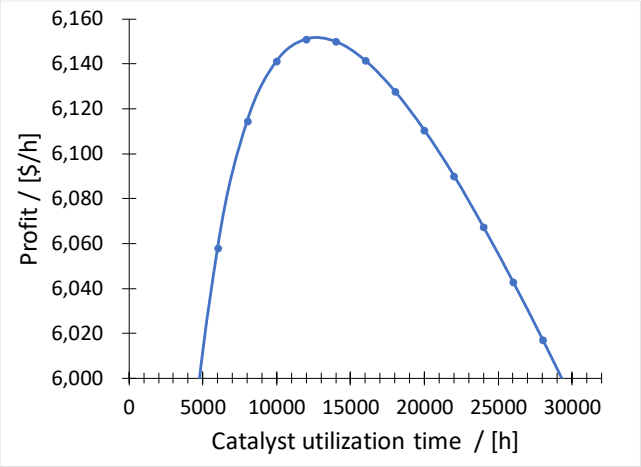

Fig. 10. The average profit variation with the catalyst's utilization time at a cost of 4 $/kg catalyst.

Cheap syngas scenario

If we consider the scenario where the syngas is cheap (for example, 10 $/TCM of syngas), it is better to change the catalyst a bit later than in the base case. While the catalysis is deactivating, more raw material is purged. However, this affects the profit less, compared to the cost of catalyst replacement. **Fig. 11** presents the results of this scenario's analysis, where it can be seen that the optimum time to change the catalyst is slightly lower than 16000 hours (2 years).

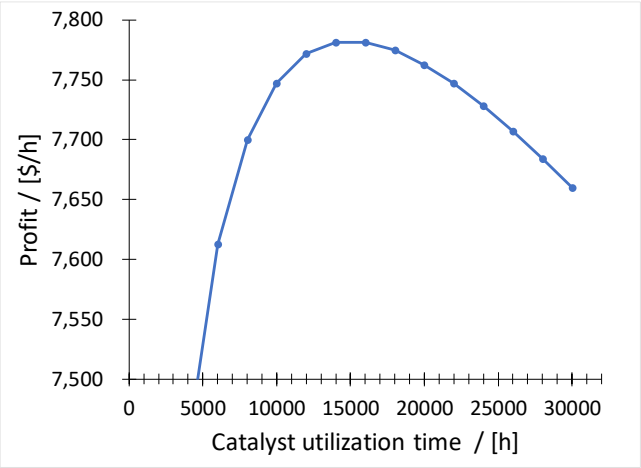

Fig. 11. The average profit variation with the catalyst's utilization time at a cost of 10 $/TCM of syngas.

5. Conclusions

This article considers the optimal design of a cooled multi-tubular methanol reactor, taking into account catalyst deactivation. First, the optimal values of reactor length and purge fraction are found, for a plant producing 150 kt methanol /year in a quasi-isothermal reactor operated at 242°C. The optimal design involves a 6092 tubes reactor, with the length of 8 m, and a purge fraction of 0.016. The methanol purification is achieved by means of a 7-tray stripping column and of a 36-tray distillation column.

Next, a reactor model including catalyst deactivation is developed. The model can be solved by an iterative procedure, where the steady state reactor model and catalyst deactivation equation are successively solved. For the reactor considered in this study, the catalyst activity drops to about 50% after 4 years of operation. Due to almost isothermal regime along the reactor, the assumption of constant catalyst activity along the reactor bed is reasonable.

Finally, the average hourly profit is calculated for different values of operation time between two catalyst replacements. It turns out that changing the catalyst every two years leads to the highest profit. The cost of the catalyst replacement affects the optimal value of the operation time. The cost of syngas has a strong effect on the profit, but is less important when considering the optimal operation time.

The procedure developed here could be extended by considering other variables affecting the economics of the profit, for example, reactor-inlet and coolant temperatures, superficial velocity, temperature and pressure of the vapour-liquid (flash) separation, and syngas composition.

REFERENCES

[1] Kunio, H., Nakamura, H., Shoji, K., Optimum catalytic reactor design for methanol synthesis with TEC MRF-Z reactor, *Catalysis Surveys from Asia*, 2(1), (1998), 99-106.

[2] Wender, I. Reactions of synthesis gas, *Fuel Processing Technology*, 48(3), (1996), 189-297.

[3] Dimian, A.C., Bildea, C.S., Kiss, A.A., 2014, Integrated design and simulation of chemical processes, Second Edition, Elsevier Science.

[4] Graaf, G.H., Scholtens, H., Stamhuis, E.J., Beenackers, A., Intra-particle diffusion limitations in low-pressure methanol synthesis, *Chem. Eng. Sci*., 45, (1990), 773-783.

[5] Bozga G., Muntean, O., 2001, Chemical Reactors, vol. II: Heterogeneous reactors, Ed. Tehnică Bucuresti.

[6] Pei, P., Korom, S.F., Ling, K., Nasah, J. Cost comparison of syngas production from natural gas conversion and underground coal gasification, *Mitigation and adaptation strategies for global change*, 21(4), (2016), 629–643

[7] Bertau, M., Offermanns, H., Plass, L., Schmidt, F., Wernicke, H.-J., 2014, Methanol: The Basic Chemical and Energy Feestock of the Future, Springer-Verlag Berlin Heidelberg.

[8] Lovik, I., Hillestad, M., Hertzberg, T., Long term dynamic optimization of a catalytic reactor system, *Computers and Chemical Engineering*, 22, (1998), 707-710.

[9] Lovik I., 2001, Modelling, Estimation and Optimization of the Methanol Synthesis with Catalyst Deactivation, PhD Thesis, Norwegian University of Science and Technology.

MODELLING AND OPTIMIZATION OF MIDDLE VESSEL BATCH DISTILLATION

Elena-Alina GĂLBĂU, Costin Sorin BÎLDEA[1]

University Politehnica of Bucharest, Department of Chemical and Biochemical Engineering

Abstract
The middle vessel column is an attractive alternative for simultaneous separation of a ternary mixture by batch distillation. This article analyzes the performance of two column configurations, corresponding to different arrangements of the vapour and liquid streams around the middle vessel. Two operation types are considered: a) reflux rate and boil-up are constant b) two temperatures inside the column are controlled. The mathematical models neglect the heat loses and the pressure drop along the column and assume perfect mixing of liquid and vapour on the plates, theoretical plates, constant molar overflow and constant holdup for condenser and reboiler. Model solution shows that passing the vapour through the middle vessel together with temperature control leads to larger product amounts, lower energy requirements and reduced batch time.

Key words: batch distillation, middle vessel column, modelling, operation strategy

1. Introduction

The middle vessel configuration (MVC) was originally proposed by Robinson and Gilliland in 1950 [1]. Diwekar presents the middle vessel as a rectifier and an inverted column connected by a still vessel [2], as shown in Fig. 1. The products are simultaneously withdrawn from the top and the bottom of the column [3]. Since this column consist of a rectifier and an inverted column connected by the reservoir in the middle, its behaviour becomes less predictable compared to a conventional batch distillation column [2].
A detailed analysis of MVC started recently due to the market change from quantity-oriented to quality-oriented products [4]. A significant number of studies concern the operation strategy for this process. Barolo and co-workers introduced an operating policy consisting of running the column at infinite reflux and reboil ratio for the whole operation. The distillation can proceed without supervision

[1] Corresponding author; Email address: s_bildea@upb.ro (Costin Sorin Bîldea)

until the liquid in the feed vessel reaches the desired composition [5]. For a ternary zeotropic system, Warter et al. showed the influence of the design and operational parameters on the system performance, by computer-based simulations. They studied the influence of the total number of stages and of the location of the middle vessel on the total energy demand [6]. Hegely and Lang studied the operation of a middle vessel column in closed (without product withdrawal) and open operation modes [7]. Rao and Barik developed a rigorous mathematical model to describe the operating behaviour of a conventional middle vessel batch distillation column. The model takes into account varying molar holdup, varying distillate flow rate, varying reflux flow rate [4].
From the point of view of the energy efficiency and of the production rate the middle vessel column configurations are generally found to be better than regular columns, and the benefit is more prominent when separating mixtures with more components [1].

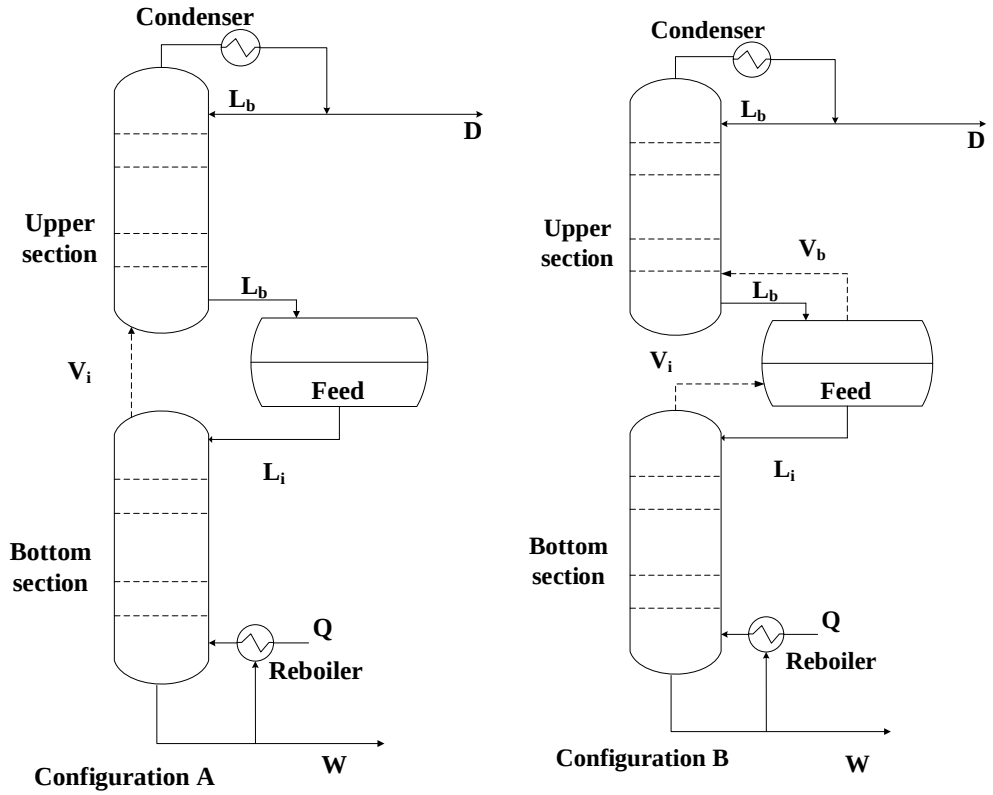

Fig. 1. Stream configurations around the vessel in a middle vessel configuration (A - the vapour from the bottom section are directed to the upper section; B - the vapour from the bottom section are directed to the middle vessel)

There can be great variety within this configuration, which is defined by the way in which the liquid and vapour streams are arranged between the middle vessel and the rectifying and stripping section (Fig. 1). Most studies have mainly concentrated on Configuration A because this alternative is clearly the easiest to handle. In this configuration, the whole liquid stream is diverted into the vessel from the bottom tray in the upper column section, and the liquid stream from the vessel is fed back to the top tray of the lower column section. The vapour from the bottom section is directed to the bottom of the upper section [1]. However, there is also an opportunity to introduce the vapour from the lower section into the vessel, and an additional vapour stream originating from the vessel is then possible (Configuration B). In this work, a comparison between Configuration A and B will be presented. For each configuration, mathematical models for operation at constant reflux rate and vapour flow and operation at variable reflux rate and vapour flow are developed. To solve the mathematical models, an equimolar mixture of benzene, toluene and o-xylene is considered. The middle vessel is fed with a quantity of 3000 kmol of mixture. For the first 10 minutes a total reflux operation is assumed.

2. Operation at Constant Reflux and Vapour Flow

In this section, the mathematical model of the middle vessel column, operated at constant reflux and vapour flow, are presented. The model assumes negligible pressure drop through the column, adiabatic operation, constant molar overflow, theoretical plates, constant reboiler and condenser holdup, and perfect mixing of liquid and vapour.

Configuration A

The first mathematical model introduced is the one for Configuration A (Fig. 1). The liquid resulted from the upper section, L_b, is mixed with the liquid from the middle vessel. The vapour flow generated in the reboiler of the lower section passes directly to the upper section, without passing through the middle vessel. V_i and V_b are numerically equal, but different notations will be used in the top and bottom section of the column, for clarity.
The model describes the accumulation of component *i* on every tray.
On the first tray ($k = 1$, condenser) the accumulation is given by the difference between the vapours arriving from the column and the liquid that leaves as distillate and reflux:

$$\frac{dn_i(k)}{dt} = V_b \cdot y_i(k+1) - L_b \cdot x_i(k) - D \cdot x_i(k) \tag{1}$$

The distillate rate, D, and is calculated with (2).

$$D = V_b - L_b \tag{2}$$

From $k = 2$ to $k = NI - 2$ the mass balance is given by equation (3).

$$\frac{dn_i(k)}{dt} = V_b \cdot \left(y_i(k+1) - y_i(k)\right) + L_b \cdot \left(x_i(k-1) - x_i(k)\right) \tag{3}$$

For the tray above the middle vessel ($k = NI - 1$), equation (4) is used.

$$\frac{dn_i(k)}{dt} = V_b \left(y_i(k+2) - y_i(k)\right) + L_b \left(x_i(k-1) - x_i(k)\right) \tag{4}$$

Equation (5) describes the mass balance around the middle vessel. As can be observed the quantity of i in the middle vessel is given by the difference of the liquid phase L_b which comes from the top section of the column, and the liquid phase L_i that leaves the middle vessel and passes to the lower section of the column.

$$\frac{dn_i(k)}{dt} = L_b \cdot x_i(k-1) - L_i \cdot x_i(k) \tag{5}$$

The mass balance for the trays from $k = NI + 1$ to $k = NT - 1$ is given by an equation similar with (3), but L_b is replaced by L_i (equation (6)).

$$\frac{dn_i(k)}{dt} = V_i \cdot \left(y_i(k+1) - y_i(k)\right) + L_i \cdot \left(x_i(k-1) - x_i(k)\right) \tag{6}$$

The last equation gives the mass balance of the reboiler ($k = NT$), where the bottom product of the column, W, is calculated with (8).

$$\frac{dn_i(k)}{dt} = L_i \cdot x_i(k-1) - V_i \cdot y_i(k) - W \cdot x_i(k) \tag{7}$$

$$W = L_i - V_i \tag{8}$$

Table 1.

Antoine equation constants (Aspen Plus Database)

Component	Boiling point (1 atm) / [K]	C_1	C_2	C_3	C_4	C_5	C_6	C_7
Benzene	353.28	71.59407	-6486.2	0	0	-9.2194	6.9844	2
Toluene	383.83	65.43207	-6729.8	0	0	-8.179	5.3017	2
O-xylene	417.55	78.89207	-7955.2	0	0	-10.086	5.9594	2

The liquid composition is given by (9), where m represents the total number of components.

$$x_i(k) = \frac{n_i}{\sum_{i=1}^{m} n_i} \tag{9}$$

The temperature profile and the composition of the vapour phase are found using Raoult Law (10). $P_{vap,i}$ is the vapour pressure of i, calculated with Antoine equation (11). $C_{n,i}$ (n = 1…7) are Antoine constants, presented in Table 1.

$$y_i(k) = \frac{P_{vap,i}\left(T(k)\right) \cdot x_i(k)}{P} \tag{10}$$

$$\ln\left(P_{vap,i}(k)/[atm]\right) = C_{1,i} + \frac{C_{2,i}}{T(k) + C_{3,i}} + C_{4,i} \cdot T(k) + C_{5,i} \cdot \ln\left(T(k)\right) + C_{6,i} \cdot T(k)^{C_{7,i}}$$

with T in K (11)

To find the temperature on each tray, *T(k)*, equation (12) is solved. Once this variable is known, it is possible to determine the mole fraction in the vapour phase by using (10).

$$P = \sum_i P_{vap,i}\left(T(k)\right) \cdot x_i(k) \tag{12}$$

The energy requirement is calculated with equation (13), where $\bar{r}$ is latent heat of vaporization of the mixture. As the latent heat depends of the temperature, it is determined for each component with (14). The values for constants C_1-C_5 are presented in Table 2.

$$Q = \int_0^t \bar{r} \cdot V(\tau)\, d\tau \tag{13}$$

$$r_i = C_{1,i} + C_{2,i} \cdot T + C_{3,i} \cdot T^2 + C_{4,i} \cdot T^3 + C_{5,i} \cdot T^4 \tag{14}$$

Table 2.

Molar latent heat constants (Aspen Plus Database)

Substance	C_1/ 10^7 [kJ/mol]	C_2/ [kJ/mol/K]	C_3/ [kJ/mol/K^2]	C_4/ [kJ/mol/K^3]	C_5/ 10^{-4} [kJ/mol/K^4]
Benzene	3.44	130083	-831.241	1.71787	-13.9
Toluene	4.60	35862.7	-413.847	0.930371	-8.33
o-Xylene	5.88	-30487.9	-218.991	0.658801	-6.69

An equimolecular mixture (3000 kmol) of benzene, toluene and o-xylene is considered. The liquid from the upper section L_b is set at 58 kmol/min and the liquid from the bottom section at 62 kmol/min. The vapour flow is constant on

both sections of the column and is set at 60 kmol/min. The distillation takes place in a column with 15 plates and the middle vessel is the 7th plate.
The high volatile component represents the larger quantity in distillate (Fig. 2 – (a)). The molar fraction of benzene is 91.87 %, the rest being toluene. The heavy component is recovered in bottoms with a molar fraction of 93.40 % (Fig. 2 – (b)). At the end of the distillation, about 859 kmol of middle-boiling component are recovered in the middle vessel. The molar fraction of toluene in middle vessel is 97 % ((Fig. 2 – (c)). The temperature increases through the column. The decreasing slope around middle vessel is caused by vapours absence in the middle vessel ((Fig. 2 – (d)). The distillation time is of 545 min. The total energy consumption is 1134 MJ.

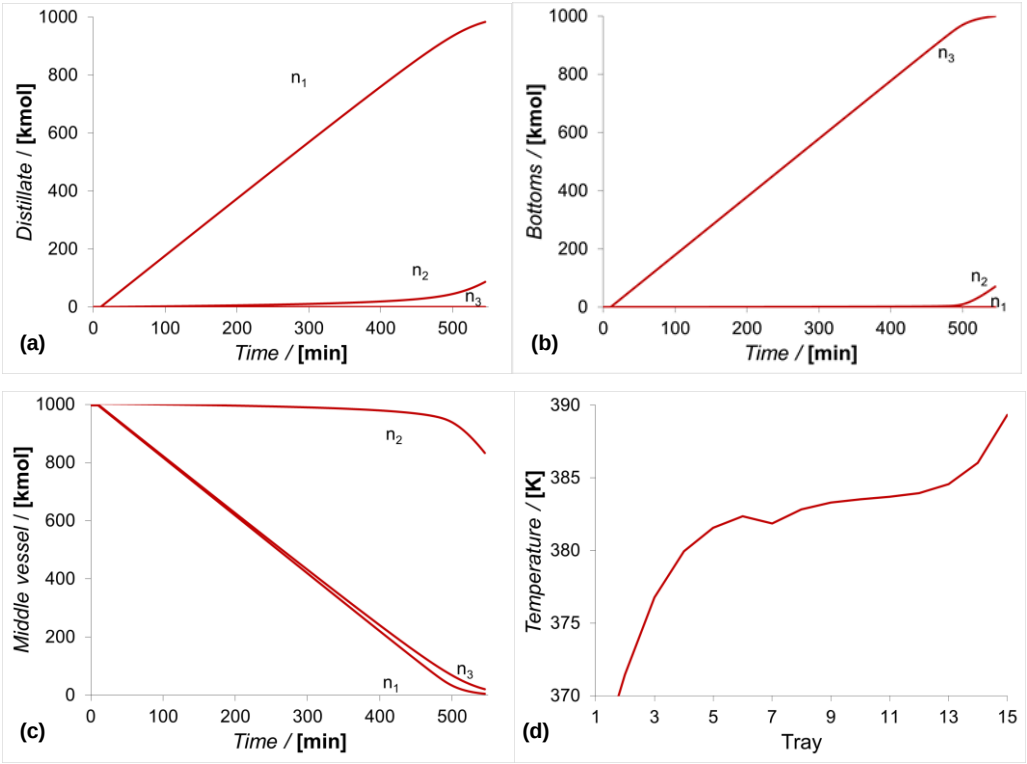

Fig. 2. Middle-vessel distillation – configuration A. V = 60 kmol/min, L_b = 58 kmol/min, L_i = 62 kmol/min. (a) – (c): Distillate, Bottoms and Middle vessel composition. (d): Temperature profile at the end of distillation.

Configuration B

The same equimolar mixture of benzene, toluene, and o-xylene is distilled, but this time the vapour flow generated in reboiler is directed to the middle vessel.

The upper section of the column is fed with vapours from the middle vessel. The column has 15 plates and the middle vessel is 7th plate. The same values as in the previous case for L_b, L_i, V_i and V_b are considered.
The mass balance of the first tray (k = 1) is given by the equation (1). The distillate flow is calculated by (2). The equation (3) will be applied for k = 2 to k = j -1.
The mole balance of the middle vessel is given by (15). In this case the vapour flow from the upper section, V_b, is equal to the vapour flow from the lower section, V_i.

$$\frac{dn_i(k)}{dt} = V_i \cdot y_i(k+1) - V_b \cdot y_i(k) + L_b \cdot x_i(k-1) - L_i \cdot x_i(k) \qquad (15)$$

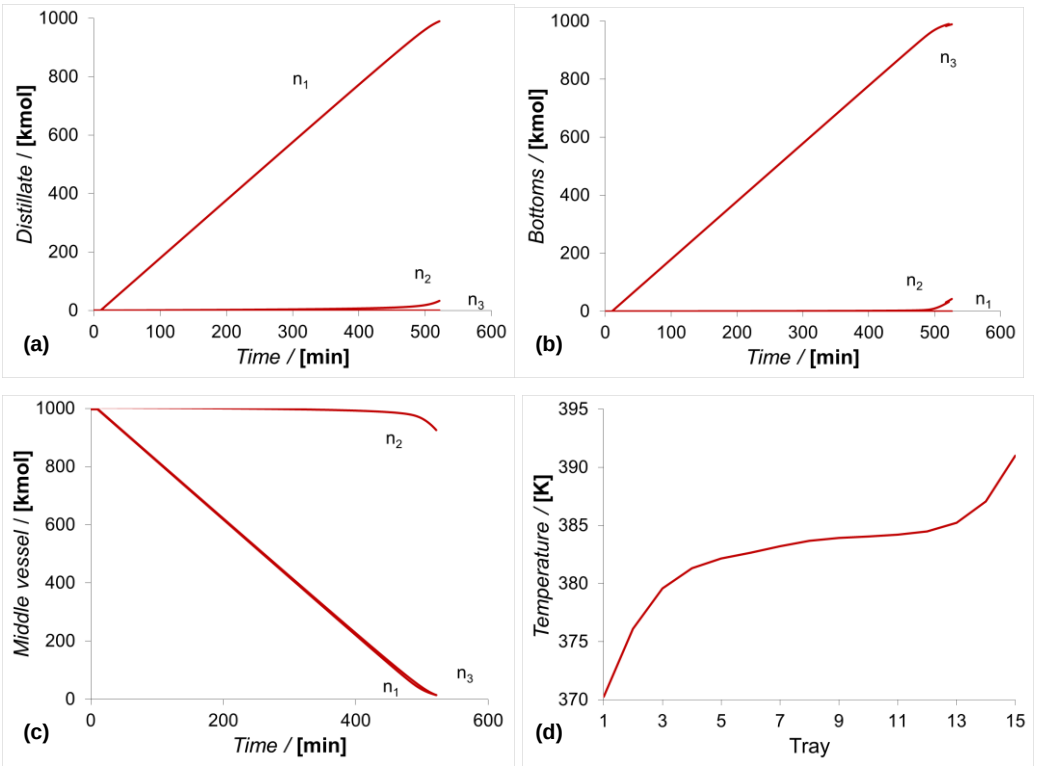

Fig. 3. Middle-vessel distillation – configuration B. V = 60 kmol/min, L_b = 58 kmol/min, L_i = 62 kmol/min. (a) – (c): Distillate, Bottoms and Middle vessel composition. (d): Temperature profile at the end of distillation

A significant amount of benzene (molar fraction 96.76 %) is recovered in distillate (Fig. 3 – (a)). It can be observed that the least volatile compound is obtained in bottoms (molar fraction 96.79 %) ((Fig. 3 – (b)). At the end of the distillation toluene mole fraction in the middle vessel is 97 % ((Fig. 3 – (c)). The

temperature increases along the column. In this case, the decreasing slope observed for configuration A is not found because vapour passes through the middle vessel ((Fig. 3 – (d)). The energy demand is of 1086 MJ and the distillation time is of 520 min.
Comparing with the results obtained for Configuration A, using the same operating parameters (V, L_b and L_i), it can be observed that the purity increased significantly for all three products, while the distillation time and the energy requirement are reduced.

3. Operation at Variable Reflux Ratio and Variable Vapour Flow

The middle vessel column has more degrees of freedom than a regular one, and some form of control of at least some of these is required. For the most common mode of operation, this involves controlling the compositions in each vessel to meet their respective specifications [1].
The control strategy chosen in this work consists in inferential composition control based on temperature measurements. Composition measurement may sometimes be difficult to obtain and a simpler solution is this one. A simple feedback control strategy is used in this case, where the temperature in each column section is controlled. The set point for each controller is set to be near the boiling temperature of the light and heavy components.
The results obtained in the previous section proves that middle vessel configuration is a good option to separate ternary mixtures. It still remains a time and energy consuming process. The results of the mathematical models presented above (distillation time, purities and energy consumption) are strongly impacted by the values of V_b, L_i, L_b. For this reason, operation at variable reflux rate and variable vapour flow should be considered.
The mathematical models presented in the previous section are completed by equations that describes the change of the liquid flow from upper section (L_b) and vapour flow (V_i) through the column needed to achieve constant temperatures on two selected trays. It is expected an improvement of the heat consumption and a decrease of distillation time. The equimolar mixture of benzene, toluene and xylene is distilled using a column with 20 theoretical plates. The middle vessel is the 10th stage.
The control strategy presented in Fig. 4 works as follows: Controller TC_1 looks at the 3rd plate temperature and decides how to change the valve position that allows the liquid flow L_b (reflux) in column, to satisfy its set point T_{SP1}. Control action in this case is direct. Controller TC_2, having reverse action, adjusts the reboiler duty such that the temperature on the 17th plate is kept constant to its set point, T_{SP2}.

$$L_b = L^* + K_c \cdot \left(\left(T - T_{SP1}\right) + \frac{1}{T_i} \int_0^t \left(T - T_{SP1}\right)(\tau)\, d\tau \right) \tag{16}$$

$$V_i = V^* - K_c \cdot \left(\left(T - T_{SP2}\right) + \frac{1}{T_i} \int_0^t \left(T - T_{SP2}\right)(\tau)\, d\tau \right) \tag{17}$$

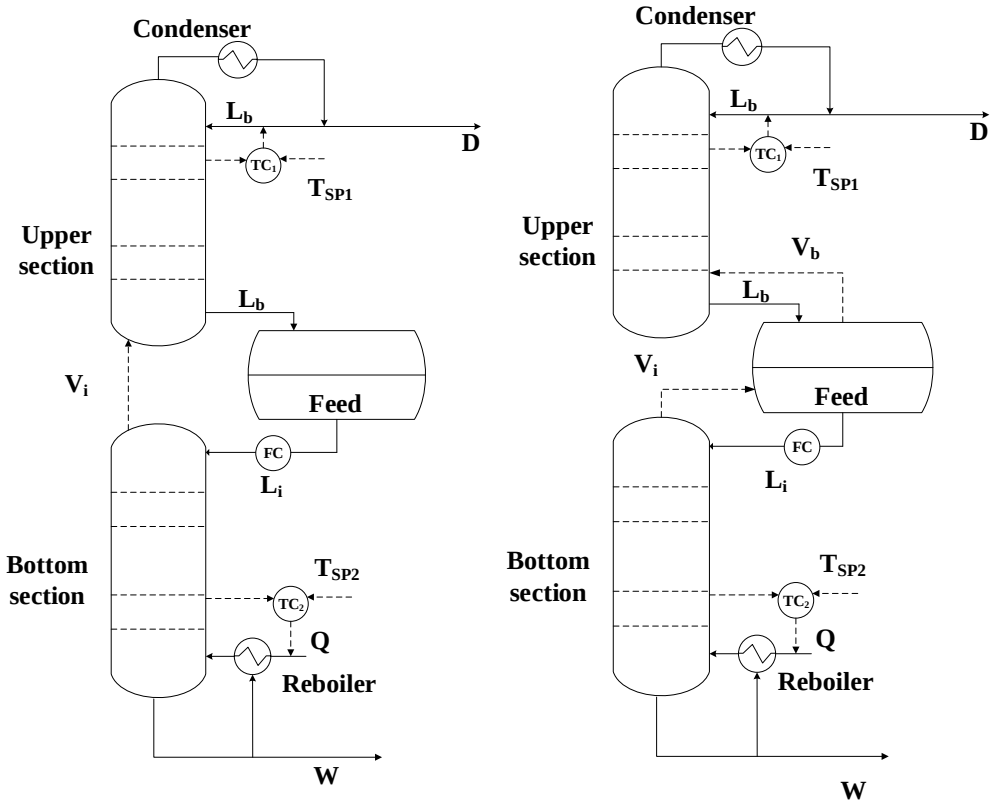

Fig. 4. Control strategy for Configuration A (left) and B (right)

The controller gain K_c is set to 1 kmol/(min·K), and the integration time, T_i, is equal to 10 min. The temperature is kept constant on the 3rd plate by changing the liquid flow L_b. The set point, T_{SP1} is 355 K. In the bottom part, the temperature is kept constant on the 17th plate by modifying the flow of heating agent. The set point of this controller, T_{SP2}, is 413.5 K. The liquid that leaves the middle vessel, L_i, is set at 55 kmol/h. These values were chosen such that, at the end of the distillation time, the mole fraction is at least 95%, for all three products.

Configuration A

The first case studied is the one without vapour passing through the middle vessel. Low-boiling component is recovered in the top of the column (Fig. 5 – (a)). The

molar fraction obtained for benzene is 95.49 %. The bottom product contains 95.21 % xylene (Fig. 5 – (b)).
It can be observed that the low- and high-boiling components are slowly removed from the middle vessel. At the end of the distillation, the middle vessel contains toluene, with a molar fraction of 95 % (Fig. 5 – (c)).
The linear growth of temperature is stopped near the middle vessel due of vapour absence. In the bottom section of the column, where the vapours are generated, it can be noticed that the temperature profile is strongly increasing (Fig. 5 – (d)).
The batch time is 211 min with a total energy consumption of 353 MJ. The distillation time obtained in this study is about 2.5 smaller than the one obtained for constant reflux and vapour operation of Configuration A. The energy consumption is also significantly reduced (3.2 times).

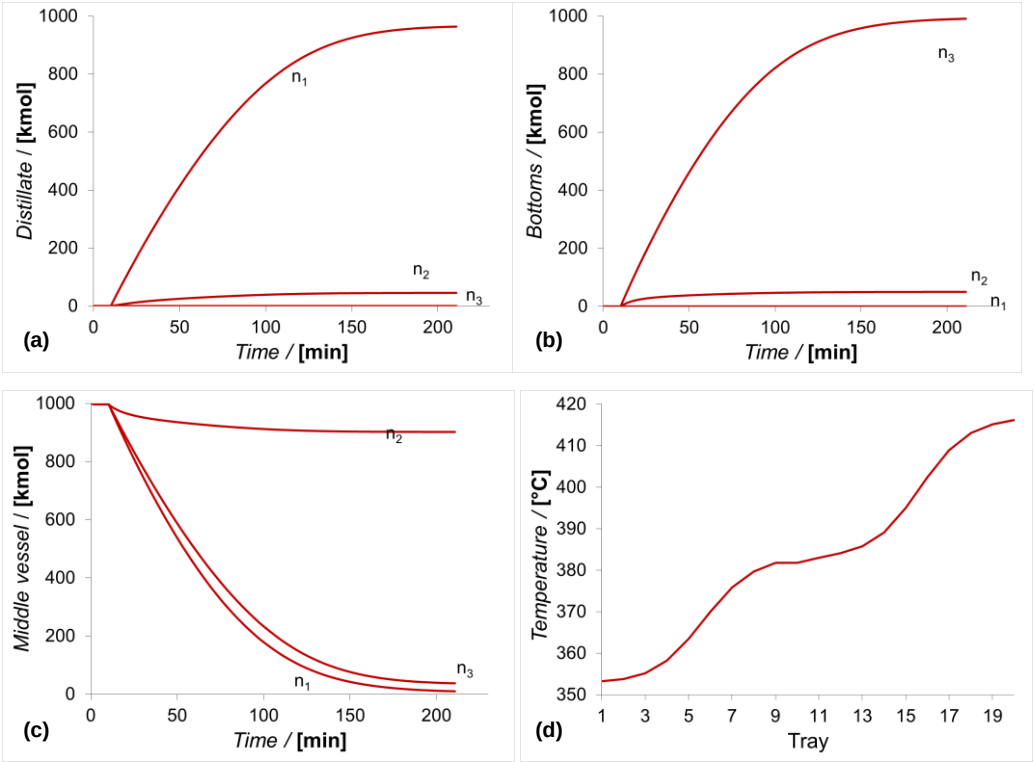

Fig. 5. Middle-vessel distillation – configuration A. T_{SP1} = 355 K, T_{SP2} = 413.5 K, L_i= 55 kmol/h. (a) – (c): Distillate, Bottoms and Middle vessel composition. (d): Temperature profile at the end of distillation

Configuration B

In this section, the results for the case when the vapours pass through the middle vessel are presented.

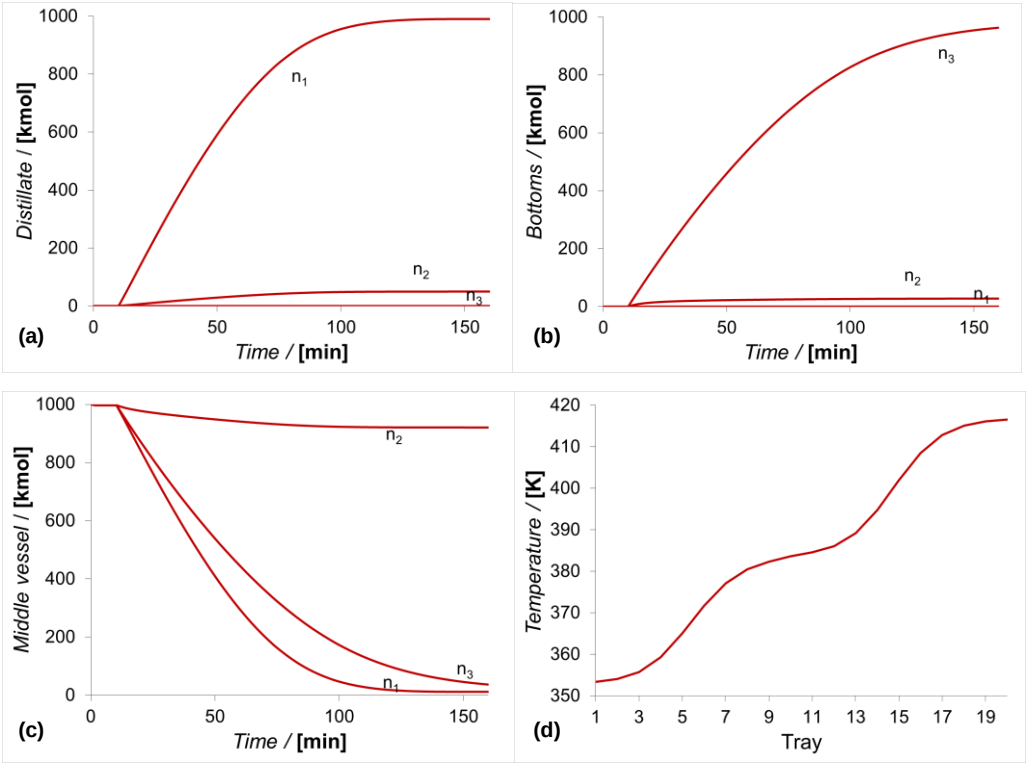

Fig. 6. Middle-vessel distillation – configuration B. T_{SP1} = 355K, T_{SP2} = 413.5 K, L_b = 55 kmol/h. (a) – (c): Distillate, Bottoms and Middle vessel composition. (d): Temperature profile at the end of distillation

A large amount of benzene is found in the distillate (Fig. 6 – (a)). Xylene is obtained as main product in bottoms (Fig. 6 – (b)) and toluene in the middle vessel (Fig. 6 – (c)). More than that, Fig. 6 – (c) shows that the most volatile compound is removed faster than the one with high boiling point. At the end of the distillation the toluene from the middle vessel will be mostly contaminated with xylene. The molar fraction for the low, intermediate and high volatile compounds at the end of the distillation are 95.19 %, 95 % and 97.23 %.

The temperature increases along the column (Fig. 6 – (d)). Near middle vessel the temperature varies less compared with the plate zones in the upper and lower section of the column. This happens due of the temperature differences of the vapour that pass in the middle vessel and of the liquid present there.

The necessary time for distillation is 160 min, shorter than the one obtained when the mixture was separated using Configuration A. The energy consumption is also improved, this time only 257 MJ being necessary to entertain the process.

4. Discussions

For the purpose of analyzing the performance of middle vessel column two models were investigated: when the vapour from the bottom section (configuration A) are directed to the upper section and when the vapour from the bottom section are directed to the middle vessel (configuration B). More than that, two operation strategies were proposed: in the first one the liquid flow from the upper section and the vapours are kept constant and in the second one, these are changed in time.

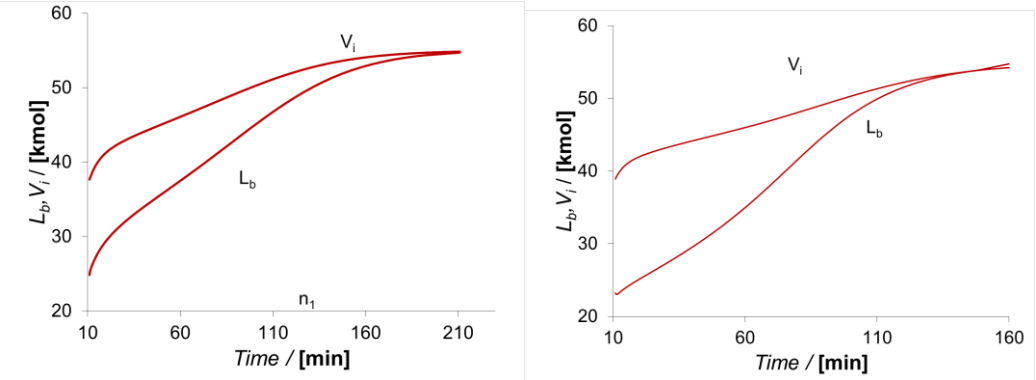

Fig. 7. Liquid flow in the upper section and vapour flow through the column during distillation (Configuration A - left, Configuration B - right) – operation with variable L_b and V_i.

Operation at constant parameters lead to greater values for energy demand and batch time and lower purities for the final products. This behaviour is caused by using the same operating parameters at different composition profiles in columns.
The performance of the middle vessel column is improved when an operation strategy with variable V_i and L_b is used. The distillation time is reduced by more than half and the energy consumed is more than three times smaller.
When operated at constant tray temperature, Configuration A works with a greater liquid flow than B (Fig. 7). In the both studies presented, the results for configuration B are more convenient (Table 3).

Table 3.

The results of the mathematical models for Configuration A and B when an operation strategy with constant and L_b and V_i is used.

Parameters	Configuration A		Configuration B	
	Constant L_b, V_i	Variable L_b, V_i	Constant L_b, V_i	Variable L_b, V_i
T_{SP1} / [K]	-	355	-	355
T_{SP2} / [K]	-	413.5	-	413.5
L_b / [kmol]	58	varies	58	Varies
L_i / [kmol]	62	55	62	55
V_i / [kmol]	60	varies	60	Varies
$x_{benzen,\ distillate}$	0.919	0.955	0.968	0.952
$x_{xylene,\ bottoms}$	0.934	0.952	0.968	0.950
$x_{toluene,\ middle\ vessel}$	0.970	0.950	0.970	0.972
t / [min]	545	211	520	160
Q_{total} / [MJ]	1134	353	1086	257

5. Conclusions

- Middle vessel distillation column is an attractive option for batch separation of a ternary mixture
- Operation at constant liquid and vapour flow is time consuming and requires more energy, because the concentration profile is changing with time in column.
- The energy requirement and batch time is reduced and superior values for purities are obtained when an operation strategy with variable liquid and vapour flow is used.
- Configuration with vapour passing through middle vessel is more convenient from the point of view of energy demand, batch time and products quality.

6. Nomenclature and Abbreviations

D = distillate flow, [kmol/min]
i = component number (1-3)
k = stage number
K_c = controller gain, [(kmol/min) / K]
L_b = liquid flow in the upper section of the column, [kmol/min]
L_i = liquid flow in the bottom section of the column, [kmol/min]

L^* = proposed liquid flow of controller [kmol/min]
m = total number of components in the mixture
n_i = molar quantity of i, [kmol]
NT = total number of trays
NI = middle vessel tray number
P = working pressure, [atm]
$P_{vap,i}$ = vapour pressure of *i*, [atm]
Q = energy demand, [MJ]
$\bar{r}$ = latent heat, [kmol/min]
t = time, [min]
T = temperature, [K]
T_i = integration time
$T_{SP1/2}$ = temperature set point of controller, [K]
V_b = vapour flow in the upper section, [kmol/min]
V_i = vapour flow in the lower section, [kmol/min]
x = molar fraction in liquid
y = molar faction in vapour
W = bottoms flow, [kmol/min]

Acknowledgement

C.S. Bildea gratefully acknowledges the financial support of the European Commission through the European Regional Development Fund and of the Romanian state budget, under the grant agreement POC P-37-449 (acronym ASPiRE).

REFERENCES

[1] Sorensen, E., 2014, Design and Operation of Batch Distillation. Oxford, Elsevier, Vol. Distillation: Fundamentals and Principles, 187-220.
[2] Diwekar, U, 2012, Batch distillation - simulation, optimal design and control. New York, CRC Press, 139-159
[3] Kim, K., Diwekar, U., 2005, Batch Processes. Cincinnati, CRC Press, 107-147
[4] Rao, C., Barik K., Modeling, Simulation and Control of a Middle Vessel Distillation Column. Procedia Engineering Elsevier, 38, (2012), 2383-2397.
[5] Barolo, M., et al. Some issues in the design and operation of a batch distillation column with a middle vessel. *Computers Chem. Eng*, 20, (1996), 37-42.
[6] Warter, M., Demicoli, D.. Stichlmair, J., Batch Distillation of Zeotropic Mixtures in a Column with a Middle Vessel. *European Symposium on Computer Aided Process Engineering*, 12, (2002), 385-391.
[7] Hegely, L., Lang, P., Study of Closed Operation Modes of Batch Distillation Columns. *21st European Symposium on Computer Aided Process Engineering*, 21, (2011), 1050-1055.

PARETO-OPTIMAL OPERATING POLICIES OF A MECHANICALLY AGITATED SEMICONTINUOUS REACTOR USED FOR THE OXIDATION OF D-GLUCOSE ON CO-IMMOBILIZED PYRANOSE OXIDASE AND CATALASE

Mara CRIȘAN, Gheorghe MARIA[1]

University Politehnica of Bucharest, Department of Chemical & Biochemical Engineering

Abstract

One essential engineering problem when developing an industrial enzymatic process concerns the choice of the reactor operating alternative based on à-priori knowledge of the process kinetics and enzyme inactivation characteristics. For a multi-enzymatic system, involving complex interactions among enzymes that exhibit optimal activity on different parametric domains, and a high-order deactivation, this problem requires an extended analysis. The engineering problem becomes difficult when a multi-objective optimization problem is formulated. An elegant option developed in this paper is to obtain sets of Pareto optimal solutions, also called Pareto-optimal fronts, each one generated for the case of at least two adverse objectives. Then, the final choice of the enzymatic reactor operating policy results from the comparative analysis of these fronts. Exemplification is made for the case of the oxidation of D-glucose (DG) to 2-keto-D-glucose (kDG) in the presence of P2Ox (oxygen 2-oxidoreductase, EC 1.1.3.10) and catalase, mechanically agitated continuous reactor (MASCR) with co-immobilized enzymes on alginate beads. Optimal reactor choice is based on the minimum amount of required P2Ox that ensures an imposed reaction conversion and maximum reactor productivity under various technological constraints, at 30°C and various catalase / P2Ox ratios.

Keywords: mechanically agitated reactor optimization; D-glucose oxidation; pyranose oxidase; catalase; Pareto-optimal fronts; optimal operating policies.

1. Introduction

Multi-enzymatic reactors exhibit a wide range of applications (Fig. 1). When developing an industrial enzymatic process, one essential engineering problem concerns the choice of the reactor optimal operating policy based on à-priori knowledge of the process kinetics and enzyme inactivation characteristics. For a multi-enzymatic system, involving complex interactions among enzymes that exhibit optimal activity on different parametric domains, and a high-order deactivation, this problem requires an extended analysis (Fig. 2). The engineering problem becomes difficult when a multi-objective optimization problem is formulated. An elegant option developed in this paper is to obtain sets of Pareto

[1] Corresponding author. Email address: gmaria99m@hotmail.com

optimal solutions, also called Pareto-optimal fronts, each one generated for the case of at least two adverse objectives. Then, the final choice of the enzymatic reactor operating policy results from the comparative analysis of these fronts.
The aim of this paper is to extend the MASCR optimization analysis step, by determining multiple Pareto-front optimal solutions generated for successive pairs of adverse objectives, thus facilitating the final choice of the optimal setpoint.
Exemplification is made for the case of the oxidation of D-glucose (DG) to 2-keto-D-glucose (kDG) in the presence of P2Ox (oxygen 2-oxidoreductase) and catalase, continuously operated in a mechanically agitated semicontinuous reactor (MASCR) with co-immobilized enzymes on alginate beads (Fig. 3).

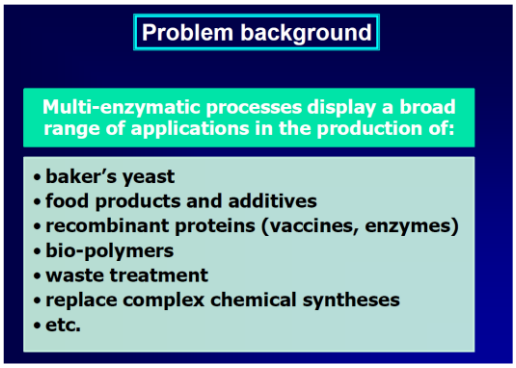

Fig. 1. Multi-enzymatic reactors exhibit a wide range of applications [1,2]

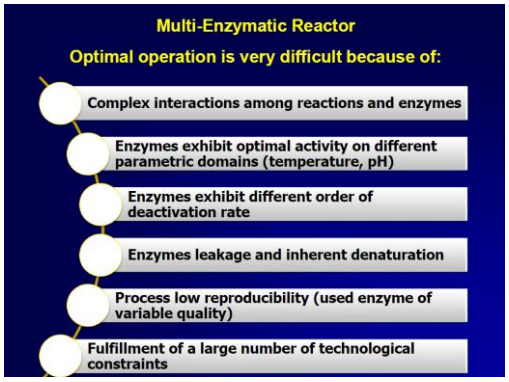

Fig. 2. Optimal operation of multi-enzymatic reactors is a major but difficult engineering problem [1].

2. The math models of the enzymatic process and MASCR reactor

The MASCR reactor is a semicontinuously operated three-phase-fluidized-bed reactor (TPFB) with the two enzymes (P2Ox, and catalase) co-immobilized on alginate beads (Fig. 3). The kinetic model of the bi-enzymatic process of D-glucose oxidation on P2Ox and catalase is presented in Fig. 4 [1,4-5].
To perform the MASCR optimization, a dynamic ideal model was adopted from literature [1,3] corresponding to an isothermal, perfectly mixed reactor of constant volume, with vigorous aeration and mechanical stirring, fed with substrate solution, and including suspended solid particles (spherical beads) with immobilized enzymes (Fig. 5). The current model also considers P2Ox activity decay due to their chemical interactions, but also due to its leaking following the hydrodynamic stress, and its inherent denaturation over time (see P2Ox balance in Fig. 3.). The MASCR reactor main characteristics and nominal conditions are presented in the Fig. 3.

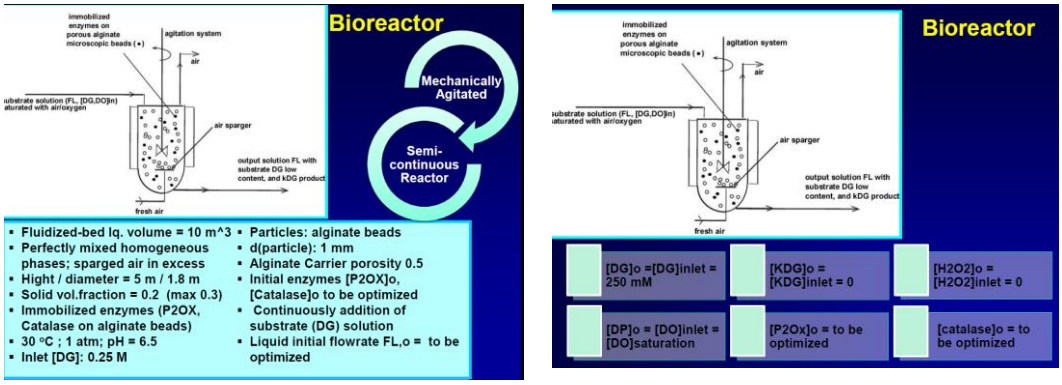

Fig. 3. The main characteristics and nominal operating conditions (left) of the semi-continuous MASCR enzymatic reactor used for D-glucose oxidation [1,2]. (right) Batch initial conditions.

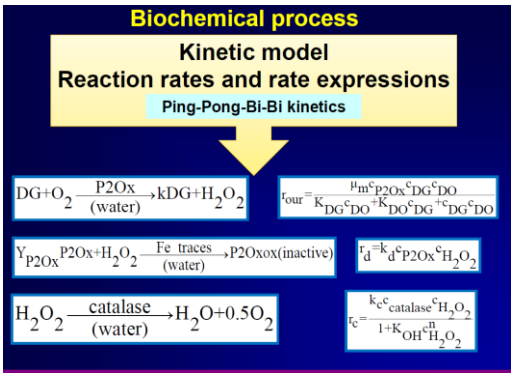

Fig. 4. The kinetic model of the enzymatic oxidation of D-glucose on P2Ox and catalase [1,4-5]

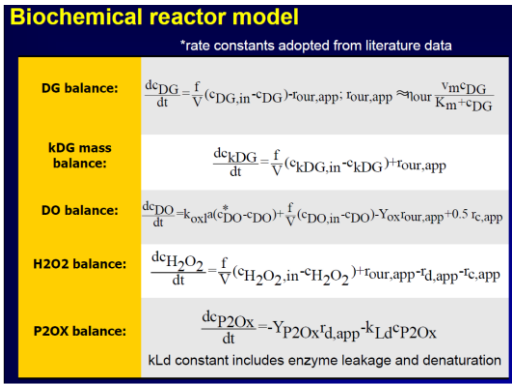

Fig. 5. The semi-continuous MASCR enzymatic reactor model used for D-glucose oxidation [1,4-5]

3. Formulation of the optimization problem for the MASCR enzymatic reactor operation

The optimal operating policy choice is that requiring minimum P2Ox amount but ensuring an imposed reaction conversion and maximum reactor productivity under various technological constraints (Fig. 6). These three considered optimization objectives are presented in the Fig. 6 in a math formulation.

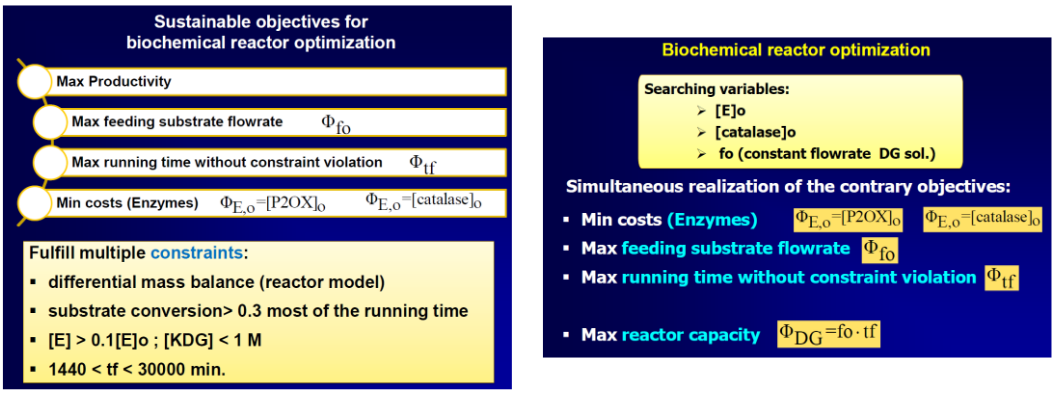

Fig. 6. (left) The considered three objectives for optimization of the MASCR enzymatic reactor used for D-glucose oxidation, and technological constraints [1,4-5]. (right) Optimization objectives, and searching variables [1].

One elegant and more precise option is to obtain the set of Pareto optimal solutions, also called Pareto-front for the case of only two adverse objectives. A Pareto solution is one where any improvement in one objective can only take place at the cost of the other objective, being in fact the best trade-off between the two objectives (Fig. 7). The disadvantage of the Pareto-front optimal solutions is the existence on the Pareto-curve of infinity of optimal operating solutions.
By inspecting the formulated objectives of Fig. 6, it can be easily observed that most of them are adverse, that is realization of one of them is made to the detriment of another. For instance, realization of Φ_{fo} and Φ_{DG} requires lot of $c_{E,s,o}$, which, in turn, will lead to the diminishment of $\Phi_{E,o}$. Consequently, the following Pareto problems have been formulated by considering pairs of adverse objectives, as followings (Fig. 7):
Pareto-front no. 1 (PF1): $\Phi_{E,o}$ (f2) vs. Φ_{fo} (f1)

Pareto-front no. 2 (PF2): Φ_{tf} (f2) vs. Φ_{fo} (f1)

Pareto-front no. 3 (PF3): $\Phi_{E,o}$ (f2) vs. Φ_{DG} (f1)

4. Derivation of the Pareto optimal fronts and result discussion

To obtain the best trade-off optimisation solution, when multiple Pareto-optimal fronts exist (three in the present case, see the previous chapter, and PF1-PF3 in the Fig. 8), Maria and Crișan [1] proposed a three-step computational strategy, as following (Fig. 8):
i) a setpoint (SP) from PF1 is chosen that better matches the objectives of Fig. 6. Then, ii) a check of the operating policy is performed by process

simulation to examine the realized t_f without constraint violation and, iii) finally, the validity of the chosen SP is checked again in relation to PF2 and PF3.

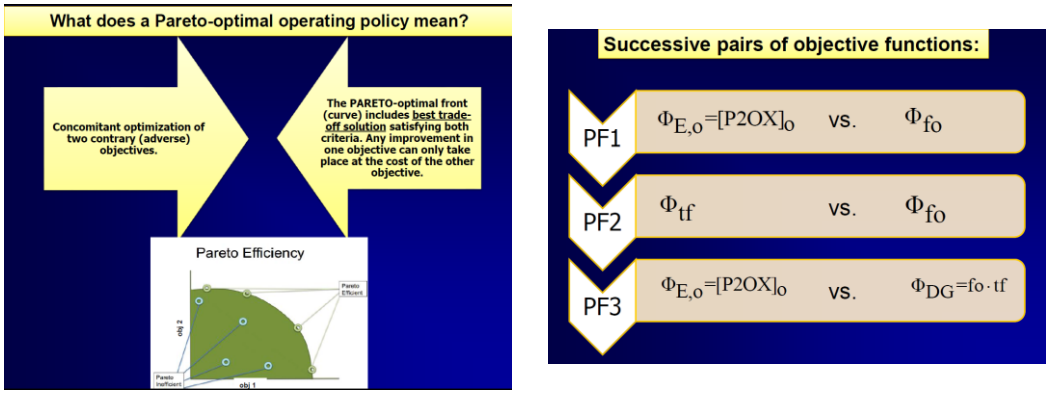

Fig. 7. (left) Explanation of the Pareto-optimal front method [1]. (right) The two-by-two Pareto-optimal fronts (PF1-PF3) formulated using the three objectives for optimization of the MASCR enzymatic reactor used for D-glucose oxidation. [1].

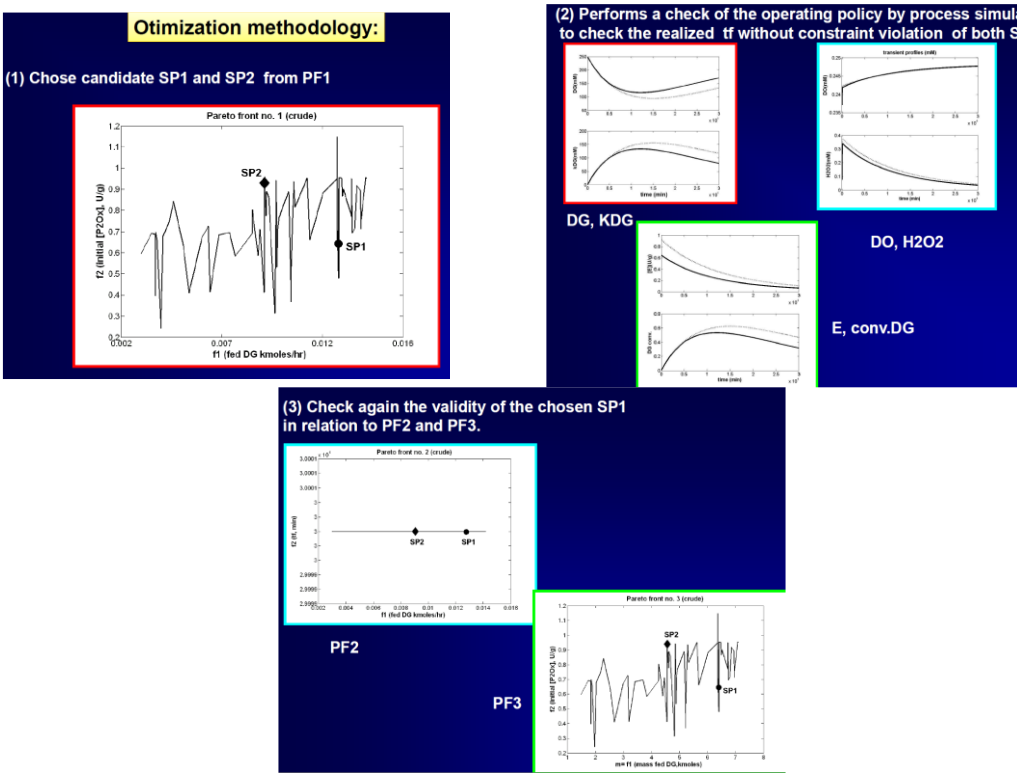

Fig. 8. The three-step methodology proposed by Maria and Crișan [1] to get the optimal setpoint SP1, based on the three Pareto-optimal fronts PF1-PF3.

To exemplify this proposed procedure, two candidate setpoints were selected, that is SP1 and SP2, displayed in Fig. 8, with [[P2Ox]s,o(U/g); [catalase]s,o(U/g); FL,o(kmol DG/hr.)] of the following values for SP1= [0.65; 170; 0.013], and SP2=[0.922; 204; 0.009]. The SP1 was selected because it uses low initial amount of P2Ox enzyme (that is [P2Ox]o= 0.65 U/g), a relatively high DG-solution feed flow-rate (0.013 kmol DG/h), and a lower catalase initial amount ([Catalase],o= 170 U/g). For comparison, the selected SP2 from PF1 (plotted in Fig. 8), uses a higher initial amount of P2Ox enzyme ([P2Ox],o= 0.922 U/g), a lower DG-solution feed flow-rate (0.009 kmol DG/h), and a higher catalase initial amount ([Catalase],o= 204 U/g). It clearly appears that SP2 operating policy is inferior to SP1 in terms of several objectives.

To check the validity of the SP1 choice, the dynamics of the MASCR was comparatively simulated for SP1 and SP2 setpoints using the process/reactor model of Fig. 4-5. The obtained state-variable trajectories comparatively plotted in Fig. 8-up, reveal some important conclusions: I) all constrains (4) are fulfilled over the whole running time [0, tf = 30000 min]; ii) the reactor presents a transient regime tending to the steady-state which is never reached due to the continuous decline of the P2Ox (E) enzyme activity; iii) DG-conversion is higher than the imposed threshold of 0.3 for most of the running time; iv) operation is stopped after tf = 30000 min when enzyme activity is too low, i.e. [E]s< 0.1 [E]s,o, where E = P2Ox.

By calculating the reactor productivity objective m = Φ(DG) for both of the tried setpoints, it results the values 6.375 kmoles DG for SP1 and 4.55 kmoles DG for SP2. These values sit perfectly on the PF2-curve in Fig. 8, confirming that SP1 is superior to SP2 concerning the reactor productivity. The same result is obtained when the two SP-s are plotted on the PF3 in Fig. 8. The policy SP1 realizes a higher productivity m = Φ(DG) using a smaller amount of initial enzyme [P2Ox]o.

Finally, based on this successive and comparative analysis of the optimal PF1- PF3 we can retain the SP1 as being the optimal operating policy of the MASCR that realizes the best trade-off between the formulated optimization objectives in the presence of the technological constraints of Fig. 6.

5. Conclusions

Derivation of the most suitable operating alternative and reactor type for multi-enzymatic systems of complex kinetics is a difficult task, requiring: I) steady experimental efforts to get enough information on the process kinetics, on the free-/immobilized-enzyme stability and optimal activity conditions and, ii) an intensive model-based computational analysis to determine alternative operating

policies of the reactor realizing the best trade-off among adverse/concurrent criteria, such as a high imposed conversion, a high reactor productivity, and enzyme minimum consumption in the presence of multiple technological constraints.
The employed method to generate Pareto-optimal fronts for pairs of adverse optimization objectives, followed by their comparative analysis facilitates decisions concerning optimal operating alternatives, by determining the operating condition limits within the operation of a certain reactor is economically efficient. By paying the cost of a relatively high computational effort, the proposed model-based approach to solve the reactor optimization problem presents the advantage of finding the best design alternative, by pointing out differences between operating policies in terms of flexibility, productivity, and substrate/enzyme consumption.

Acknowledgment. First author is grateful for the participation grant to the 20th Romanian International Conference on Chemistry and Chemical Engineering offered with generosity by the Romanian Chemical Engineering Society.

REFERENCES

[1] *Maria, G., Crișan, M.,* Evaluation of optimal operation alternatives of reactors used for D-glucose oxidation in a bi-enzymatic system with a complex deactivation kinetics, *Asia-Pacific Journal of Chemical Engineering*, 10 (2015) 22-44. DOI: 10.1002/apj.1825.
[2] *Crișan, M., Maria, G.,* Pareto-optimal Operating Policies of a Mechanically Agitated Continuous Reactor used for the Oxidation of D-Glucose on co-Immobilized Pyranose Oxidase and Catalase, 20th Romanian International Conference on Chemistry and Chemical Engineering, Poiana Brasov (Romania), 6-9 Sept. 2017. http://riccce20.chimie.upb.ro/
[3] *Maria, G.,* Enzymatic reactor selection and derivation of the optimal operation policy by using a model-based modular simulation platform, *Computers & Chemical Engineering* 36 (2012), 325–341. DOI: 10.1016/j.compchemeng.2011.06.006.
[4] *Maria, G., Ene, M.D., Jipa, I.,* Modelling enzymatic oxidation of D-glucose with pyranose 2-oxidase in the presence of catalase, *Journal of Molecular Catalysis B: Enzymatic*, 74 (2012) 209-218.
[5] *Ene, M.D., Maria, G.,* Temperature decrease (30-25°C) influence on bi-enzymatic kinetics of D-glucose oxidation, *Journal of Molecular Catalysis B: Enzymatic*, 81 (2012) 19-24.

FOAM GLASS PRODUCED BY MICROWAVE HEATING TECHNIQUE

Lucian PAUNESCU[1*], Bogdan Traian GRIGORAS[1], Marius Florin DRAGOESCU[1], Sorin Mircea AXINTE[2], Alexandru FITI[3]

[1] Daily Sourcing & Research SRL, 95-97 E CaleaGrivitei, sector 1, 010705, Bucharest, Romania
[2] University "Politehnica" of Bucharest, Department of Applied Chemistry and Materials Science, 1-7 Gh. PolizuStreet,sector 1, 011061, Bucharest, Romania
[3]Cosfel Actual SRL, 95-97 E Calea Grivitei, sector 1, 010705, Bucharest, Romania

Abstract

An important contribution to the improvement of the manufacturing process of foam glass from waste by the use of microwave energy is presented in the paper. The powder mixture of waste glass and foaming agent (calcium carbonate), introduced into a silicon carbide crucible with thin wall (2.5 mm) and subjected to microwave irradiation, is preponderantly direct heated up to the sintering and foaming temperature, the center of high temperature being initiated in the middle of sample and partially indirect by the thermal radiation of the inner surface of the crucible wall. The process is significantly intensified compared to the case of using a thick wall crucible (of over 20 mm), the heating duration and the specific consumption of electricity being reduced, obtaining similar physical, mechanical and structural characteristics of the foam glass.

Keywords*:* Foam glass, Waste glass, Microwave, Silicon carbide crucible, Direct heating.

1. INTRODUCTION

In the last decades the interest in recycling of various materials is a result of the requirements of a sustainable development. The glass recycling, due to its high amount of material involved, is one of the most important domains. The deposits of glass, which in Romania are estimated at some hundred thousand tones/ year, became a valuable resource for the foam glass industry. By its properties, foam glass is one of the certitudes in the future of the market of building materials. This is a vitreous material with a porous macrostructure obtained by a thermal treatment at high temperatures (700 – 1100 ºC) of waste glass by addition of a foaming agent. In a more complicated composition, with additives like fly ashes and others, the resulted material is a glass-ceramic with the same macrostructure and different mechanical properties. For both materials the commercial name is "foam glass".

Its main features are low density and thermal conductivity and, in the same time, a good mechanical strength, being usable as thermal and sound insulator, floors and wall tiles, architectural panels, filters, absorbers, gas sensors. Also, it can be used as aggregate for

* Corresponding author, Email address: lucianpaunescu16@gmail.com

lightweight concrete, in road construction, infrastructures foundations, sports grounds etc. [1 – 3].

The current paper presents the achievements in using the microwave heating in the manufacture of the vitreous material with the macrostructure of the “foam glass”.

In the last year the Romanian company Daily Sourcing & Research SRL Bucharest carried out several experiments for manufacturing the foam glass from waste bottle glass, using the microwave energy. This economical, fast and “clean” heating technique is not yet used in the making process of foam glass, worldwide being preferred the conventional techniques (fuels burning or electric resistances) [3, 4]. The experiments carried out in the company Daily Sourcing & Research used different foaming agent types, additional materials, technological equipment and tools. The processing methods of the raw material and foaming agent mixture consisted in the finely grinding and homogeneity and, in some cases, their water wetting and pressing. Having an experimental character, all tests were carried out in a discontinuous operation regime, with low thermal efficiency and high specific consumption of electricity, higher than the industrial continuous processes. The research results are shown in the work [5] and other several papers in process of publishing in Romania [6 - 8].

The first scientific observations on the influence of microwave radiation on the glass have been issued by M. Knox and G. Copley in their work [9], taken over later by other authors [1, 3]. These remark that at the ambient temperature the commercial glass compositions are not transparent to the microwave radiation. However, at higher temperatures (over 500 ^{o}C) the glass structure relaxes and the microwave absorption increase rapidly, producing the glass heating.

Referring to the industrial manufacturing process of foam glass using preponderantly waste glass as raw material and having into account the feature of this material noted above, J. Hurley recommends in his work [3] the use of electric resistances to preheat the material up to 500 ^{o}C in the first part of the length of a tunnel type oven and further the use of the microwave energy up to the sintering temperature at which the foaming is produced. These considerations, which will be challenged by the experimental results presented in the current paper, influenced negatively the development of the manufacturing techniques of foam glass based on the microwave energy, worldwide being used at an industrial scale only the conventional heating techniques (fuels consumption or electric resistances).

Because, between all tested techniques of producing foam glass, the most economical is the technique of using calcium carbonate as foaming agent, which allows to revaluate the waste glass in very high proportions and the sintering and foaming temperature has the lowest values, the experiments presented in the paper were oriented to this manufacturing method.

The literature contains more information about the use of calcium carbonate as foaming agent. This material is used in weight proportion of 5% to obtain foam glass from certain silicate wastes (cathode ray tube glass or oil shale ash [2, 10, 11]. Other authors [12] produce foam glass from coal ash and waste glass in 40/ 60 weight ratio using only 0.5 wt.% calcium carbonate and a supplementary addition (30 wt.%) of borax as fluxing agent. Also, a very low weight proportion of calcium carbonate (1%) is used to manufacture a foam glass with high porosity from 99 wt.% waste glasses [13]. The powder mixture of raw material and foaming agent is homogenized and pressed at 40 MPa in conditions of 8 wt.% humidity. The technique of water wetting the powder mixture in the case of using calcium carbonate as foaming agent is recommended also in the paper [1]. All manufacturing techniques of the foam glass described above are based on conventional heating methods (fuels consumption or electric resistances).

2. EXPERIMENTAL WORK

2. 1. Methodology of experimentation

As previously noted, the team of researchers from Daily Sourcing & Research conducted several experiments to produce foam glass using the microwave energy. The current paper refers to techniques for obtaining this product from waste bottle glass (98.0 – 99.0 wt.%) using calcium carbonate (0.1 – 2.0 wt.%) as foaming agent. The powder mixture of these components obtained by fine grinding, homogenization and pressing offers the advantages of a lower foaming temperature (below 900 ºC) compared to the use of other foaming agent (so, with a smaller consumption of electricity) as well as a very high revaluation degree of waste glass (over 98%).

The thermal decomposition of calcium carbonate applied in the foaming process of waste glass consists in releasing the carbon dioxide inside the viscous glass mass in the temperature range 730 – 900 ºC [14]. An appropriate viscosity ensures blocking the gas and its pressure is gradually increased, forcing the expansion of the melted glass mass. By the subsequent cooling, the melted glass is solidified forming a cellular structure. A maximum expansion of a soda-lime colourless glass of over 450% can be obtained with 2 wt.% calcium carbonates [1].

Also, by the decomposition of calcium carbonate, the calcium oxide is released, being incorporated in the melted glass mass. It acts as a modifier of the glass, whose viscosity is altered [1]. A low addition of calcium oxide, resulted from the carbonate decomposition, contributes to forming a melting with high surface tension, but low viscosity, allowing the increase of the melted glass volume by expansion.

The glass foaming by addition of calcium carbonate is improved by wetting the glass particles, due to that the partial leaching the alkaline metal oxides from the glass surface produces the adhesion of particles at lower temperatures compared to the temperature of the beginning the decomposition of calcium carbonate [1]. According to the work [15], it was found that the water is suitable to obtain very low pore size in the foam glass mass.

The thermal decomposition of calcium carbonate occurs according to the following reaction:

$$CaCO_3 = CaO + CO_2 \quad (1)$$

The equipment used for the experiments is a 0.8 kW domestic microwave oven adapted to working at high temperature around 1000 ºC, mainly, by replacing the usual rotation mechanism with one made of a high temperature resistant material and air cooling of some components (figure 1). The powder mixture is loaded into a silicon carbide crucible placed on a support which is rotated around its axis during the operation of the magnetron. To avoid the thermal losses, the side wall and the upper area of the crucible are protected with ceramic fiber. For the same reason, the crucible is placed on ceramic fiber mats and a ceramic refractory material mounted above the mobile component of the oven rotation mechanism.

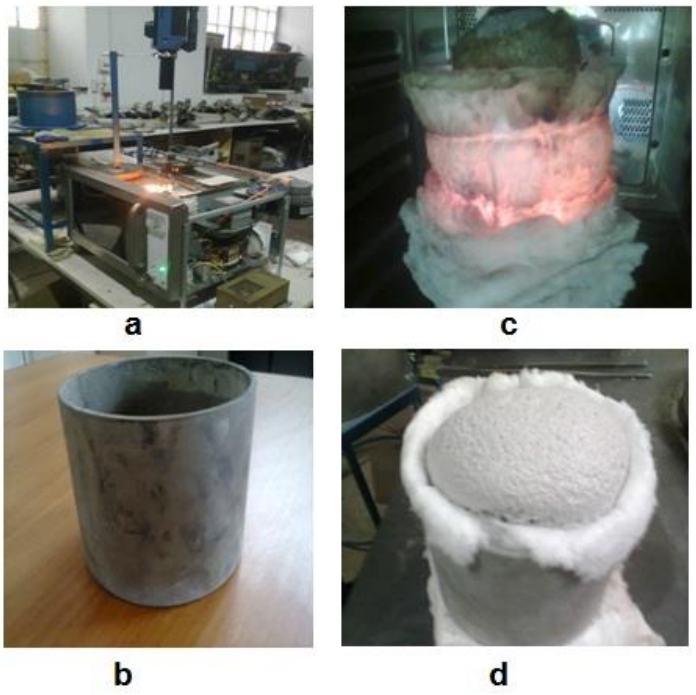

Fig. 1. 0.8 kW microwave oven adapted to produce foam glass
a – microwave oven; b – silicon carbide crucible with thin wall; c - image of the crucible during the foaming process into the oven; d - image of the crucible at the end of process.

Previous tests carried out on this experimental equipment, whose results are presented in the paper as reference data, used a cylindrical silicon carbide crucible with the wall thickness of 20 mm, the inner diameter of 130 mm and the height of 100 mm. Silicon carbide is a microwave susceptible material. Due to the large thickness of the crucible, this material largely absorbs the microwaves, converting their energy in thermal energy and causing the fast and high heating of the crucible wall. The powder mixture inside the crucible receives the necessary heat in the sintering and foaming process preponderantly by thermal radiation.

The last experiments on the same microwave oven described above are based on ensuring technical conditions for preponderantly microwave direct heating of the powder mixture, involving the penetration of the silicate carbide crucible wall by the microwave field emitted by the magnetron. The wall thickness of the new crucible made from the same material is only 2.5 mm, its inner diameter and height remaining unchanged (see figure 1b).

2. 2. Raw material

The chemical composition of waste bottle colourless glass used as raw material is shown in table 1.

Table 1

Chemical composition of waste bottle colourless glass

SiO_2	Al_2O_3	CaO	MgO	Na_2O
71.8	1.9	12.0	1.0	13.3

The recycled waste bottle glass was broken and ground in a ball mill, its grain size being below 130 μm.

Calcium carbonate was used without other mechanical processing such as it was purchased from the market, having a very fine grain size below 40 μm.

After the dosage of the raw material and foaming agent amounts, the powder mixture was homogenized together with the water addition amount in a low size laboratory installation.

2.3. Characterization of the foam glass samples

The foam glass samples, resulted after the sintering process described above, were tested in laboratory to determine the physical, mechanical and structural characteristics. The characterizations were performed in Daily Sourcing & Research SRL Bucharest, Faculty of Applied Chemistry and Materials Science of University "Politehnica" of Bucharest and Metallurgical Research Institute, aiming apparent density, porosity, water absorption, compressive strength, thermal conductivity, hydrolytic stability and crystallographic structure of the foam glass samples.

The apparent density was determined by the gravimetric method with the pycnometer [16]. The porosity was calculated by the comparison method of true and apparent densities of the material, experimentally measured [17]. The volumetric proportion of the water absorption was determined by the method of water immersion of the sample (for 30 minutes). Determining the thermal conductivity was performed by the guarded-comparative-longitudinal heat flow technique, according to ASTM E 1225 – 04. The compressive strength was measured with an uniaxial hydraulic press. The hydrolytic stability of the samples was measured by the standard procedure ISO 719:1985 with a 0.01M HCl solution [18, 19].

3. EXPERIMENTAL RESULTS AND DISCUSSION

The experiments, whose results are shown in this chapter, aimed to highlight the influence of the microwave susceptible character of the raw material mixture during the producing process of foam glass (direct heating) compared to the indirect heating method by the thermal radiation of the crucible wall. Practically, the difference between the two heating methods is obtained by sizing the wall thickness of the silicon carbide crucible, which allows or not its penetration by the microwave field. The experiments were carried out using successively two constructive variants of crucible, with the wall thickness of 2.5 mm (for direct heating) and, respectively, 20 mm (for indirect heating).

Six variants of weight proportions of the components of raw material mixture, presented in table 2, were tested in conditions of using the thin wall crucible (variants A1 – A6) and the thick wall crucible (variants B1 – B6).

Table 2

Distribution of the powder mixture components, wt.%

Variant	Waste bottle colourless glass	Calcium carbonate	Water addition
1	98.0	2.0	8.0
2	99.0	1.0	8.0
3	99.3	0.7	10.0
4	99.5	0.5	10.0
5	99.7	0.3	13.0
6	99.9	0.1	20.0

The main parameters of the sintering and foaming process corresponding to the two constructive variants of crucible are presented in table 3.

Table 3

Parameters of the sintering and foaming process

Var.	Raw material/ foam glass amount (g)	Sintering and foaming temperature (ºC)	Average speed, (ºC/ min)		Heating process duration (min)	Specific consumption of electricity (kWh/ kg)
			Heating	Cooling		
A. Thin wall crucible (2.5 mm)						
A1	235/ 224.0	830	26.4	5.6	31	1.60
A2	235/ 223.3	822	26.9	5.8	30	1.50
A3	235/ 222.6	827	26.7	5.4	30	1.55
A4	235/ 223.1	825	26.5	5.3	30	1.53
A5	235/ 223.2	830	25.4	5.5	32	1.60
A6	235/ 222.8	829	26.6	5.6	31	1.58
B. Thick wall crucible (20 mm)						
B1	235/ 222.8	845	16.2	5.9	51	3.05
B2	235/ 223.0	840	17.1	6.5	48	2.87
B3	235/ 222.8	845	16.5	6.5	50	2.99
B4	235/ 223.1	852	15.1	5.9	55	3.29
B5	235/ 222.9	850	15.7	5.8	53	3.17
B6	235/ 223.3	845	16.2	5.3	51	3.05

The main observations resulted from the data presented in table 3 are: very high increase (with 64%) of the heating speed from 16.1 ºC/ min (average value of variant B) to 26.4 ºC/ min, decrease of the heating process duration from 46.3 min (variant B) to 30.7 min (variant A) i.e. with 33.7% as well as the significant reduction (with 49.2%) of the specific consumption of electricity from 3.07 kWh/ kg (variant B) to 1.56 kWh/ kg (variant A). Excepting the wall size of the two crucibles, the other test conditions were similar for both variant.

Obviously, these significant changes of the functional parameters of process are due to the differences caused by the way heat is transmitted to the material by direct or indirect heating.

The graph in figure 2 is suggestive of accelerating the process in the case of preponderantly direct heating comparative to the process achieved by indirect heating.

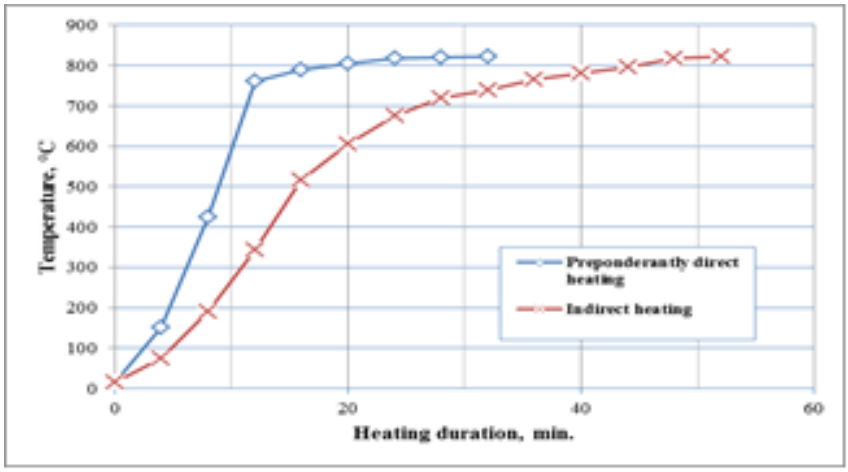

Fig. 2. The graph of microwave direct (preponderantly) and indirect heating of the raw material based on waste glass

Previous tests of microwave direct heating carried out in the adapted 0.8 kW domestic microwave oven on samples obtained by pressing the powder mixture, placed in the microwave field, demonstrated experimentally that the mixture reaches rapidly the sintering and foaming temperature (820 – 850 ºC), starting from the ambient temperature. The thermal process begins inside the sample, where the temperature increases rapidly, directly influenced by the microwave radiation. The foaming process is produced from inside and is propagated to the peripheral area of the sample (see figure 3).

Fig. 3. The direct microwave heating test of the powder mixture based on waste glass

The test result is opposable to M. Knox and G. Copley's theory of glass feature being microwave susceptible only at over 500 ºC [9]. Thus, the technical solution of preponderantly direct heating of the mixture based on waste glass from the ambient temperature became practically viable.

The main disadvantage of the microwave direct heating is the extremely high heating speed, which generates major imbalances in the structure of the material (non-homogeneous structure characterized by high pore size, sometimes even containing very large goals). Therefore, it is necessary to simultaneously perform direct (preponderantly) and indirect heating, achievable by using the silicon carbide crucible with thin wall.

The physical, mechanical and structural features of the foam glass samples experimentally determined are shown in table 4.

Table 4

Physical, mechanical and structural characteristics

Var.	Index of volume growth	Apparent density, (g/ cm^3)	Porosity, (%)	Compressive strength, (MPa)	Thermal conducti-vity, (W/m·K)	Water absorp-tion, (%)	Pore size, (mm)
A. Thin wall crucible (2.5 mm)							
A1	1.75	0.46	79.0	1.9	0.054	6.6	0.6 – 1.7
A2	2.00	0.36	83.6	1.3	0.042	5.9	0.5 – 1.5
A3	1.55	0.45	79.5	1.9	0.055	5.3	0.4 – 1.3
A4	1.50	0.46	79.1	1.8	0.057	4.4	0.3 – 1.0
A5	1.40	0.58	73.6	3.0	0.070	3.8	0.2 – 0.8
A6	1.25	0.86	60.9	4.3	0.091	3.6	0,1 – 0.7
B. Thick wall crucible (20 mm)							
B1	1.80	0.45	79.5	1.7	0.053	6.7	0.6 – 1.6
B2	2.00	0.37	83.2	1.4	0.043	5.9	0.5 – 1.5
B3	1.60	0.45	79.5	1.8	0.055	5.4	0.4 – 1.2
B4	1.50	0.47	78.6	1.8	0.057	4.5	0.3 – 1.0
B5	1.40	0.60	72.7	2.9	0.072	3.6	0.2 – 0.7
B6	1.30	0.85	61.4	4.3	0.090	3.6	0.1 – 0.7

The reproducibility dispersion of the characterization data is +/- 3%. The porosity value is reproducible in proportion of +/- 0.5%.

According to the data from table 4, generally, the physical and mechanical features of the samples obtained by the two variants are similar. Therefore, the microwave heating mode does not influence significant the physical, mechanical and structural characteristics of the samples. The lowest apparent density values correspond to the variantsA2 (0.36 g/ cm^3) and B2 (0.37 g/ cm^3) obtained from 99.0 wt.% waste glass, 1.0 wt.% calcium carbonate and 8.0 wt.% water addition. High porosity values (83.6% and respectively 83.2%) correspond to this density value. The thermal conductivity of the material has low values (0.042 – 0.043 W/ m·K) and the compressive strength is also relative small of 1.3 – 1.4 MPa. The pores size varies between 500 μm and 1.6 mm. A material with these features is a good insulator material usable in construction. The increase of the weight proportion of waste glass, the corresponding reduction of the weight proportion of calcium carbonate and the increase of the mixture moistening with water addition allow to obtain more dense materials, having higher compressive strengths and thermal conductivities. These materials are appropriate for using as aggregate for lightweight concretes in construction.

The structural features of the foam glass samples are obviously influenced by the amounts of water added in the powder mixture of raw material as well as the reduction of the weight proportion of calcium carbonate by diminishing the pores size and improving the homogeneity of their distribution. Images of all samples experimentally obtained in both variants are shown in figures 4 – 15.

Fig. 4. Sample 1A

Fig. 10. Sample 1B

Fig. 5. Sample 2A

Fig. 11. Sample 2B

Fig. 6. Sample 3A

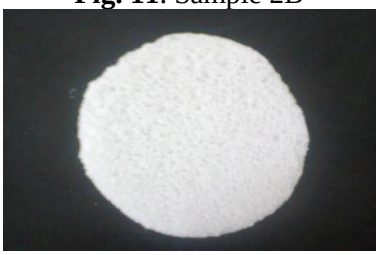

Fig. 12. Sample 3B

Fig. 7. Sample 4A

Fig. 13. Sample 4B

Fig. 8. Sample 5A

Fig. 14. Sample 5B

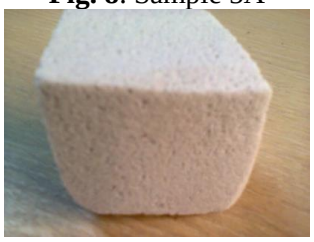

Fig. 9. Sample 6A

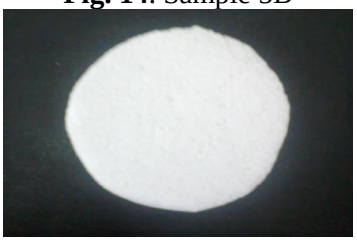

Fig. 15. Sample 6B

The samples with the finest porosities are the samples 5 and 6 (variants A and B), characterized by calcium carbonate proportions between 0.1 – 0.3 wt.% and water addition proportions between 13 – 20 wt.%. According to the data from Table 4, the pores size reaches values below 1 mm: between 200 – 800 µm (sample 5 – figures 8 and 14) and, respectively, between 100 – 700 µm (sample 6 - figures 9 and 15).

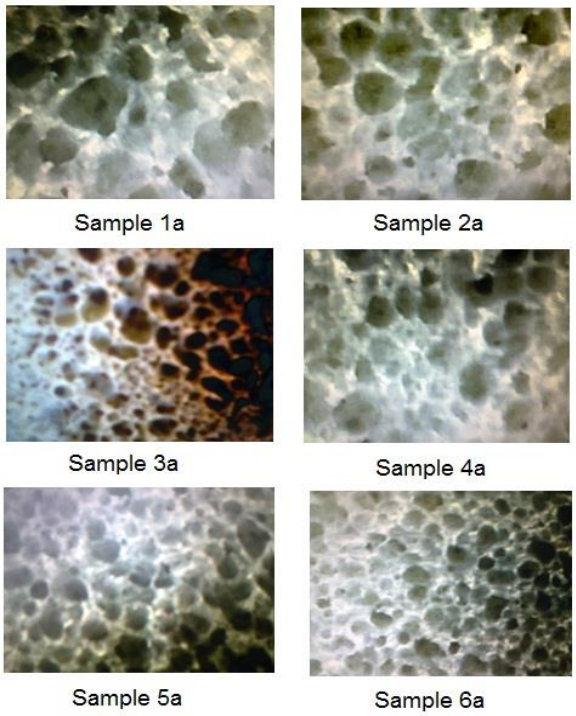

Fig. 16. Images of pores structure determined with a macro-epidiascope with image analyzer

Images of the pores structure of the samples 1 – 6A were obtained with a macro-epidiascope with image analyzer, being shown in figure 16.

The tests for determining the hydrolytic stability of samples, using 0.15 ml of 0.01M HCl solution to neutralize the extracted Na_2O, showed that the stability joins in the hydrolytic class 2, the extracted Na_2O equivalent being in the range 31 - 50 μg.A.

4. ESTIMATED ECONOMIC EFFECT AND THE ENVIRONMENT IMPACT

The use of the feature of raw material based on waste glass to be a microwave susceptible material, tested in the experiments described above, led to significant improvements of the functional parameters of the manufacturing process of foam glass (thermal efficiency, specific consumption of energy and productivity), the physical, mechanical and structural characteristics of the products being not changed.

Having into account the amount of heat required to develop the sintering process of waste glass at 830 ºC (0.15 kWh/ kg [20]) and the average value of specific consumption of electricity of the current experimental process (variant A) carried out in a discontinuous operation regime (1.56 kWh/ kg), results that its thermal efficiency is: $\eta = 0.15/ 1.56 = 0.096$. This value, small by comparison with an industrial continuous technological process, is significant increased about two time compared to the average thermal efficiency of the experimental manufacturing processes of foam glass which do not use the raw material feature of microwave susceptible – variant B ($\eta = 0.049$). Also, the productivity is improved due to the decrease of the heating process duration from 46.3 minutes to 30.7 minutes, i. e. with 33.7%. The specific consumption of electricity determined in the current experiments (1.56 kWh/ kg) is much lower compared to the average specific consumption of the reference experiments of 3.07kWh/ kg.

Generally, the literature does not provide information on the specific consumption of the industrial manufacturing processes of foam glass by the conventional heating methods. Obviously, there are not data on similar tests of using the microwave energy.

From the environmental protection point of view, the manufacturing technique of foam glass, used as replacer of different materials in construction, from waste bottle glass, constitutes a viable revaluation solution of this waste existing on large scale.

5. CONCLUSIONS

The objective of research, whose experimental results are presented in the paper, is the use of the feature of the raw material based on waste glass to absorb the microwave energy and convert it to heat in the manufacturing process of foam glass from waste.

Although, theoretically, the advantages of the heating of materials with the microwave energy are well known, worldwide this advanced technique is used only on a small scale.

Because the glass is not a microwave susceptible material at the ambient temperature and it obtains this feature only over 500 ºC, according to M. Knox and G. Copley's theory, led to the conclusion that the use of the microwave heating in the producing process of foam glass from waste glass is not yet interesting for the great industrial manufacturers.

The research carried out in the last time by the Romanian company Daily Sourcing & Research highlighted that the powder mixture of raw material based on waste glass has the features of a microwave susceptible material since the ambient temperature and the direct contact between this and the microwave radiation allows significant improvements of the functional parameters of the manufacturing process of foam glass.

The experiments carried out on an adapted 0.8 kW domestic microwave oven, using waste bottle glass and calcium carbonate as foaming agent into a silicon carbide crucible with thin wall, led to the reduce of the specific consumption of electricity two time, reaching 1.56 kWh/ kg. Also, the heating process duration was reduced with 33.7%, the average heating speed of the material being of over 26 ºC/ min. The physical, mechanical and structural characteristics of the products were not changed compared to the reference tests.

By the adopted technique, the revaluation degree of waste bottle glass, existing in large amounts, is very high, the experiments being carried out for its weight proportions between 98.0 – 99.9%.

REFERENCES

[1] Scheffler M., Colombo P., (2005), *Cellular ceramics: structure, manufacturing, properties and applications,* Wiley-VCH Verlag GmbH & Co. KGaA, Weinheim.

[2] Rawlings R. D., Wu J. P., Boccaccini A. R., Glass-ceramics:Their production from wastes-A review, *Journal of Materials Science,* 41(3), (2006), 733-761.

[3] Hurley J., *Glass-Research and development final report,* A UK market survey for foam glass, March 2003.

[4] Kharissova V. Oxana, Kharissov B. I., Ruiz Valdez J. J., Review: The use of microwave irradiation in the processing of glasses and their composites, *Industrial & Engineering Chemistry Research*, 49(4), (2010), 1457 - 1466.

[5] Paunescu L., Dragoescu M. F., Axinte S. M., Comparative analysis of the own experimental techniques of producing the foamed glass ceramic, *Journal of Engineering Studies and Research*, 22(2), (2016), 55-64.

[6] Paunescu L., Grigoras B. T., Dragoescu M. F., Axinte S. M., Fiti A., Production of foam glass from waste glass and calcium carbonate using the microwaves energy, *Journal of Engineering Studies and Research* (in press).

[7] Axinte S. M., Dragoescu M. F., Paunescu L., Hritac M, Advanced technique of producing glass-ceramic foams using the microwaves energy, *Scientific Bulletin of University Politehnica of Bucharest, Series B* (in press).

[8] Paunescu L., Grigoras B., T., Dragoescu M. F., Paunescu B. V., Dense foamed glass-ceramic for construction by recycling the waste bottle glass, *Constructii*, (in press).

[9] Knox M., Copley G., Use of microwave radiation for the processing of glass, *Glass Technology*, 38(3), (1997), 91-96.

[10] Bernardo E., Scarinci G., Hreglich S., Foam glass as a way recycling glasses from cathode ray tubes, *Glass Science and Technology*, 78(1), (2005), 7-11.

[11] Gorokhovsky A. V., Escalante-Garcia J. I., Mendez-Nonell J., Gorokhovsky V. A., Mescheryakov D. V., Foamed glass-ceramic materials based on oil shale by-products, *Glass Science and Technology*, 75, (2002), 259-262.

[12] Zhu M., Ji R., Li Z., Zhang Z., Preparation of glass ceramic foams for thermal insulation application from coal fly ash and waste glass, *Construction and Building Materials*, 112(1), (2016), 398-405.

[13] Stiti N., Ayadi A., Lerabi Y., Benhaoua F., Benzerga R., Legendre L., Preparation and characterization of foam glass based waste, *Asian Journal of Chemistry*, 23(8), (2011), 3384-3386.

[14] Ducman V., *Foaming process of waste glass using $CaCO_3$, MnO_2 and water glass as foaming agents.* http://books.google.ro

[15] Oakseson W. G., Lee J. G., Goyal S. K., Robson T., Cutler I., *Foam glass insulation from waste glass,* US Environmental Protection Agency, Cincinnati, Ohio, August 1977.

[16] *** *Manual of weighing applications, Part 1, Density*, February 1999.

[17] Anovitz L. M., Cole D. R., Characterization and analysis of porosity and pore structures, *Reviews in Mineralogy & Geochemistry*, 80, (2015), 61-164.

[18] ISO 719:1985, *Glass – hydrolytic resistance of glass grain at 98 ºC – Method of test and classification* (reviewed and confirmed in 2011).

[19] *Calculation of the chemical durability (hydrolytic class, corrosion) of glass.* http://glassproperties.com/chemical_durability/

[20] Ražnjević, K., *Tables and thermodynamic diagrams*, Technical Publisher, Bucharest, 1978.